Summer 8-15-2016

Functions for Murine Norovirus Protein NS1/2 in Mice and Cells

Broc Taylor Mccune
Washington University in St. Louis

WASHINGTON UNIVERSITY IN ST. LOUIS

Division of Biology and Biomedical Sciences
Immunology

Dissertation Examination Committee:
Herbert W. Virgin, Chair
Gaya Amarasinghe
Jacco Boon
Michael Diamond
Andrzej Krezel
Wayne Yokoyama

Functions for Murine Norovirus Protein NS1/2 in Mice and Cells

by

Broc Taylor McCune

A dissertation presented to the
Graduate School of Arts & Sciences
of Washington University in
partial fulfillment of the
requirements for the degree
of Doctor of Philosophy

August 2016

St. Louis, Missouri

Table of Contents

List of Figures

List of Abbreviations

BMDM	Bone-Marrow Derived Macrophage
ER	Endoplasmic Reticulum
HCV	Hepatitis C Virus
HIV	Human Immunodeficiency Virus
HPI	Hours Post Infection
HPT	Hours Post Transfection
HNoV	Human Norovirus
HSQC	Heteronuclear Single Quantum Coherence
IFN	Interferon
Ifnar/Ifnlr	Interferon alpha receptor/Interferon lambda receptor
IRF	Interferon Regulatory Factor
ISG	Interferon Stimulated Gene
LCMV	Lymphocytic Choriomeningitis Virus
LTP	Lipid Transfer Protein
MCS	Membrane Contact Site
MLN	Mesenteric Lymph Nodes
MOI	Multiplicity of Infection
MNoV	Murine Norovirus
NMR	Nuclear Magnetic Resonance
NoV	Norovirus
NS (upper case)	non-structural (viral proteins)
Ns (lower-case)	not significant
ORF	Open Reading Frame

PFU	Plaque Forming Unit
qRT-PCR	quantitative Real Time Polymerase Chain Reaction
RC	Replication Complex
STAT1	Signal transducer and activator of transcription 1
VAPA/B	(Vesicle Associated Membrane Protein) Associated Protein A/B
VP	Viral Protein, referring to proteins constituting NoV capsid
vRNA	Viral RNA
WT	Wild Type

Acknowledgments

Any substantial effort in life insists on the support of a team of people, and my dissertation exemplifies that well.

Tim Nice influenced my scientific thinking and training more than any other individual. He is a friend, a colleague, and a mentor. He shouldered the mountainous task of my mentorship willingly, without complaint, and cheerily. I admire and try to emulate him scientifically and personally.

I am grateful to my thesis advisor, Herbert "Skip" Virgin. He exhibited a great deal of patience with my adolescent-scientific tendencies. I am grateful he allowed me to explore ideas on my own. It was an inefficient way to do science, but what I learned about myself and science could have been gained in no other way.

Of all of my thesis advisor's skills, I am most grateful for his ability to attract congenial and brilliant people into his lab. I found talking science with my Virgin lab colleagues practically, technically, hedonistically, to be a highlight of my training. They are a collaborative, generous, and intelligent group, and they took my eccentricities in stride. Of the group, Robert Orchard was particularly influential. Forever generous, thoughtful, and actively modest, he is an intellectual force to reckon with. I greatly value his sledgehammer blows of logic and insight. He is great friend and colleague. Craig Wilen and Megan Baldridge took an active interest in my project and training, and I am grateful to them. Megan helped polish much of my writing, and attended many practice talks. She is a real team player.

Thanks to my thesis committee, Michael Diamond, Wayne Yokoyama, Jacco Boon, Andrzej Krezel, and Gaya Amarasinghe. Gaya particularly took an active interest in helping me

take responsibility for my training. That is inherently painful, but a crucial attitude to take early on.

I am grateful to the many collaborators. They have all been patient, generous, and professional. Andrzej Krezel performed the studies that made the NS1/2-VAPA interaction an interesting phenomenon. Ian Goodfellow, and many scientists in his lab, made important contributions through the years.

I am grateful for my spiritual and religious convictions. Perhaps God must not be invoked in the scientific method, nevertheless I felt Divine assistance scientifically, emotionally, intellectually, and spiritually through the intense experience of earning a PhD. I believe He does know all the answers, but for His children's sake is committed to the scientific method for scientific matters.

I wish to write an endless soliloquy for my wife, Melanie. I put her through fire and hell, and she came through it gloriously. She is my best friend, confidant, sounding board, and best and greatest support. I love her dearly. My children Janessa, Jaxton, and Carsten are the best scientists in the family! They are precious to me and I appreciate their support. My parents and parents-in-law are intelligent, inquisitive people, and have been actively supportive through the entire PhD. Thanks to them all.

Finally, I am grateful for financial support. Funding agencies had no influence on the studies herein, nor does this work reflect funding agencies' views. I was supported by Siteman Cancer Center and NIH-NCI award F31CA177194-01.

Broc McCune

Washington University in St. Louis

August 2016

ABSTRACT OF THE DISSERTATION

Functions for Murine Norovirus Protein NS1/2 in Mice and Cells

by

Broc Taylor McCune

Doctor of Philosophy in Biology and Biomedical Sciences

Immunology

Washington University in St. Louis, 2016

Professor Herbert Virgin, Chair

Noroviruses are a leading cause of epidemic gastroenteritis and a major health burden worldwide. One source for outbreaks is individuals who shed virus asymptomatically and persistently. Viral persistence is a successful strategy for viruses to spread, but the mechanisms and consequences of norovirus persistent infection are unknown. In this dissertation, we sought to determine the norovirus determinant(s) of persistence and explore the functions of the associated viral molecules.

To determine the viral determinants of persistent infection and tropism, we used the murine norovirus model system in mice. Using plasmid infectious clones for persistent strain CR6 and non-persistent strain CW3, we mapped the viral persistence determinant to the poorly understood non-structural gene NS1/2. The NS1 domain of NS1/2^{CR6} was necessary and sufficient for persistence. A single amino acid change, NS1/2^{D94E}, conferred persistence on CW3. Viral persistence was restricted to replication and shedding in the intestine, and NS1/2 conferred intestinal tropism. In contrast, the capsid protein VP1 conferred acute replication in the spleen. Moreover, CW3 grew more rapidly in macrophages *ex vivo*, and this difference mapped to VP1.

Therefore, NS1/2 and VP1 are the major determinants for persistence and tropism *in vivo* and *ex vivo*.

To determine a molecular function of NS1/2, we characterized its interaction with the host protein Vamp-Associated Protein A (VAPA). Murine norovirus replication was delayed in *Vapa*$^{-/-}$ cells and this was rescued by exogenous VAPA. Moreover, in *Vapa*$^{-/-}$ cells, NS1/2 protein levels were decreased early during viral infection as well as with electroporated viral RNA. The interaction of murine norovirus NS1/2 with VAPA occurred in a region within the poorly conserved NS1 domain of NS1/2. Investigations in the structural basis of NS1/2-VAPA interaction revealed sequence and functional mimicry between the VAPA binding region of NS1 and the host diphenylalanine-acidic-tract (FFAT)-motif that binds VAPA. The NS1/2-FFAT-mimic interacted with VAPA similarly to bona fide host FFAT motifs. Furthermore, mutations within NS1/2 that disrupted interaction with VAPA inhibited viral replication. Thus, VAPA is a pro-norovirus host factor interacting directly with a norovirus protein that functionally mimics FFAT motifs to co-opt VAPA function.

In conclusion, we mapped the norovirus determinants of persistence and tropism to NS1/2 and VP1. Furthermore, we determined that the NS1/2 interaction with VAPA enhanced murine norovirus infection. These are the first structural and functional studies to characterize NS1/2 in molecular detail. This work provides the basis for further exploration to identify the function of NS1/2 that contributes to persistent infection in mice.

Chapter 1:
Introduction

1.1 Gastrointestinal viruses and Persistence

1.1.1 Viral models for gastrointestinal infection

The mammalian intestinal virome is a crucial nexus of health and disease (1-7). Many viral families can be found in the intestine or stool of mammals, including *Retroviridae, Herpesviridae, Coronaviridae, Parvoviridae, Adenoviridae, Astroviridae, Caliciviridae, Reoviridae,and Picornaviridae, Picobirnaviridae, Annelloviridae, Circoviridae*, and many different families of bacteriophage. Several of these viruses can establish long-lasting enteric infection (8-15). Among these, murine norovirus (MNoV) is a powerful model virus to study enteric persistence. Understanding the mechanisms of persistent, enteric viral infection using the MNoV model system is the over-arching goal of this dissertation.

1.1.2 Viral Persistence

The establishment of a long-lasting, persistent infection is a successful strategy for dissemination and replication for many viruses. During persistence, viruses may continuously replicate (ex. Lymphocytic Choriomeningitis Virus (LCMV), Hepatitis C Virus (HCV), Papillomaviruses (HPV)), persist as non-replicating, latent genomes that reactivate upon stimulation, (ex. Herpesviruses), or may integrate into their host's genomes (ex. Lentiviruses and Retroviruses). For viruses that continuously replicate, the LCMV model system has yielded detailed insight into host and viral mechanism of persistence. Particularly, single amino acid variants within two LCMV proteins, glycoprotein and polymerase, contribute to persistence (16-20). The glycoprotein variant is associated with viral tropism *in vivo* (18), and variants within glycoprotein and polymerase that are associated with persistence permit LCMV replication in macrophages *in vitro* (16). These observations linked viral mechanisms of replication and

tropism with viral persistence. However, detailed mechanisms for enteric viral persistence are lacking.

Viral persistence can have profound effects on their hosts. Persistent viral infection can lead to immune related pathologies (21), such as immunodeficiency (HIV and LCMV (22)), immunopathology (HCV), and autoimmunity (LCMV). Many persistent viral infections are associated with cancer, such as HCV, HPV, Human T-Lymphotropic Virus, Simian Virus 40, Epstein-Barr Virus, and Rous Sarcoma virus (23). It is unknown if persistent viral infections in the intestine are associated with cancer, though for bacteria persistent *Helicobacter pylori* infection leads to gastric and esophageal cancer (24). A persistent strain of MNoV is associated with pathology found in inflammatory bowel disease patients (2). In contrast, persistent infections can have beneficial effects on their hosts as well. Chronic herpesvirus infection can help mice resist lethal bacterial challenges (25), and reverses the effects of a specific immunodeficiency (26). Therefore, the mechanisms and consequences of persistent viral infection is an important research goal.

1.2 Norovirus

1.2.1 Norovirus Persistence

Human Norovirus (HNoV) can establish persistent infections (27). Additionally, persistent HNoV infection is frequently asymptomatic (28-32). This may be of epidemiological importance because asymptomatically infected individuals may serve as reservoirs for NoV between outbreaks. Indeed, NoV from these individuals has been reported to initiate NoV outbreaks (33-36). Of additional concern are potential consequences of persistent HNoV infection on individuals. Multiple case reports have described severe outcomes for HNoV

infection (37-43). The inability for HNoV to grow robustly in small animal models has prevented studying the mechanisms and consequences of NoV persistence. The 1) discovery of MNoV, 2) the observation that not all MNoV strains establish persistent infections (15, 44), and 3) the engineering of genetically tractable infectious clones for MNoV (45), have collectively enabled the possibility to determine the mechanisms of NoV persistence.

1.2.2 Norovirus Health Consequences

HNoVs are the leading cause of non-bacterial gastroenteritis, and the primary cause of epidemic acute gastroenteritis (46-48). While most healthy individuals recover without complication, HNoVs cause significant morbidity and mortality among the young and old. HNoV also pose an economic burden due to lost productive work, hospitalization costs, and closure of hospital wards during nosocomial outbreaks. Direct healthcare costs alone are estimated to be $500 million annually in the US (49), and $4.2 billion worldwide ((50)). There are no norovirus vaccines, yet several candidates are under development (51-56). However, study of the basic mechanisms of replication and pathogenesis have been limited as efforts to robustly and reproducibly grow HNoV in small animal models or in cell culture have been unsuccessful.

1.2.3 MNoV Pathogenesis and Immune Responses

The discovery of Murine Norovirus (MNoV) has greatly facilitated the study of virus-host interactions in the intestines, and specifically NoV pathogenesis and replication *in vivo* and *in vitro*. Major discoveries *in vivo* include a role for NoV in the development of the intestine (3), antiviral immunity in the intestine (57-59), a role for viruses in inflammatory bowel disease pathogenesis (2), and bacteria-virus interactions (58). However, it is an imperfect model of

HNoV pathogenesis. HNoV causes gastroenteritis, including vomiting and diarrhea, but there are no overt clinical signs in MNoV infection in WT animals. However, in *Stat1*$^{-/-}$ mice, MNoV-1 causes gastric bloating and loose stool (60). These signs of disease imperfectly model HNoV pathogenesis, but it should be noted that mice do not have an emetic reflex (61), so it is reasonable to predict MNoV evolved other mechanisms of transmission and pathogenesis.

Viruses must in some way evade or antagonize immune responses to establish persistent infections (62-64). Both innate and adaptive immune responses are important for control of MNoV-1 in mice, which is cleared acutely in WT mice. The founding strain of MNoV, MNoV-1, was isolated during intracranial serial passaging in mice devoid of adaptive immunity and IFN signaling, *Rag1/Stat1*$^{-/-}$ mice (65). For adaptive immune responses, MNoV-1 can persist in *Rag1*$^{-/-}$ mice (66, 67). Moreover, antibody production by B cells, CD4+ and CD8+ T cells are necessary for rapid clearance of MNoV-1 (66, 67). Furthermore, the persistent MNoV strain CR6 induces MNoV-specific T cells, but these cells are less functional (57). Further studies are needed to characterize the role of adaptive immune responses against persistent MNoV strains such as CR6.

Innate immune responses are important for control of MNoV. MNoV-1 is lethal in *Stat1*$^{-/-}$ and *Ifnar*$^{-/-}$ mice, but is cleared acutely from immunocompetent mice (65, 68), indicating lack of interferon (IFN) signaling alone is sufficient for MNoV-1 lethality. IFNγ signaling is also important for control of MNoV-1 in mice and bone-marrow derived macrophages (BMDMs) (69). Furthermore, MNoV-1 replication is enhanced in mice lacking the transcription factors IRF1, IRF3, IRF5, and IRF7, which are involved in IFN production and signaling (68, 70, 71). Moreover, deletion of *Ifnar*$^{-/-}$ only in macrophages or dendritic cells permits a non-lethal persistent MNoV-1 infection of mice (72). Host detection of MNoV-1 is mediated by the pattern

recognition receptor MDA-5 (73). Additionally, MNoV-1 growth *in vivo* is enhanced by *Nlrp6*$^{-/-}$, a recently identified RNA-virus sensor (74). Work on the role of individual IFN-stimulated genes for MNoV is limited, except ISG15 has antiviral function against MNoV (75). Furthermore, autophagy proteins are necessary for the antiviral function of IFNγ in mice and in BMDMs (69), suggesting that these proteins interact with ISG(s) to restrict MNoV replication.

Immune control of different MNoV strains is not universal. MNoV strains isolated from feces, such as CR6, have reduced lethality in immunocompromised mice (15, 76). Furthermore, IFNλ controls CR6, but not MNoV-1 subtype CW3 (59). These observations opened the possibility to map viral determinants for susceptibility/resistance to immune responses. A critical advance to accomplish this aim was the creation of DNA-plasmid infectious clones for MNoV-1.CW3 and the CR6 (45). Single gene chimera between CW3 and CR6 revealed that the viral protein VP1 determines MNoV lethality in immunocompromised mice (77, 78) and is a partial determinant for sensitivity to IFNλ in mice (59). This viral genetic system will permit further mapping of the viral genetic determinants of traits that differ between CW3 and CR6.

1.2.4 Norovirus Tropism

A substantial limitation for NoV studies is the lack of definitive evidence for the cell types in which NoV replicates *in vivo* in immunocompetent and tractable model organisms. Exhaustive efforts have been made to this end (reviewed in (79)). Evidence to date does not support a role of replication in epithelial cells, but rather in macrophages (80-82), dendritic cells (80, 83), and B cells (84, 85). Detailed studies of mechanisms of NoV pathogenesis, immune responses, mechanisms of persistence, and many other studies will require this breakthrough.

Host factors determine an individual's susceptibility to infection by NoV. In a strain dependent fashion, HNoV requires carbohydrates, specifically histo-blood group antigens

(HGBAs), at the cell surface to enable virus attachment (86-93). This has profound consequences for HNoV host range. Individuals who lack the protein FUT2, an enzyme necessary for production of HGBAs, are not susceptible to challenge infections by HNoV (87). MNoV also binds carbohydrates at the cell surface (94, 95). Mutations in VP1 that attenuate the ability for MNoV to bind carbohydrates exhibit altered tropism in mice (95).

1.2.5 Norovirus Molecular Virology

NoV is genus within the *Caliciviridae* family. The NoV genus is further organized into seven phylogenetically classified "genogroups" based on VP1 sequence (96, 97). NoVs are small, non-enveloped viruses encoded by a single-stranded positive-sense RNA genome. The 5' terminus of vRNA is covalently linked to a small viral protein (VPg). The genome is organized into three Open Reading Frames (ORFs), and a fourth ORF unique to MNoV (Figure 1.1A). ORF1 contains the Non-Structural (NS) proteins NS1/2 through NS7. ORFs 2 and 3 encode the structural proteins VP1 and VP2, which make up the viral capsid (98). ORF4 overlaps with ORF2 and encodes an immune-evasion molecule, VF1, which is unique to MNoV (99).

On a cellular level, some details of the NoV life cycle are known (Figure 1.1B). Both MNoV and HNoV bind to carbohydrates at the cell surface (94, 100). Recently, a proteinaceous receptor for MNoV was discovered, CD300lf (in press). MNoV is taken up through an endocytic process mediated by dynamin, cholesterol (101, 102), and possibly ceramide (103), and releases viral genome into the cytoplasm. ORF1 polyprotein is translated from the virion RNA. This is mediated by interactions of VPg with eIF4G (104, 105) and eIF4E (106) and results in NoV regulating host translation (107). The ORF1 polyprotein is proteolytically processed into non-structural proteins by the virally encoded protease (NS6) (108). Non-structural proteins then collaborate to re-organize host membranes to form a membranous structure on which viral

replication occurs, i.e. the replication complex (RC) (80, 109). It is undefined what functions of NoV and host proteins, lipids, and pathways are required for formation of RCs. Nevertheless, precedents from other viruses are discussed below. However, all MNoV non-structural proteins localize with RCs during infection (109), and when transiently transfected, NSs localize with different markers of membranous sub-cellular structures (110). Virally encoded RNA-Dependent RNA Polymerase (NS7) synthesizes negative-strand RNA. This negative strand then serves as template for amplification of genomic viral RNA (vRNA) as well as the sub-genomic RNA. ORFs 2-4 are translated from sub-genomic RNAs. vRNA and capsid proteins VP1 and VP2 assemble into virions that are released from cells.

As a single-stranded RNA virus, the NoV genome is folded into higher order secondary and tertiary structures (111-114). These structures have been observed at the 5' and 3' termini of the genome, thus overlapping the coding sequence for NS1/2 and NS7 respectively. Another structured region immediately precedes the sub-genomic RNA within NS7 gene, called the sub-genomic promoter (112). These structures are critical for viral replication. These RNA structures overlap coding sequence for NS1/2, NS7, and VP2, thus placing additional constraints on the ability for these proteins to evolve.

1.3 Norovirus Non-Structural Protein NS1/2

NS1/2 is the first NoV protein translated upon infection of a cell. It is rapidly cleaved at its C-terminus by the viral protease NS6, separating NS1/2 from NS3 (108). Therefore, NS1/2 likely functions independently of its temporary conjugation to NS3 in the MNoV polyprotein.

1.3.1 NS1/2 Domains

Three domains comprise NS1/2, the NS1, NS2, and predicted trans-membrane domains (115-117). Nearly nothing is known about the NS1 domain.However, the MNoV NS1 domain in isolation has a structured fold preceded by an unstructured region (117, 118). The NS2 domain is well conserved among the NoV genus. Importantly, the NS2 domain contains a predicted protein fold, termed NlpC/P60, seen in all kingdoms of life (119). Proteins with this fold have enzymatic activities, including phospholipases, proteases, and acyltransferases, suggesting that NS1/2 may be an enzyme. NS2 specifically resides in a clade whose prototypical member is mammalian-encoded Lecithin Retinol Acyltransferase (LRAT). LRAT and LRAT-like Hrev107 modify lipids, and Hrev107 modulates cellular proliferation (120, 121). Two genera within *Picornaviridae* also encode LRAT-like molecules, which include the viruses Aichi Virus (AiV), Avian encephalomyelitis Virus (AeV), Human Parechovirus (HPaV), and Ljungan virus (LjV) (119, 122, 123), which will be discussed below. Finally, a predicted trans-membrane region (TM) occupies the C-terminal portion of NS2 domain.

Some evidence evokes the idea that NS1 and NS2 may act independently of each other. Two caspase-3 cleavage site separate MNoV NS1 and NS2 (108), and cleavage products are visible by 12 hours post-infection (HPI) (108, 117). In collaboration with cellular factors, NS6 may cleave a site near the HNoV NS1/NS2 predicted junction (124). These observations support the possibility that NS1 and NS2 can function both together and separately during the virus life cycle. Functional significance of NS1/2 cleavage is lacking.

1.3.2 NS1/2 Subcellular Localization

NS1/2 associates with membranes and the viral RC. The RC is a membranous structure organized by many RNA-viruses that permits efficient virus replication (reviewed in (125-128).

RCs also serve immune evasive function in two ways: 1) by secluding viral molecular patterns such as dsRNA sensed by host proteins that activate antiviral responses, and by 2) disrupting host membranes necessary for expression and secretion of antiviral molecules (129). Two separate strains of HNoV NS1/2 associate with Golgi markers as seen by microscopy and sub-cellular fractionation (115, 116). These strains also disrupt the Golgi apparatus morphology (115). NS1/2 acts as an integral membrane protein, though this was not dependent on its predicted TM (116), possibly by binding strongly to the integral membrane protein VAMP (Vesicle-Associated Membrane Protein)-Associated Protein (VAPA). It is neither known if MNoV binds VAPA nor if this interaction is important for replication. For MNoV NS1/2, overexpressed NS1/2 localizes with ER markers, but not Golgi markers (110). Moreover, during infection NS1/2 overlaps entirely with double-stranded RNA, which forms during viral RNA synthesis and is a definitive feature of RCs. NS1/2 also forms puncta outside RCs (109). It is unknown what cellular markers these puncta localize with or what functions they serve.

1.3.3 NS1/2 Protein Interactions

A number of host and viral proteins have been reported to interact with NS1/2. As discussed above, VAPA interacts with NS1/2. NS1/2 also interacts with the viral protein NS4 (130), but the contributions of this interaction to viral replication have not been investigated. Lastly, HSP90, a host chaperone that stabilizes and assists proper protein folding, also binds NS1/2 (131). NS1/2 is produced in lower levels upon pharmacological inhibition of HSP90 (131), while this was not true for all viral proteins. This is intriguing as the NS proteins cleaved from the polyprotein are produced in relatively equimolar ratios in WT cells. This argues NS1/2 production is uniquely influenced by the function of HSP90. However, while HSP90 was demonstrated to be beneficial for MNoV growth, it cannot be imputed this is primarily due to

HSP90-NS1/2 interaction as HSP90 also binds and stabilizes VP1 and the 5' end of MNoV genomes (131). Identification of additional NS1/2 client proteins, and uncovering their roles in MNoV infection, will be critical to understanding the role of NS1/2 during MNoV infection.

The interaction of NS1/2 with HSP90 represents an example of how proteostasis, the regulation of protein production and degradation within the cell, can influence NoV infection. Further evidence for the importance of proteostasis during MNoV infection comes from studies on the unfolded protein response (UPR). The UPR is a key regulator of proteostasis. Activation of the UPR is detrimental to MNoV replication (132). How NS1/2 production is regulated during infection, and if the UPR plays a role, will be resolved with further experimentation.

1.3.4 NS1/2 Functions

Many observations support that NS1/2 is involved in basic virus replication. First, NS1/2 co-localizes with the viral RC (109). Second, mutagenizing the NlpC/p60 predicted catalytic residue in NS1/2, MNoV-NS1/2^{C216A}, prevents recovery of plasmid-derived virus (unpublished data). Third, Thorne et al. created a library of MNoV clones whose genomes were saturated with small insertions (130). Among viruses with insertions in NS1/2, viruses were recovered in cell culture only with insertions in three discrete regions, all confined to the NS1 domain. This suggests the NS2 domain has critical function(s) for virus replication, as disruption of NS2 with small insertions did not produce virus. Fourth, NS1/2 enhances RNA synthesis activity of NS7 in a cell-based functional assay (133). Fifth, virus-encoded homologues of NS2 contribute to virus replication, discussed next.

The functions of homologues for the NS2-domain suggest NS1/2 has a fundamental role in viral replication. For example, the AiV homologue for NS1/2, the 2A protein, is required for viral replication as mutating the predicted catalytic sites within the NlpC/P60 fold inhibits

synthesis of viral RNA both in cells and in a cell-free system (134). The initial round of translation is unaffected in these systems, strongly supporting that the defect is at a step downstream of protein synthesis. In support of a function at RNA replication, AiV 2A binds to AiV 3CD protein shown by M2H (135) which has a role in replication of viral RNA. Furthermore, 2A in HPaV binds specifically to the 3'UTR of the genome, consistent with a role for RNA synthesis (136). Finally, HPaV 2A associates with viral RC (137), though notably extra-RC 2A diffuses throughout the entire cellular space, in contrast to cytoplasmic puncta formed by NoV NS1/2. The mechanisms through which these homologues function may help predict NS1/2 function in MNoV lifecycle.

In line with the finding that over-expressed NS1/2 associates with ER and Golgi membranes, two additional observations support that NS1/2 disrupts secretion. First, over-expressing NS1/2 disrupts the Golgi apparatus (115). Second, over-expressed VSV-G normally accumulates on the plasma membrane. Simultaneous over-expression of NS1/2 and VSV-G prevents cell surface expression of VSV-G (116). These results suggest NS1/2 participates in membrane re-modeling during viral replication or perhaps immune evasion.

1.4 VAPA

VAPA is a type II endoplasmic reticulum (ER) resident protein that is conserved in eukaryotes (138). VAPA is comprised of a Major Sperm Protein (MSP) domain, a Coiled-Coil domain (CCD), and a transmembrane domain. Initially found to bind SNAREs (139-141), VAPA also binds a variety of client interacting proteins (138). Importantly, through the cytosolic MSP domain, VAPA interacts with client proteins. These proteins interact with VAPA-MSP via a diphenylalanine acidic tract (FFAT) linear motif (142-146). VAPA client proteins have roles in diverse cellular processes, including proteostasis (147-154), non-vesicular lipid transfer (138,

145, 155-160), membrane morphology (154, 161, 162), and membrane contacts (154, 157, 159, 163-165),

VAPA performs important functions during infection as both microbes and antimicrobial host molecules target VAPA and its client proteins. VAPA and its paralog VAPB enhance the replication of Hepatitis C virus (166, 167), rhinoviruses (168), tombusvirus (169, 170), and the intracellular bacteria *Chlamydia trachomatis* (171, 172). Some of these microbes encode molecules that interact with VAPA, VAPB, and/or its client proteins, including HCV proteins NS5a and NS5b (166, 167), tombusvirus p33 (169, 170), and *C. trachomatis* IncD (171, 172). VAPA and VAPA client proteins may assist in organization of membranous structures critical for virus replication (173, 174), possibly by manipulating the lipid composition of these membranes (168-170). Furthermore, VAPA binds to the interferon stimulated genes IFITM3 (175) and RSAD2 (176, 177), suggesting that VAPA may be involved in antiviral responses.

Regulation of VAPA function by competition between VAPA-client proteins has been observed in several settings. First, VAPA interacts competitively with FFAT motifs and either FAF1 or ATF6 that may mediate switching between regulating lipid trafficking and ER quality control (150). Second, IFITM3 competitively binds VAPA away from lipid transfer proteins (LTPs); this correlates with cholesterol accumulation in endosomes and impaired entry of VSV and influenza into cells (175). It is unknown if IFITM family members are antagonistic to NoV replication. A separate IFN stimulated VAPA-client protein, RSAD2, antagonizes HCV infection by disrupting VAPA-NS5a interaction (176, 177). Together these observations raise the question how frequently VAPA is regulated by competition in physiological processes or during microbial infection.

In addition to those discussed above, non-vesicular, protein-mediated lipid transfer is the primary function of VAPA and the most studied function in relation to microbial infection. Examples from positive-sense RNA viruses demonstrate possible functions in NoV. Picornaviruses, Hepatitis C Virus (HCV), and tombusviruses require VAP proteins (166, 168, 169, 173, 178-180) and the VAP-client protein OSBP (168, 169, 181). Domain mapping of OSBP revealed OSBP-VAP interaction is required to enhance HCV replication. Cholesterol is enriched at RCs for HCV and picornaviruses (182-187), and OSBP is thought to be a major mechanism for this enrichment (168, 186-188). Proper recruitment and activity of OSBP requires the accumulation of PI4P at picornaviruses and HCV replication complexes (187-190). PI4P lipid-modification recruits OSBP via a PH-PI4P binding domain. This recruitment is required for HCV replication, as reconstitution of OSBP depleted cells with OSBP lacking the PH domain does not rescue viral replication (188). The specific role of cholesterol in HCV infection is unclear, but cholesterol enrichment does induce biophysical changes to membranes, such as causing negative curvature and reduced membrane fluidity. These characteristics may be necessary for proper replication complex assembly and function. It is unknown if cholesterol or PI4P are enriched at NoV replication complexes, or if disruption of lipid trafficking perturbs viral replication. However, in a STAT1- and IRF1-dependent fashion, IFNγ inhibits cholesterol and lipid metabolism (70), suggesting the possibility that lipid metabolism is a pro-viral host process.

VAP proteins make membrane contact sites (MCS) which are associated with the viral replication of tombusviruses, a genus of plant viruses. Tombusviruses require VAP protein homologues to replicate efficiently (169). OSPB Related Proteins (ORPs) are required to enrich tombusvirus RCs with cholesterol (169, 170). Critically, MCSs can be detected in close

proximity to tombusvirus replication complexes (169). Thus, tombusviruses may thus take advantage of MCSs to channel the appropriate lipids to replication complexes.

Lastly, the intracellular bacteria *Chlamydia trachomatis* also requires VAP proteins, and encodes a virulence factor IncD that interacts with the VAP-client protein CERT (171, 172). VAP and CERT localize with IncD at ER-bacterial inclusion MCSs. At these sites, CERT transfers ceramide to the bacterial inclusion that is processed to sphingomyelin and used by the bacterium. There are no precedents for viruses requiring CERT. While there is some evidence for a role for ceramide in NoV entry into cells (103), it is unknown if CERT, ceramide, or sphingomyelin are required for viral replication.

1.5 Rationale

NoV is an important human pathogen, yet there is limited understanding of viral and host molecules that regulate replication *in vivo* and in cell culture. Furthermore, there are additionally few tractable model systems to study virus-host interactions during enteric viral persistence. Virus persistence within individuals is an important mechanism for maintaining reservoirs to infect others, but also has consequences for the host. Furthermore, the study of persistent extra-intestinal viral infection has resulted in many important immunological and virological observations, but it is unclear if these observations are relevant to enteric virus infection. Therefore, understanding the mechanisms and consequences of enteric viral persistence is an important goal.

We aimed to determine the MNoV molecular determinants of persistence and tropism in the intestine, then to characterize the function of these molecules. We found NS1/2 is the major determinant of tropism and persistence, and further described in detail the molecular interaction between NS1/2 and the host protein VAPA.

1.6 Contribution to Field

In this dissertation, we describe the mapping of MNoV genetic determinants for persistent replication and tropism in the intestine. These studies advanced our understanding of how viruses and hosts interact in the intestinal tract and provide a starting point to understanding the viral mechanisms of persistent infection. This work is also the first detailed structure-function description of the NoV protein NS1/2. We also identified the first microbial mimic of the FFAT host protein motif.

1.7 References

1. **Norman JM, Handley SA, Baldridge MT, Droit L, Liu CY, Keller BC, Kambal A, Monaco CL, Zhao G, Fleshner P, Stappenbeck TS, McGovern DP, Keshavarzian A, Mutlu EA, Sauk J, Gevers D, Xavier RJ, Wang D, Parkes M, Virgin HW.** 2015. Disease-specific alterations in the enteric virome in inflammatory bowel disease. Cell **160:**447-460.

2. **Cadwell K, Patel KK, Maloney NS, Liu TC, Ng AC, Storer CE, Head RD, Xavier R, Stappenbeck TS, Virgin HW.** 2010. Virus-plus-susceptibility gene interaction determines Crohn's disease gene Atg16L1 phenotypes in intestine. Cell **141:**1135-1145.

3. **Kernbauer E, Ding Y, Cadwell K.** 2014. An enteric virus can replace the beneficial function of commensal bacteria. Nature **516:**94-98.

4. **Virgin HW.** 2014. The Virome in Mammalian Physiology and Disease. Cell **157:**142-150.

5. **Cadwell K.** 2015. The virome in host health and disease. Immunity **42:**805-813.

6. **Duerkop BA, Hooper LV.** 2013. Resident viruses and their interactions with the immune system. Nature Immunology **14:**654-659.

7. **Pfeiffer JK, Virgin HW.** 2016. Viral immunity. Transkingdom control of viral infection and immunity in the mammalian intestine. Science **351**.

8. **Kapusinszky B, Minor P, Delwart E.** 2012. Nearly constant shedding of diverse enteric viruses by two healthy infants. J Clin Microbiol **50:**3427-3434.

9. **Nelson JA, Wiley CA, Reynolds-Kohler C, Reese CE, Margaretten W, Levy JA.** 1988. Human immunodeficiency virus detected in bowel epithelium from patients with gastrointestinal symptoms. Lancet **1:**259-262.

10. **Veazey RS, DeMaria M, Chalifoux LV, Shvetz DE, Pauley DR, Knight HL, Rosenzweig M, Johnson RP, Desrosiers RC, Lackner AA.** 1998. Gastrointestinal tract as a major site of CD4+ T cell depletion and viral replication in SIV infection. Science **280:**427-431.

11. **Cinek O, Witso E, Jeansson S, Rasmussen T, Drevinek P, Wetlesen T, Vavrinec J, Grinde B, Ronningen KS.** 2006. Longitudinal observation of enterovirus and adenovirus

in stool samples from Norwegian infants with the highest genetic risk of type 1 diabetes. J Clin Virol **35:**33-40.

12. **Maldonado Y, Cantwell M, Old M, Hill D, Sanchez ML, Logan L, Millan-Velasco F, Valdespino JL, Sepulveda J, Matsui S.** 1998. Population-based prevalence of symptomatic and asymptomatic astrovirus infection in rural Mayan infants. J Infect Dis **178:**334-339.

13. **Phillips G, Lopman B, Rodrigues LC, Tam CC.** 2010. Asymptomatic rotavirus infections in England: prevalence, characteristics, and risk factors. Am J Epidemiol **171:**1023-1030.

14. **Nice TJ, Strong DW, McCune BT, Pohl CS, Virgin HW.** 2013. A single-amino-acid change in murine norovirus NS1/2 is sufficient for colonic tropism and persistence. J Virol **87:**327-334.

15. **Thackray LB, Wobus CE, Chachu KA, Liu B, Alegre ER, Henderson KS, Kelley ST, Virgin HW.** 2007. Murine noroviruses comprising a single genogroup exhibit biological diversity despite limited sequence divergence. J Virol **81:**10460-10473.

16. **Matloubian M, Kolhekar SR, Somasundaram T, Ahmed R.** 1993. Molecular determinants of macrophage tropism and viral persistence: importance of single amino acid changes in the polymerase and glycoprotein of lymphocytic choriomeningitis virus. J Virol **67:**7340-7349.

17. **Salvato M, Borrow P, Shimomaye E, Oldstone MB.** 1991. Molecular basis of viral persistence: a single amino acid change in the glycoprotein of lymphocytic choriomeningitis virus is associated with suppression of the antiviral cytotoxic T-lymphocyte response and establishment of persistence. J Virol **65:**1863-1869.

18. **Ahmed R, Hahn CS, Somasundaram T, Villarete L, Matloubian M, Strauss JH.** 1991. Molecular basis of organ-specific selection of viral variants during chronic infection. J Virol **65:**4242-4247.

19. **Matloubian M, Somasundaram T, Kolhekar SR, Selvakumar R, Ahmed R.** 1990. Genetic basis of viral persistence: single amino acid change in the viral glycoprotein affects ability of lymphocytic choriomeningitis virus to persist in adult mice. JExpMed **172:**1043-1048.

20. **Salvato M, Borrow P, Shimomaye E, Oldstone MB.** 1991. Molecular basis of viral persistence: a single amino acid change in the glycoprotein of lymphocytic choriomeningitis virus is associated with suppression of the antiviral cytotoxic T-lymphocyte response and establishment of persistence. JVirol **65:**1863-1869.

21. **Heise MT, Virgin HW.** 2013. Pathogenesis of Viral Infection, p 254-285. *In* Knipe DM, Howley PM (ed), Fields Virology, 6th ed, vol One. Lippincott Williams & Wilkins, Philadelphia, PA.

22. **Heise MT, Virgin HW.** 2013. Pathogenesis of Viral Infection, p 254-285. *In* Knipe DM, Howley PM (ed), Fields Virology, 6 ed, vol 1. Lippincott, Williams, and Wilkins, Philadelphia, PA USA.

23. **DiMaio D, Fan H.** 2013. Viruses, Cell Transformation, and Cancer, p 153-188. *In* Knipe DM, Howley PM (ed), Fields Virology, 6 ed, vol 1. Lippincott Williams and Wilkins, Philadelphia, PA USA.

24. **Ernst PB, Gold BD.** 2000. The disease spectrum of Helicobacter pylori: the immunopathogenesis of gastroduodenal ulcer and gastric cancer. Annu Rev Microbiol **54:**615-640.

25. **Barton ES, White DW, Cathelyn JS, Brett-McClellan KA, Engle M, Diamond MS, Miller VL, Virgin HW.** 2007. Herpesvirus latency confers symbiotic protection from bacterial infection. Nature **447:**326-329.

26. **MacDuff DA, Reese TA, Song C, Lee JS, Zhang X, Kambal A, Duan E, Carerro J, Boisson B, Colonna M, Sibley LD, Edelson BT, Stallings C, Casanova J-L, Iwai K, Virgin HW.** 2014. Complementation of genetic immunodeficiency by chronic herpesvirus infection. eLife**:**In revision.

27. **Milbrath MO, Spicknall IH, Zelner JL, Moe CL, Eisenberg JN.** 2013. Heterogeneity in norovirus shedding duration affects community risk. Epidemiol Infect **141:**1572-1584.

28. **Graham DY, Jiang X, Tanaka T, Opekun AR, Madore HP, Estes MK.** 1994. Norwalk virus infection of volunteers: new insights based on improved assays. J Infect Dis **170:**34-43.

29. **Gallimore CI, Cubitt D, du Plessis N, Gray JJ.** 2004. Asymptomatic and symptomatic excretion of noroviruses during a hospital outbreak of gastroenteritis. J Clin Microbiol **42:**2271-2274.

30. **Murata T, Katsushima N, Mizuta K, Muraki Y, Hongo S, Matsuzaki Y.** 2007. Prolonged norovirus shedding in infants <or=6 months of age with gastroenteritis. PediatrInfectDisJ **26:**46-49.

31. **Atmar RL, Opekun AR, Gilger MA, Estes MK, Crawford SE, Neill FH, Graham DY.** 2008. Norwalk virus shedding after experimental human infection. Emerg Infect Dis **14:**1553-1557.

32. **Sukhrie FH, Siebenga JJ, Beersma MF, Koopmans M.** 2010. Chronic shedders as reservoir for nosocomial transmission of norovirus. J Clin Microbiol **48:**4303-4305.

33. **Barrabeig I, Rovira A, Buesa J, Bartolome R, Pinto R, Prellezo H, Dominguez A.** 2010. Foodborne norovirus outbreak: the role of an asymptomatic food handler. BMC Infect Dis **10:**269.

34. **Gallimore CI, Cubitt D, du Plessis N, Gray JJ.** 2004. Asymptomatic and symptomatic excretion of noroviruses during a hospital outbreak of gastroenteritis. Journal of Clinical Microbiology **42:**2271-2274.

35. **Ozawa K, Oka T, Takeda N, Hansman GS.** 2007. Norovirus infections in symptomatic and asymptomatic food handlers in Japan. J Clin Microbiol **45:**3996-4005.

36. **Schmid D, Kuo HW, Hell M, Kasper S, Lederer I, Mikula C, Springer B, Allerberger F.** 2011. Foodborne gastroenteritis outbreak in an Austrian healthcare facility caused by asymptomatic, norovirus-excreting kitchen staff. J Hosp Infect **77:**237-241.

37. **Chan CM, Chan CW, Ma CK, Chan HB.** 2011. Norovirus as cause of benign convulsion associated with gastro-enteritis. J Paediatr Child Health **47:**373-377.

38. **Stuart RL, Tan K, Mahar JE, Kirkwood CD, Andrew Ramsden C, Andrianopoulos N, Jolley D, Bawden K, Doherty R, Kotsanas D, Bradford J, Buttery JP.** 2010. An outbreak of necrotizing enterocolitis associated with norovirus genotype GII.3. Pediatr Infect Dis J **29:**644-647.

39. **Obinata K, Okumura A, Nakazawa T, Kamata A, Niizuma T, Kinoshita K, Shimizu T.** 2010. Norovirus encephalopathy in a previously healthy child. Pediatr Infect Dis J **29:**1057-1059.

40. **Medici MC, Abelli LA, Dodi I, Dettori G, Chezzi C.** 2010. Norovirus RNA in the blood of a child with gastroenteritis and convulsions--A case report. J Clin Virol **48:**147-149.

41. **Chen SY, Tsai CN, Lai MW, Chen CY, Lin KL, Lin TY, Chiu CH.** 2009. Norovirus Infection as a Cause of Diarrhea-Associated Benign Infantile Seizures. Clinical Infectious Diseases **48:**849-855.

42. **Turcios-Ruiz RM, Axelrod P, St JK, Bullitt E, Donahue J, Robinson N, Friss HE.** 2008. Outbreak of necrotizing enterocolitis caused by norovirus in a neonatal intensive care unit. J Pediatr **153:**339-344.

43. **Marshall JK, Thabane M, Borgaonkar MR, James C.** 2007. Postinfectious irritable bowel syndrome after a food-borne outbreak of acute gastroenteritis attributed to a viral pathogen. Clin GastroenterolHepatol **5:**457-460.

44. **Hsu CC, Riley LK, Wills HM, Livingston RS.** 2006. Persistent infection with and serologic cross-reactivity of three novel murine noroviruses. Comp Med **56:**247-251.

45. **Ward VK, McCormick CJ, Clarke IN, Salim O, Wobus CE, Thackray LB, Virgin HW, Lambden PR.** 2007. Recovery of infectious murine norovirus using pol II-driven expression of full-length cDNA. Proc Natl Acad Sci U S A **104:**11050-11055.

46. **Patel MM, Hall AJ, Vinje J, Parashar UD.** 2009. Noroviruses: a comprehensive review. J Clin Virol **44:**1-8.

47. **CDC.** 2016. Norovirus Worldwide, *on* Center for Disease Control. http://www.cdc.gov/norovirus/worldwide.html. Accessed 8/1.

48. **Ahmed SM, Hall AJ, Robinson AE, Verhoef L, Premkumar P, Parashar UD, Koopmans M, Lopman BA.** 2014. Global prevalence of norovirus in cases of gastroenteritis: a systematic review and meta-analysis. Lancet Infect Dis **14:**725-730.

49. **Lopman BA, Hall AJ, Curns AT, Parashar UD.** 2011. Increasing rates of gastroenteritis hospital discharges in US adults and the contribution of norovirus, 1996-2007. Clin Infect Dis **52:**466-474.

50. **Bartsch SM, Lopman BA, Ozawa S, Hall AJ, Lee BY.** 2016. Global Economic Burden of Norovirus Gastroenteritis. PLoS One **11:**e0151219.

51. **Tacket CO, Mason HS, Losonsky G, Estes MK, Levine MM, Arntzen CJ.** 2000. Human immune responses to a novel norwalk virus vaccine delivered in transgenic potatoes. JInfectDis **182:**302-305.

52. **Kocher J, Bui T, Giri-Rachman E, Wen K, Li G, Yang X, Liu F, Tan M, Xia M, Zhong W, Jiang X, Yuan L.** 2014. Intranasal P particle vaccine provided partial cross-variant protection against human GII.4 norovirus diarrhea in gnotobiotic pigs. J Virol **88:**9728-9743.

53. **Tamminen K, Lappalainen S, Huhti L, Vesikari T, Blazevic V.** 2013. Trivalent combination vaccine induces broad heterologous immune responses to norovirus and rotavirus in mice. PLoS One **8:**e70409.

54. **Ball JM, Graham DY, Opekun AR, Gilger MA, Guerrero RA, Estes MK.** 1999. Recombinant Norwalk virus-like particles given orally to volunteers: phase I study. Gastroenterology **117:**40-48.

55. **Guerrero RA, Ball JM, Krater SS, Pacheco SE, Clements JD, Estes MK.** 2001. Recombinant Norwalk virus-like particles administered intranasally to mice induce systemic and mucosal (fecal and vaginal) immune responses. JVirol **75:**9713-9722.

56. **Jiang X, Wang M, Graham DY, Estes MK.** 1992. Expression, self-assembly, and antigenicity of the Norwalk virus capsid protein. J Virol **66:**6527-6532.

57. **Tomov VT, Osborne LC, Dolfi DV, Sonnenberg GF, Monticelli LA, Mansfield K, Virgin HW, Artis D, Wherry EJ.** 2013. Persistent enteric murine norovirus infection is associated with functionally suboptimal virus-specific CD8 T cell responses. J Virol **87:**7015-7031.

58. **Baldridge MT, Nice TJ, McCune BT, Yokoyama CC, Kambal A, Wheadon M, Diamond MS, Ivanova Y, Artyomov M, Virgin HW.** 2015. Commensal microbes and interferon-λ determine persistence of enteric murine norovirus infection. Science **16:**266-269.

59. **Nice TJ, Baldridge MT, McCune BT, Norman JM, Lazear HM, Artyomov M, Diamond MS, virgin HW.** 2015. Interferon-lambda cures persistent murine norovirus infection in the absence of adaptive immunity. Science **347:**269-273.

60. **Kahan SM, Liu G, Reinhard MK, Hsu CC, Livingston RS, Karst SM.** 2011. Comparative murine norovirus studies reveal a lack of correlation between intestinal virus titers and enteric pathology. Virology **421:**202-210.

61. **Horn CC, Kimball BA, Wang H, Kaus J, Dienel S, Nagy A, Gathright GR, Yates BJ, Andrews PL.** 2013. Why can't rodents vomit? A comparative behavioral, anatomical, and physiological study. PLoS One **8:**e60537.

62. **Kane M, Golovkina T.** 2010. Common threads in persistent viral infections. J Virol **84:**4116-4123.

63. **Oldstone MB.** 2009. Anatomy of viral persistence. PLoS Pathog **5:**e1000523.

64. **Virgin HW, Wherry EJ, Ahmed R.** 2009. Redefining chronic viral infection. Cell **138:**30-50.

65. **Karst SM, Wobus CE, Lay M, Davidson J, Virgin HW.** 2003. STAT1-dependent innate immunity to a Norwalk-like virus. Science **299:**1575-1578.

66. **Chachu KA, Strong DW, LoBue AD, Wobus CE, Baric RS, Virgin HW.** 2008. Antibody is critical for the clearance of murine norovirus infection. Journal of Virology **82:**6610-6617.

67. **Chachu KA, LoBue AD, Strong DW, Baric RS, Virgin HW.** 2008. Immune mechanisms responsible for vaccination against and clearance of mucosal and lymphatic norovirus infection. PLoS Pathog **4:**e1000236.

68. **Thackray LB, Duan E, Lazear HM, Kambal A, Schreiber RD, Diamond MS, Virgin HW.** 2012. Critical role for interferon regulatory factor 3 (IRF-3) and IRF-7 in type I interferon-mediated control of murine norovirus replication. J Virol **86:**13515-13523.

69. **Hwang S, Maloney NS, Bruinsma MW, Goel G, Duan E, Zhang L, Shrestha B, Diamond MS, Dani A, Sosnovtsev SV, Green KY, Lopez-Otin C, Xavier RJ, Thackray LB, Virgin HW.** 2012. Nondegradative role of Atg5-Atg12/ Atg16L1 autophagy protein complex in antiviral activity of interferon gamma. Cell Host Microbe **11:**397-409.

70. **Maloney NS, Thackray LB, Goel G, Hwang S, Duan E, Vachharajani P, Xavier R, Virgin HW.** 2012. Essential cell-autonomous role for interferon (IFN) regulatory factor 1 in IFN-gamma-mediated inhibition of norovirus replication in macrophages. J Virol **86:**12655-12664.

71. **Lazear HM, Lancaster A, Wilkins C, Suthar MS, Huang A, Vick SC, Clepper L, Thackray L, Brassil MM, Virgin HW, Nikolich-Zugich J, Moses AV, Gale M, Jr., Fruh K, Diamond MS.** 2013. IRF-3, IRF-5, and IRF-7 Coordinately Regulate the Type I IFN Response in Myeloid Dendritic Cells Downstream of MAVS Signaling. PLoS Pathog **9:**e1003118.

72. **Nice TJ, Osborne LC, Tomov VT, Artis D, Wherry EJ, Virgin HW.** 2016. Type I Interferon Receptor Deficiency in Dendritic Cells Facilitates Systemic Murine Norovirus Persistence Despite Enhanced Adaptive Immunity. PLoS Pathog **12:**e1005684.

73. **McCartney SA, Thackray LB, Gitlin L, Gilfillan S, Virgin HW, Colonna M.** 2008. MDA-5 recognition of a murine norovirus. PLoS Pathog **4:**e1000108.

74. **Wang P, Zhu S, Yang L, Cui S, Pan W, Jackson R, Zheng Y, Rongvaux A, Sun Q, Yang G, Gao S, Lin R, You F, Flavell R, Fikrig E.** 2015. Nlrp6 regulates intestinal antiviral innate immunity. Science **350:**826-830.

75. **Rodriguez MR, Monte K, Thackray LB, Lenschow DJ.** 2014. ISG15 functions as an interferon-mediated antiviral effector early in the murine norovirus life cycle. J Virol **88:**9277-9286.

76. **Shortland A, Chettle J, Archer J, Wood K, Bailey D, Goodfellow I, Blacklaws BA, Heeney JL.** 2014. Pathology caused by persistent murine norovirus infection. J Gen Virol **95:**413-422.

77. **Bailey D, Thackray LB, Goodfellow IG.** 2008. A single amino acid substitution in the murine norovirus capsid protein is sufficient for attenuation in vivo. JVirol **82:**7725-7728.

78. **Strong DW, Thackray LB, Smith TJ, Virgin HW.** 2012. Protruding domain of capsid protein is necessary and sufficient to determine murine norovirus replication and pathogenesis in vivo. J Virol **86:**2950-2958.

79. **Karst SM, Wobus CE, Goodfellow IG, Green KY, Virgin HW.** 2014. Advances in Norovirus Biology. Cell Host Microbe **15:**668-680.

80. **Wobus CE, Karst SM, Thackray LB, Chang KO, Sosnovtsev SV, Belliot G, Krug A, Mackenzie JM, Green KY, Virgin HW.** 2004. Replication of Norovirus in cell culture reveals a tropism for dendritic cells and macrophages. PLoS Biol **2:**e432.

81. **Mumphrey SM, Changotra H, Moore TN, Heimann-Nichols ER, Wobus CE, Reilly MJ, Moghadamfalahi M, Shukla D, Karst SM.** 2007. Murine Norovirus 1 Infection Is Associated with Histopathological Changes in Immunocompetent Hosts, but Clinical Disease Is Prevented by STAT1-Dependent Interferon Responses. JVirol **81:**3251-3263.

82. **Perdue KA, Green KY, Copeland M, Barron E, Mandel M, Faucette LJ, Williams EM, Sosnovtsev SV, Elkins WR, Ward JM.** 2007. Naturally occuring murine norovirus infection in a large research institution. Journal of the American Association for Laboratory Animal Science **46:**38-44.

83. **Bok K, Parra GI, Mitra T, Abente E, Shaver CK, Boon D, Engle R, Yu C, Kapikian AZ, Sosnovtsev SV, Purcell RH, Green KY.** 2011. Chimpanzees as an animal model for human norovirus infection and vaccine development. Proc Natl Acad Sci U S A **108:**325-330.

84. **Chan MC, Ho WS, Sung JJ.** 2011. In vitro whole-virus binding of a norovirus genogroup II genotype 4 strain to cells of the lamina propria and Brunner's glands in the human duodenum. J Virol **85:**8427-8430.

85. **Jones MK, Watanabe M, Zhu S, Graves CL, Keyes LR, Grau KR, Gonzalez-Hernandez MB, Iovine NM, Wobus CE, Vinjé J, Tibbetts SA, Wallet SM, Karst SM.** 2014. Enteric bacteria promote human and mouse norovirus infection of B cells. Science **346:**755-759.

86. **Marionneau S, Ruvoen N, Moullac-Vaidye B, Clement M, Cailleau-Thomas A, Ruiz-Palacois G, Huang P, Jiang X, Le Pendu J.** 2002. Norwalk virus binds to histo-blood group antigens present on gastroduodenal epithelial cells of secretor individuals. Gastroenterology **122:**1967-1977.

87. **Lindesmith L, Moe C, Marionneau S, Ruvoen N, Jiang X, Lindblad L, Stewart P, LePendu J, Baric R.** 2003. Human susceptibility and resistance to Norwalk virus infection. NatMed **9:**548-553.

88. **Hutson AM, Airaud F, LePendu J, Estes MK, Atmar RL.** 2005. Norwalk virus infection associates with secretor status genotyped from sera. Journal of Medical Virology **77:**116-120.

89. **Larsson MM, Rydell GE, Grahn A, Rodriguez-Diaz J, Akerlind B, Hutson AM, Estes MK, Larson G, Svensson L.** 2006. Antibody prevalence and titer to norovirus (genogroup II) correlate with secretor (FUT2) but not with ABO phenotype or Lewis (FUT3) genotype. JInfectDis **194:**1422-1427.

90. **Lindesmith L, Moe C, LePendu J, Frelinger JA, Treanor J, Baric RS.** 2005. Cellular and humoral immunity following Snow Mountain virus challenge. J Virol **79:**2900-2909.

91. **Hutson AM, Atmar RL, Marcus DM, Estes MK.** 2003. Norwalk virus-like particle hemagglutination by binding to h histo-blood group antigens. J Virol **77:**405-415.

92. **Huang PW, Farkas T, Zhong WM, Thornton S, Morrow AL, Xi J.** 2005. Norovirus and histo-blood group antigens: Demonstration of a wide spectrum of strain specificities and classification of two major binding groups among multiple binding patterns. Journal of Virology **79:**6714-6722.

93. **Shirato H, Ogawa S, Ito H, Sato T, Kameyama A, Narimatsu H, Xiaofan Z, Miyamura T, Wakita T, Ishii K, Takeda N.** 2008. Noroviruses distinguish between type 1 and type 2 histo-blood group antigens for binding. J Virol **82:**10756-10767.

94. **Taube S, Perry JW, Yetming K, Patel SP, Auble H, Shu LM, Nawar HF, Lee CH, Connell TD, Shayman JA, Wobus CE.** 2009. Ganglioside-Linked Terminal Sialic Acid Moieties on Murine Macrophages Function as Attachment Receptors for Murine Noroviruses. Journal of Virology **83:**4092-4101.

95. **Taube S, Perry JW, McGreevy E, Yetming K, Perkins C, Henderson K, Wobus CE.** 2012. Murine noroviruses bind glycolipid and glycoprotein attachment receptors in a strain-dependent manner. J Virol **86:**5584-5593.

96. **Zheng DP, Ando T, Fankhauser RL, Beard RS, Glass RI, Monroe SS.** 2006. Norovirus classification and proposed strain nomenclature. Virology **346:**312-323.

97. **Vinje J.** 2015. Advances in laboratory methods for detection and typing of norovirus. J Clin Microbiol **53:**373-381.

98. **Thorne LG, Goodfellow IG.** 2014. Norovirus gene expression and replication. J Gen Virol **95:**278-291.

99. **McFadden N, Bailey D, Carrara G, Benson A, Chaudhry Y, Shortland A, Heeney J, Yarovinsky F, Simmonds P, Macdonald A, Goodfellow I.** 2011. Norovirus regulation of the innate immune response and apoptosis occurs via the product of the alternative open reading frame 4. PLoS Pathog **7:**e1002413.

100. **Le Pendu J, Ruvoen-Clouet N, Kindberg E, Svensson L.** 2006. Mendelian resistance to human norovirus infections. Semin Immunol **18:**375-386.

101. **Gerondopoulos A, Jackson T, Monaghan P, Doyle N, Roberts LO.** 2010. Murine norovirus-1 cell entry is mediated through a non-clathrin-, non-caveolae-, dynamin- and cholesterol-dependent pathway. J Gen Virol **91:**1428-1438.

102. **Perry JW, Wobus CE.** 2010. Endocytosis of murine norovirus 1 into murine macrophages is dependent on dynamin II and cholesterol. J Virol **84:**6163-6176.

103. **Shivanna V, Kim Y, Chang KO.** 2015. Ceramide formation mediated by acid sphingomyelinase facilitates endosomal escape of caliciviruses. Virology **483:**218-228.

104. **Leen EN, Sorgeloos F, Correia S, Chaudhry Y, Cannac F, Pastore C, Xu Y, Graham SC, Matthews SJ, Goodfellow IG, Curry S.** 2016. A Conserved Interaction between a C-Terminal Motif in Norovirus VPg and the HEAT-1 Domain of eIF4G Is Essential for Translation Initiation. PLoS Pathog **12:**e1005379.

105. **Chung L, Bailey D, Leen EN, Emmott EP, Chaudhry Y, Roberts LO, Curry S, Locker N, Goodfellow IG.** 2014. Norovirus translation requires an interaction between the C Terminus of the genome-linked viral protein VPg and eukaryotic translation initiation factor 4G. J Biol Chem **289:**21738-21750.

106. **Chaudhry Y, Nayak A, Bordeleau ME, Tanaka J, Pelletier J, Belsham GJ, Roberts LO, Goodfellow IG.** 2006. Caliciviruses differ in their functional requirements for eIF4F components. J Biol Chem **281:**25315-25325.

107. **Royall E, Doyle N, Abdul-Wahab A, Emmott E, Morley SJ, Goodfellow I, Roberts LO, Locker N.** 2015. Murine norovirus 1 (MNV1) replication induces translational

control of the host by regulating eIF4E activity during infection. J Biol Chem **290:**4748-4758.

108. **Sosnovtsev SV, Belliot G, Chang KO, Prikhodko VG, Thackray LB, Wobus CE, Karst SM, Virgin HW, Green KY.** 2006. Cleavage map and proteolytic processing of the murine norovirus nonstructural polyprotein in infected cells. J Virol **80:**7816-7831.

109. **Hyde JL, Sosnovtsev SV, Green KY, Wobus C, Virgin HW, Mackenzie JM.** 2009. Mouse norovirus replication is associated with virus-induced vesicle clusters originating from membranes derived from the secretory pathway. J Virol **83:**9709-9719.

110. **Hyde JL, Mackenzie JM.** 2010. Subcellular localization of the MNV-1 ORF1 proteins and their potential roles in the formation of the MNV-1 replication complex. Virology **406:**138-148.

111. **McFadden N, Arias A, Dry I, Bailey D, Witteveldt J, Evans DJ, Goodfellow I, Simmonds P.** 2013. Influence of genome-scale RNA structure disruption on the replication of murine norovirus--similar replication kinetics in cell culture but attenuation of viral fitness in vivo. Nucleic Acids Res **41:**6316-6331.

112. **Yunus MA, Lin X, Bailey D, Karakasiliotis I, Chaudhry Y, Vashist S, Zhang G, Thorne L, Kao CC, Goodfellow I.** 2015. The murine norovirus core subgenomic RNA promoter consists of a stable stem-loop that can direct accurate initiation of RNA synthesis. J Virol **89:**1218-1229.

113. **Bailey D, Karakasiliotis I, Vashist S, Chung LM, Rees J, McFadden N, Benson A, Yarovinsky F, Simmonds P, Goodfellow I.** 2010. Functional analysis of RNA structures present at the 3' extremity of the murine norovirus genome: the variable polypyrimidine tract plays a role in viral virulence. J Virol **84:**2859-2870.

114. **Simmonds P, Karakasiliotis I, Bailey D, Chaudhry Y, Evans DJ, Goodfellow IG.** 2008. Bioinformatic and functional analysis of RNA secondary structure elements among different genera of human and animal caliciviruses. NucleicAcids Res **36:**2530-2546.

115. **Fernandez-Vega V, Sosnovtsev SV, Belliot G, King AD, Mitra T, Gorbalenya A, Green KY.** 2004. Norwalk virus N-terminal nonstructural protein is associated with disassembly of the Golgi complex in transfected cells. J Virol **78:**4827-4837.

116. **Ettayebi K, Hardy ME.** 2003. Norwalk virus nonstructural protein p48 forms a complex with the SNARE regulator VAP-A and prevents cell surface expression of vesicular stomatitis virus G protein. J Virol **77:**11790-11797.

117. **Baker ES, Luckner SR, Krause KL, Lambden PR, Clarke IN, Ward VK.** 2012. Inherent structural disorder and dimerisation of murine norovirus NS1-2 protein. PLoS ONE **7:**e30534.

118. **Borin BN, Tang W, Nice TJ, McCune BT, Virgin HW, Krezel AM.** 2013. Murine norovirus protein NS1/2 aspartate to glutamate mutation, sufficient for persistence, reorients side chain of surface exposed tryptophan within a novel structured domain. Proteins doi:10.1002/prot.24484.

119. **Anantharaman V, Aravind L.** 2003. Evolutionary history, structural features and biochemical diversity of the NlpC/P60 superfamily of enzymes. GenomeBiol **4:**R11.

120. **Sers C, Emmenegger U, Husmann K, Bucher K, Andres AC, Schafer R.** 1997. Growth-inhibitory activity and downregulation of the class II tumor-suppressor gene H-rev107 in tumor cell lines and experimental tumors. J Cell Biol **136:**935-944.

121. **Sers C, Husmann K, Nazarenko I, Reich S, Wiechen K, Zhumabayeva B, Adhikari P, Schroder K, Gontarewicz A, Schafer R.** 2002. The class II tumour suppressor gene H-REV107-1 is a target of interferon-regulatory factor-1 and is involved in IFNgamma-induced cell death in human ovarian carcinoma cells. Oncogene **21:**2829-2839.

122. **Hughes PJ, Stanway G.** 2000. The 2A proteins of three diverse picornaviruses are related to each other and to the H-rev107 family of proteins involved in the control of cell proliferation. J GenVirol **81:**201-207.

123. **Johansson S, Niklasson B, Maizel J, Gorbalenya AE, Lindberg AM.** 2002. Molecular analysis of three Ljungan virus isolates reveals a new, close-to-root lineage of the Picornaviridae with a cluster of two unrelated 2A proteins. J Virol **76:**8920-8930.

124. **Seah EL, Marshall JA, Wright PJ.** 2003. Trans activity of the norovirus Camberwell proteinase and cleavage of the N-terminal protein encoded by ORF1. J Virol **77:**7150-7155.

125. **den Boon JA, Diaz A, Ahlquist P.** 2010. Cytoplasmic viral replication complexes. Cell Host Microbe **8:**77-85.

126. **Sasvari Z, Nagy PD.** 2010. Making of viral replication organelles by remodeling interior membranes. Viruses **2:**2436-2442.

127. **Belov GA, van Kuppeveld FJ.** 2012. (+)RNA viruses rewire cellular pathways to build replication organelles. Curr Opin Virol **2:**740-747.

128. **den Boon JA, Ahlquist P.** 2010. Organelle-like membrane compartmentalization of positive-strand RNA virus replication factories. Annu Rev Microbiol **64:**241-256.

129. **Belov GA, Altan-Bonnet N, Kovtunovych G, Jackson CL, Lippincott-Schwartz J, Ehrenfeld E.** 2007. Hijacking components of the cellular secretory pathway for replication of poliovirus RNA. J Virol **81:**558-567.

130. **Thorne L, Bailey D, Goodfellow I.** 2012. High-resolution functional profiling of the norovirus genome. J Virol **86:**11441-11456.

131. **Vashist S, Urena L, Gonzalez-Hernandez MB, Choi J, de Rougemont A, Rocha-Pereira J, Neyts J, Hwang S, Wobus CE, Goodfellow I.** 2015. Molecular chaperone Hsp90 is a therapeutic target for noroviruses. J Virol **89:**6352-6363.

132. **Perry JW, Ahmed M, Chang KO, Donato NJ, Showalter HD, Wobus CE.** 2012. Antiviral activity of a small molecule deubiquitinase inhibitor occurs via induction of the unfolded protein response. PLoS Pathog **8:**e1002783.

133. **Subba-Reddy CV, Goodfellow I, Kao CC.** 2011. VPg-primed RNA synthesis of norovirus RNA-dependent RNA polymerases by using a novel cell-based assay. J Virol **85:**13027-13037.

134. **Sasaki J, Taniguchi K.** 2008. Aichi virus 2A protein is involved in viral RNA replication. Journal of Virology **82:**9765-9769.

135. **Ishikawa K, Sasaki J, Taniguchi K.** 2010. Overall linkage map of the nonstructural proteins of Aichi virus. Virus Res **147:**77-84.

136. **Samuilova O, Krogerus C, Poyry T, Hyypia T.** 2004. Specific interaction between human parechovirus nonstructural 2A protein and viral RNA. J Biol Chem **279:**37822-37831.

137. **Krogerus C, Samuilova O, Poyry T, Jokitalo E, Hyypia T.** 2007. Intracellular localization and effects of individually expressed human parechovirus 1 non-structural proteins. J Gen Virol **88:**831-841.

138. **Lev S, Ben Halevy D, Peretti D, Dahan N.** 2008. The VAP protein family: from cellular functions to motor neuron disease. Trends Cell Biol **18:**282-290.

139. **Skehel PA, Martin KC, Kandel ER, Bartsch D.** 1995. A VAMP-binding protein from Aplysia required for neurotransmitter release. Science **269:**1580-1583.

140. **Weir ML, Klip A, Trimble WS.** 1998. Identification of a human homologue of the vesicle-associated membrane protein (VAMP)-associated protein of 33 kDa (VAP-33): a broadly expressed protein that binds to VAMP. Biochem J **333 (Pt 2):**247-251.

141. **Weir ML, Xie H, Klip A, Trimble WS.** 2001. VAP-A binds promiscuously to both v- and tSNAREs. Biochem Biophys Res Commun **286:**616-621.

142. **Furuita K, Jee J, Fukada H, Mishima M, Kojima C.** 2010. Electrostatic interaction between oxysterol-binding protein and VAMP-associated protein A revealed by NMR and mutagenesis studies. J Biol Chem **285:**12961-12970.

143. **Mikitova V, Levine TP.** 2012. Analysis of the key elements of FFAT-like motifs identifies new proteins that potentially bind VAP on the ER, including two AKAPs and FAPP2. PLoS One **7:**e30455.

144. **Kaiser SE, Brickner JH, Reilein AR, Fenn TD, Walter P, Brunger AT.** 2005. Structural basis of FFAT motif-mediated ER targeting. Structure **13:**1035-1045.

145. **Loewen CJ, Roy A, Levine TP.** 2003. A conserved ER targeting motif in three families of lipid binding proteins and in Opi1p binds VAP. EMBO J **22:**2025-2035.

146. **Loewen CJ, Levine TP.** 2005. A highly conserved binding site in vesicle-associated membrane protein-associated protein (VAP) for the FFAT motif of lipid-binding proteins. J Biol Chem **280:**14097-14104.

147. **Brickner JH, Walter P.** 2004. Gene recruitment of the activated INO1 locus to the nuclear membrane. PLoS Biol **2:**e342.

148. **Suzuki H, Kanekura K, Levine TP, Kohno K, Olkkonen VM, Aiso S, Matsuoka M.** 2009. ALS-linked P56S-VAPB, an aggregated loss-of-function mutant of VAPB, predisposes motor neurons to ER stress-related death by inducing aggregation of co-expressed wild-type VAPB. J Neurochem **108:**973-985.

149. **Gkogkas C, Middleton S, Kremer AM, Wardrope C, Hannah M, Gillingwater TH, Skehel P.** 2008. VAPB interacts with and modulates the activity of ATF6. Hum Mol Genet **17:**1517-1526.

150. **Ernst WL, Shome K, Wu CC, Gong X, Frizzell RA, Aridor M.** 2016. VAMP-associated Proteins (VAP) as Receptors That Couple Cystic Fibrosis Transmembrane Conductance Regulator (CFTR) Proteostasis with Lipid Homeostasis. J Biol Chem **291:**5206-5220.

151. **Larroquette F, Seto L, Gaub PL, Kamal B, Wallis D, Lariviere R, Vallee J, Robitaille R, Tsuda H.** 2015. Vapb/Amyotrophic lateral sclerosis 8 knock-in mice display slowly progressive motor behavior defects accompanying ER stress and autophagic response. Hum Mol Genet **24:**6515-6529.

152. **Baron Y, Pedrioli PG, Tyagi K, Johnson C, Wood NT, Fountaine D, Wightman M, Alexandru G.** 2014. VAPB/ALS8 interacts with FFAT-like proteins including the p97 cofactor FAF1 and the ASNA1 ATPase. BMC Biol **12:**39.

153. **Moustaqim-Barrette A, Lin YQ, Pradhan S, Neely GG, Bellen HJ, Tsuda H.** 2014. The amyotrophic lateral sclerosis 8 protein, VAP, is required for ER protein quality control. Hum Mol Genet **23:**1975-1989.

154. **Manford AG, Stefan CJ, Yuan HL, Macgurn JA, Emr SD.** 2012. ER-to-plasma membrane tethering proteins regulate cell signaling and ER morphology. Dev Cell **23:**1129-1140.

155. **Wyles JP, McMaster CR, Ridgway ND.** 2002. Vesicle-associated membrane protein-associated protein-A (VAP-A) interacts with the oxysterol-binding protein to modify export from the endoplasmic reticulum. J Biol Chem **277:**29908-29918.

156. **Kawano M, Kumagai K, Nishijima M, Hanada K.** 2006. Efficient trafficking of ceramide from the endoplasmic reticulum to the Golgi apparatus requires a VAMP-associated protein-interacting FFAT motif of CERT. J Biol Chem **281:**30279-30288.

157. **Peretti D, Dahan N, Shimoni E, Hirschberg K, Lev S.** 2008. Coordinated lipid transfer between the endoplasmic reticulum and the Golgi complex requires the VAP proteins and is essential for Golgi-mediated transport. Mol Biol Cell **19:**3871-3884.

158. **Tuuf J, Wistbacka L, Mattjus P.** 2009. The glycolipid transfer protein interacts with the vesicle-associated membrane protein-associated protein VAP-A. Biochem Biophys Res Commun **388:**395-399.

159. **Alpy F, Rousseau A, Schwab Y, Legueux F, Stoll I, Wendling C, Spiegelhalter C, Kessler P, Mathelin C, Rio MC, Levine TP, Tomasetto C.** 2013. STARD3 or STARD3NL and VAP form a novel molecular tether between late endosomes and the ER. J Cell Sci **126:**5500-5512.

160. **Kumagai K, Kawano M, Shinkai-Ouchi F, Nishijima M, Hanada K.** 2007. Interorganelle trafficking of ceramide is regulated by phosphorylation-dependent cooperativity between the PH and START domains of CERT. J Biol Chem **282:**17758-17766.

161. **Amarilio R, Ramachandran S, Sabanay H, Lev S.** 2005. Differential regulation of endoplasmic reticulum structure through VAP-Nir protein interaction. J Biol Chem **280:**5934-5944.

162. **Kentala H, Pfisterer SG, Olkkonen VM, Weber-Boyvat M.** 2015. Sterol liganding of OSBP-related proteins (ORPs) regulates the subcellular distribution of ORP-VAPA complexes and their impacts on organelle structure. Steroids **99:**248-258.

163. **Wang P, Hawkins TJ, Richardson C, Cummins I, Deeks MJ, Sparkes I, Hawes C, Hussey PJ.** 2014. The plant cytoskeleton, NET3C, and VAP27 mediate the link between the plasma membrane and endoplasmic reticulum. Curr Biol **24:**1397-1405.

164. **Stoica R, De Vos KJ, Paillusson S, Mueller S, Sancho RM, Lau KF, Vizcay-Barrena G, Lin WL, Xu YF, Lewis J, Dickson DW, Petrucelli L, Mitchell JC, Shaw CE, Miller CC.** 2014. ER-mitochondria associations are regulated by the VAPB-PTPIP51 interaction and are disrupted by ALS/FTD-associated TDP-43. Nat Commun **5:**3996.

165. **Stefan CJ, Manford AG, Baird D, Yamada-Hanff J, Mao Y, Emr SD.** 2011. Osh proteins regulate phosphoinositide metabolism at ER-plasma membrane contact sites. Cell **144:**389-401.

166. **Tu H, Gao L, Shi ST, Taylor DR, Yang T, Mircheff AK, Wen Y, Gorbalenya AE, Hwang SB, Lai MM.** 1999. Hepatitis C virus RNA polymerase and NS5A complex with a SNARE-like protein. Virology **263:**30-41.

167. **Evans MJ, Rice CM, Goff SP.** 2004. Phosphorylation of hepatitis C virus nonstructural protein 5A modulates its protein interactions and viral RNA replication. Proc Natl Acad Sci U S A **101:**13038-13043.

168. **Roulin PS, Lotzerich M, Torta F, Tanner LB, van Kuppeveld FJ, Wenk MR, Greber UF.** 2014. Rhinovirus uses a phosphatidylinositol 4-phosphate/cholesterol counter-current for the formation of replication compartments at the ER-Golgi interface. Cell Host Microbe **16:**677-690.

169. **Barajas D, Xu K, de Castro Martin IF, Sasvari Z, Brandizzi F, Risco C, Nagy PD.** 2014. Co-opted oxysterol-binding ORP and VAP proteins channel sterols to RNA virus replication sites via membrane contact sites. PLoS Pathog **10:**e1004388.

170. **Barajas D, Xu K, Sharma M, Wu CY, Nagy PD.** 2014. Tombusviruses upregulate phospholipid biosynthesis via interaction between p33 replication protein and yeast lipid sensor proteins during virus replication in yeast. Virology **471-473:**72-80.

171. **Elwell CA, Jiang S, Kim JH, Lee A, Wittmann T, Hanada K, Melancon P, Engel JN.** 2011. Chlamydia trachomatis co-opts GBF1 and CERT to acquire host sphingomyelin for distinct roles during intracellular development. PLoS Pathog **7:**e1002198.

172. **Derre I, Swiss R, Agaisse H.** 2011. The lipid transfer protein CERT interacts with the Chlamydia inclusion protein IncD and participates to ER-Chlamydia inclusion membrane contact sites. PLoS Pathog **7:**e1002092.

173. **Gao L, Aizaki H, He JW, Lai MM.** 2004. Interactions between viral nonstructural proteins and host protein hVAP-33 mediate the formation of hepatitis C virus RNA replication complex on lipid raft. J Virol **78:**3480-3488.

174. **Berger KL, Randall G.** 2009. Potential roles for cellular cofactors in hepatitis C virus replication complex formation. Commun Integr Biol **2:**471-473.

175. **Amini-Bavil-Olyaee S, Choi YJ, Lee JH, Shi M, Huang IC, Farzan M, Jung JU.** 2013. The antiviral effector IFITM3 disrupts intracellular cholesterol homeostasis to block viral entry. Cell Host Microbe **13:**452-464.

176. **Wang S, Wu X, Pan T, Song W, Wang Y, Zhang F, Yuan Z.** 2012. Viperin inhibits hepatitis C virus replication by interfering with binding of NS5A to host protein hVAP-33. J Gen Virol **93:**83-92.

177. **Helbig KJ, Eyre NS, Yip E, Narayana S, Li K, Fiches G, McCartney EM, Jangra RK, Lemon SM, Beard MR.** 2011. The antiviral protein viperin inhibits hepatitis C virus replication via interaction with nonstructural protein 5A. Hepatology **54:**1506-1517.

178. **Xu G, Xin X, Zheng C.** 2013. GPS2 is required for the association of NS5A with VAP-A and hepatitis C virus replication. PLoS One **8:**e78195.

179. **Randall G, Panis M, Cooper JD, Tellinghuisen TL, Sukhodolets KE, Pfeffer S, Landthaler M, Landgraf P, Kan S, Lindenbach BD, Chien M, Weir DB, Russo JJ, Ju J, Brownstein MJ, Sheridan R, Sander C, Zavolan M, Tuschl T, Rice CM.** 2007. Cellular cofactors affecting hepatitis C virus infection and replication. Proc Natl Acad Sci USA **104:**12884-12889.

180. **Ramage HR, Kumar GR, Verschueren E, Johnson JR, Von Dollen J, Johnson T, Newton B, Shah P, Horner J, Krogan NJ, Ott M.** 2015. A combined proteomics/genomics approach links hepatitis C virus infection with nonsense-mediated mRNA decay. Mol Cell **57:**329-340.

181. **Strating JR, van der Linden L, Albulescu L, Bigay J, Arita M, Delang L, Leyssen P, van der Schaar HM, Lanke KH, Thibaut HJ, Ulferts R, Drin G, Schlinck N,**

Wubbolts RW, Sever N, Head SA, Liu JO, Beachy PA, De Matteis MA, Shair MD, Olkkonen VM, Neyts J, van Kuppeveld FJ. 2015. Itraconazole inhibits enterovirus replication by targeting the oxysterol-binding protein. Cell Rep **10:**600-615.

182. **Aizaki H, Lee KJ, Sung VM, Ishiko H, Lai MM.** 2004. Characterization of the hepatitis C virus RNA replication complex associated with lipid rafts. Virology **324:**450-461.

183. **Shi ST, Lee KJ, Aizaki H, Hwang SB, Lai MM.** 2003. Hepatitis C virus RNA replication occurs on a detergent-resistant membrane that cofractionates with caveolin-2. J Virol **77:**4160-4168.

184. **Paul D, Hoppe S, Saher G, Krijnse-Locker J, Bartenschlager R.** 2013. Morphological and biochemical characterization of the membranous hepatitis C virus replication compartment. J Virol **87:**10612-10627.

185. **Ilnytska O, Santiana M, Hsu NY, Du WL, Chen YH, Viktorova EG, Belov G, Brinker A, Storch J, Moore C, Dixon JL, Altan-Bonnet N.** 2013. Enteroviruses harness the cellular endocytic machinery to remodel the host cell cholesterol landscape for effective viral replication. Cell Host Microbe **14:**281-293.

186. **Arita M.** 2014. Phosphatidylinositol-4 kinase III beta and oxysterol-binding protein accumulate unesterified cholesterol on poliovirus-induced membrane structure. Microbiol Immunol **58:**239-256.

187. **Dorobantu CM, Albulescu L, Harak C, Feng Q, van Kampen M, Strating JR, Gorbalenya AE, Lohmann V, van der Schaar HM, van Kuppeveld FJ.** 2015. Modulation of the Host Lipid Landscape to Promote RNA Virus Replication: The Picornavirus Encephalomyocarditis Virus Converges on the Pathway Used by Hepatitis C Virus. PLoS Pathog **11:**e1005185.

188. **Wang H, Perry JW, Lauring AS, Neddermann P, De Francesco R, Tai AW.** 2014. Oxysterol-binding protein is a phosphatidylinositol 4-kinase effector required for HCV replication membrane integrity and cholesterol trafficking. Gastroenterology **146:**1373-1385 e1371-1311.

189. **Berger KL, Cooper JD, Heaton NS, Yoon R, Oakland TE, Jordan TX, Mateu G, Grakoui A, Randall G.** 2009. Roles for endocytic trafficking and phosphatidylinositol 4-kinase III alpha in hepatitis C virus replication. Proc Natl Acad Sci U S A **106:**7577-7582.

190. **Reiss S, Rebhan I, Backes P, Romero-Brey I, Erfle H, Matula P, Kaderali L, Poenisch M, Blankenburg H, Hiet MS, Longerich T, Diehl S, Ramirez F, Balla T,**

Rohr K, Kaul A, Buhler S, Pepperkok R, Lengauer T, Albrecht M, Eils R, Schirmacher P, Lohmann V, Bartenschlager R. 2011. Recruitment and activation of a lipid kinase by hepatitis C virus NS5A is essential for integrity of the membranous replication compartment. Cell Host Microbe **9:**32-45.

1.8 Figures

A

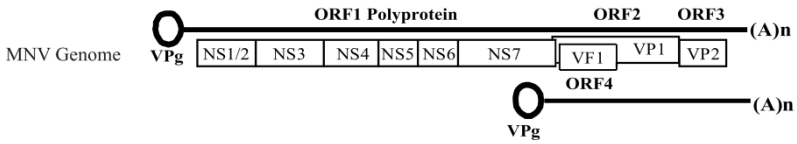

B

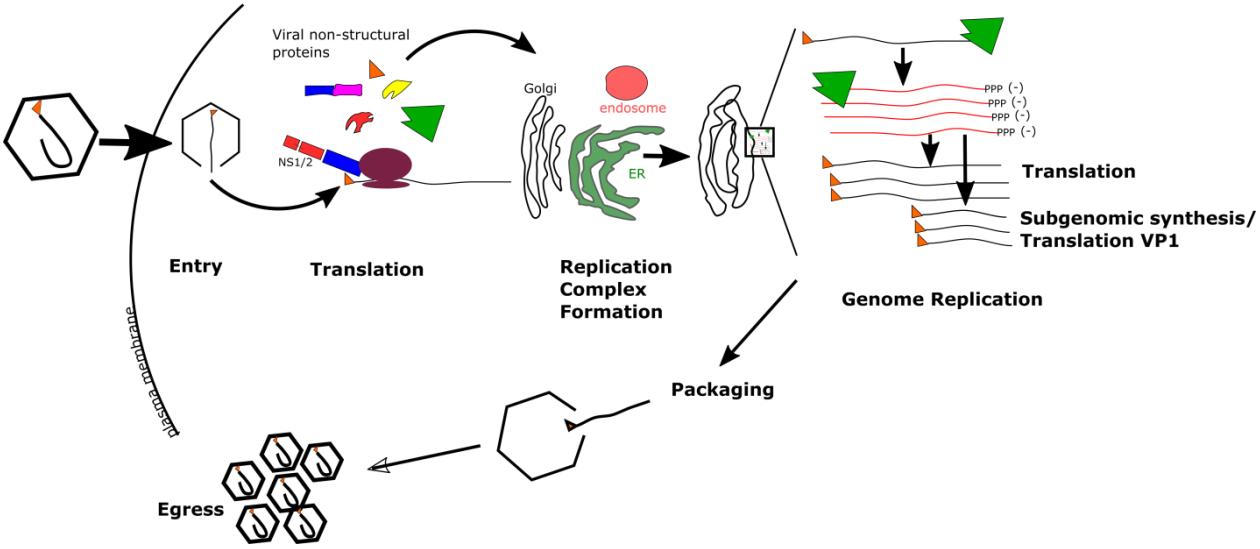

Figure 1.1. Organization of NoV genome and viral life cycle.

(A) Organization of NoV genome adapted from (14). Offset rectangles represent different Open Reading Frames (ORFs). Bolded line beneath represents subgenomic RNA, transcribed from minus strand beginning at a subgenomic promoter within NS7 coding sequence.

(B) Life cycle of NoV. Attachment is facilitated by binding carbohydrate and proteinacous receptors, followed by endocytosis. Viral genomes are released from capsid into cytoplasm where ORF1 is translated. Viral NS proteins remodel membranes to form RCs. At RCs, vRNA is copied into minus-strand, from which more vRNA is synthesized as well as sub-genomic RNAs. ORFs 2-4 are translated from sub-genomic RNAs, producing capsid proteins VP1 and VP2, as well as VF1. vRNAs are encapsidated, and virus is released through undefined mechanisms.

Chapter 2:
NS1/2 and VP1 are major murine norovirus determinants of tropism and persistence in mice

In addition to unpublished data, this chapter is adapted from:
Nice TJ, Strong DW, McCune BT, Pohl CS, Virgin HW. 2013. A Single-Amino-Acid Change in Murine Norovirus NS1/2 Is Sufficient for Colonic Tropism and Persistence. J Virol 87:327–34. DOI: 10.1128/JVI.01864-12.

2.1 Abstract

Noroviruses (NoVs) are a leading cause of epidemic gastroenteritis and a major health burden worldwide. One source for outbreaks is individuals persistently shedding virus asymptomatically. Viral persistence is a successful strategy for viruses to spread, but the mechanisms and consequences of NoV persistent infection *in vivo* are unknown. To determine the viral determinants of persistent infection and tropism, we used the murine norovirus (MNoV) model system. MNoV strains are phenotypically dimorphic for persistence; strain CR6 is persistent but CW3 is not persistent. Using plasmid infectious clones, we mapped the viral persistence determinant to the poorly understood non-structural gene NS1/2. Further, the NS1 domain of NS1/2^{CR6} was necessary and sufficient for persistence. Mutations within the NS1 domain prevented CR6 from establishing persistent infection. Strikingly, a single amino acid change, NS1/2^{D94E}, conferred persistence on CW3. NS1/2 mutants had a delay in viral release from cells in culture. Additionally, we observed persistence is restricted to replication and shedding in the intestine, and NS1/2 confers intestinal tropism. In contrast, the capsid protein VP1 conferred acute replication in the spleen. Finally, we observed CW3, but not CR6, grew rapidly in macrophages differentiated from bone marrow. This difference mapped to VP1. Therefore, persistence and intestinal tropism are conferred by NS1/2, and splenic tropism and the ability to grow in macrophages *ex vivo* is conferred by VP1. In conclusion, we mapped MNoV persistence and tropism determinants to NS1/2 and VP1. These studies highlight the strength of phenotype mapping using MNoV infectious clones.

2.2 Introduction

HNoVs are a leading cause of non-bacterial gastroenteritis, and the primary cause of epidemic gastroenteritis (reviewed in (1)). While most healthy individuals recover without complication, HNoVs cause significant morbidity and mortality among the young and old (2-8). HNoV also pose an economic burden due to lost productive work and closure of hospital wards during nosocomial outbreaks. Hospitalization costs alone are estimated to be $500 million annually in the US (9).

Multiple observations, from experimental infections to longitudinal epidemiological studies, support that HNoV can establish prolonged infections up to weeks and months (10-15). Additionally, persistent HNoV infection is frequently asymptomatic (11, 13, 15-17). This may be of epidemiological importance because asymptomatically infected individuals may serve as reservoirs for NoV in between outbreaks. Indeed, these individuals have been reported to initiate NoV outbreaks (13, 18-20).

NoV is a genus of non-enveloped, positive-sense RNA viruses within the *Caliciviridae* family. NoVs are grouped into seven clades, genogroups GI-GVII. GI, GII, and GIV cause human disease, and GV encompasses more recently discovered rodent NoVs, including MNoV (21). The NoV genome encodes nine known proteins: seven non-structural (NS) proteins derived by proteolysis of the ORF 1 polyprotein (22) and two structural proteins, VP1 and VP2 derived from ORFs 2 and 3 respectively (23). MNoV additionally encodes the virulence protein VF1 from ORF 4 (24). The host requirements for NoV replication as well as NoV pathogenesis has historically been limited by the lack of replication of HNoV in cell culture or in small animal models. Only recently has limited HNoV replication been achieved in mice or cell lines (25, 26).

As MNoV robustly replicates in mice and cells, it serves as a powerful system for functional molecular studies of NoV (23, 27).

The discovery of MNoV has greatly facilitated the study of NoV pathogenesis and replication *in vivo* and *in vitro*. The founding strain of MNoV, MNoV-1, was found during intracranial serial passaging in *Rag1/Stat1*$^{-/-}$ mice (28). It is lethal in *Stat1*$^{-/-}$ and *Ifnar*$^{-/-}$ mice, but is cleared acutely from immunocompetent mice (28, 29). However, MNoV strains subsequently isolated from feces are not lethal in immunocompromised mice (30). Furthermore, MNoV-1 does not establish persistent infection in mice, but fecal isolates predominately do persistently infect mice (30, 31). The creation of DNA-plasmid infectious clones (32) for MNoV1.CW3 and the MNoV fecal isolate CR6 aided the discovery that the viral protein VP1 determines MNoV lethality in immunocompromised mice (33, 34). However, the precise function(s) of VP1 connected to MNoV lethality has not been elucidated, nor are the MNoV genetic determinants for viral persistence known.

The N-terminal protein product in the polyprotein, NS1/2, is comprised of three domains: NS1, NS2, and a putative transmembrane (TM) domain (35). In MNoV, NS1 domain in isolation has a structured region preceded by an intrinsically disordered domain (35, 36). NS2 encodes a domain that might have enzymatic function (38). Ectopically expressed NS1/2 from GI HNoV (NS1/2^{GI}) disrupts the Golgi apparatus and vesicular trafficking (39, 40) and is reported to interact with the host protein Vamp-Associated-Protein A (VAPA) (39). The role of VAPA interactions with NS1/2 during viral replication has not been defined.

We sought to identify the viral determinants of persistent infection in mice. We found the viral gene NS1/2 from persistent MNoV strain CR6 could confer persistence on non-persistent strain CW3. Furthermore, the NS1^{CR6} domain of NS1/2 was necessary and sufficient for viral

persistence. Strikingly, a single amino change within CW3 NS1 domain, D94E, conferred persistence on CW3. The site of persistence was the gastrointestinal tract, and D94E conferred colonic replication on CW3. All viruses grew equivalently in the RAW264.7 cell line, but pCR6-NS1^{CW3} had a delay in viral release from cells. Lastly, the viral capsid protein VP1^{CW3} was associated with replication in the spleen and in primary macrophages *ex vivo*. These data extend a primary role for NS1/2 in viral persistence and roles for both NS1/2 and VP1 in viral tropism.

2.3 Results

2.3.1 MNoV strain CR6, but not CW3, is persistently shed in mice stool.

MNoV strain CR6 establishes persistent infection but CW3 does not. Using cDNA of CR6 and CW3 cloned into DNA plasmid infectious clones, we produced virus to verify plasmid-derived virus establishes persistence similar to original virus isolates. pCR6 was robustly detected in mouse stool by seven days post infection and maintained high levels of shedding as late as 70 days post infection (Figure 2.1A). pCW3 was marginally shed in stool three days post-infection, and was undetectable in stool by 14 days post infection (Figure 2.1A).

To determine what genetic elements of MNoV contribute to persistence, we generated single gene chimera between pCR6 and pCW3 (Figure 2.1B). pCW3-NS6^{CR6} did not produce virus, so we could not test this chimera for persistence (data not shown). pCW3-NS1/2^{CR6} chimera persistently shed from mice, and no other pCW3 chimera gained the ability to persist (Figure 2.1D-E). The reciprocal virus, pCR6-NS1/2^{CW3}, did not produce virus, so we could not test this mutant for the necessity of NS1/2 to establish persistence. Notably, VP1, which forms the proteinaceous exterior capsid of MNoV virions, was unrelated to persistence; pCW3-VP1^{CR6} did not persist, and pCR6-VP1^{CW3} established a persistent infection (Figure 2.1F). We concluded NS1/2^{CR6} is sufficient to confer persistence on pCW3.

2.3.2 NS1 domain is necessary and sufficient for MNoV persistence in mice.

To identify which domains contributed to persistent infection, we engineered CR6 and CW3 NS1/2 domain chimera. NS1/2 is divided into two domains, NS1 and NS2, determined by level of conservation. NS1 is poorly conserved among NoV genogroups, but NS2 is well conserved (Figure 3.8A herein). Additionally, the domains are cleaved into individual molecules

during infection, most likely at two caspase 3 cleavage sites dividing the domains (22). NS1 was sufficient to confer persistence on pCW3, but pCW3-NS2^{CR6} did not persist (Figure 2.1F). Furthermore, pCR6-NS1^{CW3} did not persist (Figure 2.1F). pCR6-NS2^{CW3} inconsistently produced virus from infectious clones, but in one experiment that did recover virus, it established persistent infection (data not shown). Therefore, the NS1^{CR6} domain is necessary and sufficient for persistence.

2.3.3 Single and combination NS1 residues are necessary and sufficient for persistence

The NS1 domains from CR6 and CW3 differ by 10 residues across 121 residues (Figure 2.2B). To map in detail which residues within NS1 contributed to persistence, we aligned the NS1 domain from persistent strains of MNoV with the non-persistent CW3. Only one residue was in common with persistent strains, E94, that differed from the CW3 residue D94 (Figure 2.2A). We introduced D94E into pCW3 and E94D into pCR6 to test the role of residue 94 in persistence. pCW3-NS1^{D94E} established persistent infection in mice (Figure 2.2C). However, pCR6-NS1^{E94D} established persistent infection, suggesting other residues contribute to persistent infection in CR6 (Figure 2.2C). To test if these other residues outside NS1 contributed to persistence in CR6, we restored D94E in non-persistent pCR6-NS1^{CW3}. pCR6-NS1$^{CW3\text{-}D94E}$ established persistent infection (Figure 2.2C).

2.3.4 Persistent and non-persistent viruses grow equivalently in cell culture, but pCR6-NS1 mutants are delayed in release from cells

To test if CW3, CR6, CW3-NS1^{D94E}, or CR6-NS1^{CW3} mutant strains replicated differently in cell lines, we infected RAW 264.7 macrophage-like cells. All viruses replicated equivalently in a single replication cycle or multiple replication cycles of growth (MOI 5 or 0.05

respectively) (Figure 2.3A). To test if all viruses are similarly released from cells, we separated cells and media at 12 hours post infection, when a complete life cycle of MNoV is completed (41). pCR6, pCW3, and pCW3-NS1^{D94E} had equivalent levels of virus in cells as supernatant, but CR6-NS1^{CW3} had lower levels of supernatant virus (Figure 2.3B). However, by 24 hours, all virus strains had equivalent levels of virus in cells or supernatant (Figure 2.3B). Therefore, the ability to persist in mice did not correlate with a virus growth advantage in a cell line. Nevertheless, a mutant NS1/2 had impaired viral release from cells.

2.3.5 VP1 and NS1/2 are determinants of tissue tropism

As pCR6 is persistently shed in stool, we reasoned the site of persistent replication is the GI tract. To determine which portion of GI tract supports persistent infection, we isolated tissues from stomach, duodenum, jejunum, ileum, cecum, proximal colon, and distal colon. We found increasing levels of MNoV genomes further down the GI tract, reaching peak levels at the proximal colon, but with low levels in the distal colon (Figure 2.4A). To assess if other tissues in mice support persistent infection, we isolated proximal colon, spleen, and mesenteric lymph nodes (MLN) infected with pCW3 or pCR6. We detected pCR6 genomes in the proximal colon and MLN from one to fourteen days post infection, but we never detected pCR6 in the spleen (Figure 2.4B). We also detected pCW3 in MLN and spleen from day three to seven, but not in the proximal colon (Figure 2.4B). However, we did not detect pCW3 genomes in any tissue by 14 days post infection (Figure 2.4B). To test if VP1 contributed to tissue tropism, we tested to which tissues pCR6-VP1^{CW3} and pCW3-VP1^{CR6} localized. We detected equivalent levels of pCR6-VP1^{CW3} and pCR6 in MLN and proximal colon seven days post infection. We also detected pCR6-VP1^{CW3} in the spleen at day 3, but not day 35 (Figure 2.4C, E). Moreover, similar to pCR6, pCR6-VP1^{CW3} replicated in the proximal colon and MLN both acutely and persistently

(Figure 2.4C, E). Like pCW3, we did not detect pCW3-VP1^{CR6} in the proximal colon. We additionally did not detect pCW3-VP1^{CR6} genomes in the spleen and reduced levels in the MLN (Figure 2.4C). Because VP1 did not govern colonic replication, and pCW3-NS1/2^{D94E} was persistently shed in stool, we wondered if NS1/2 contributed to replication in the proximal colon. We detected pCW3-NS1/2^{CR6} and pCW3-NS1/2^{D94E} genomes in the proximal colon, as well as the spleen and MLN (Figure 2.4D). Furthermore, we did not detect pCR6-NS1^{CW3} genomes in colon, spleen, or MLN. In contrast, pCR6-NS1$^{CW3\text{-}D94E}$ was robustly detected in the colon (Figure 2.4D). These results indicate the site of MNoV persistence is the GI tract. Moreover, NS1/2 and VP1 influenced tissue tropism for MNoV. VP1 dictated spread to the spleen, and NS1/2 was necessary and sufficient for colonic tropism for pCW3 and pCR6, respectively.

2.3.6 VP1 is the determinant for MNoV growth in BMDMs

The previous results mapped on a tissue level the tropism for pCW3 and pCR6. To determine the cellular tropism of pCW3 and pCR6, we tested viral growth in primary cells *ex vivo*. pCW3 grew robustly but pCR6 replicated slower in macrophages differentiated from bone marrow (i.e. bone marrow-derived macrophages (BMDMs)) (Figure 2.5A). To test if the barrier to infection for pCR6 was at viral entry, we bypassed viral entry by electroporating viral RNA from pCR6 and pCW3 into BMDMs. pCR6 and pCW3 replicated equivalently in BMDMs at 12 hours post infection, though pCR6 had diminished levels of virus at 48 hours post infection (Figure 2.5B). To identify what viral factors contributed to replication in BMDMs, we tested single gene chimera of pCW3 or pCR6. The ability to grow in BMDMs mapped to the capsid protein, VP1 (Figure 2.5C). VP1 is comprised of a shell (S) and protruding (P) domain. The protruding domain extrudes from the virion, and likely contacts putative receptors. The pCR6 expressing P^{CW3} gained the ability to grow in BMDMs (Figure 2.5C). Furthermore, pCR6-

VP1^{CW3} and pCR6-P^{CW3} replicated equivalently to CW3 at all time points, and pCW3-VP1^{CR6} replicated equivalently to pCR6 (Figure 2.5D). Therefore, VP1 is the viral determinant for growth in *ex vivo* cell type BMDMs.

2.4 Discussion

We found that the poorly studied MNoV gene NS1/2 governs enteric viral persistence. Furthermore, the NS1 domain within NS1/2 was necessary and sufficient for persistence, and a single coding change, $NS1^{D94E}$, was sufficient for pCW3 to establish persistent infection. NS1/2 also governs colonic tropism, the site of persistent infection, whereas VP1 determined splenic tropism and growth in BMDMs.

2.4.1 MNoV: a model system of enteric viral persistence.

HNoV can be shed for prolonged periods of time, which can initiate new outbreaks, thus maintaining HNoV in the population. Furthermore, astroviruses, adenoviruses, enteroviruses, and rotaviruses can all persistently infect humans (42-44). Nevertheless, MNoV is the first small animal model of viral persistence. Using this system, we identified the first genetic model of persistence. Studies using the MNoV persistence model system described herein since its original publication show the promise of MNoV to learn about viral-host interactions during persistence in the intestines (45-49).

2.4.2 NoV Tropism and Persistence

NoV persistence was associated with colonic tropism as has been reported (50, 51). Why persistence is restricted to the intestine in immunocompetent animals is unclear. A variety of mechanisms contribute to viral persistence in other models, but all viruses must escape elimination by immune responses. This is accomplished by antagonism, evasion, or antigenically shifting from innate and adaptive immune responses (52-54). For the MNoV-1 strain, adaptive and innate responses are both necessary to clear acute infection (29, 48, 55, 56). Furthermore, suboptimal intestinal innate and adaptive immune responses are associated with CR6 persistence

(47, 57, 58). These observations argue that CR6 antagonizes or evades a productive immune response. The gastrointestinal tract is a unique immunological site due to the vast abundance of the microbial flora. The microbial flora predisposes the intestine to immune regulation that CR6 may coopt to establish persistence (58).

2.4.3 NS1/2 and Persistence and Tropism

pCW3-NS1^{D94E} and pCR6-VP1^{CW3} both establish persistent infection, leading us to conclude that NS1/2 is the major viral determinant of persistence. However, additional experimentation revealed NS1/2 is sufficient only at a low viral dose (3 x 10^4 PFU). pCW3-NS1^{D94E} sporadically establishes persistence at higher doses (1x10^6 PFU), but the double mutant pCW3-NS1^{D94E}-VP1^{CR6} invariably establishes persistence at high dose (57). Furthermore, VP1^{CW3} is a determinant for IFNλ induction in mice (57). pCW3-NS1^{D94E} at high dose persists in *Ifnlr-/-*, arguing VP1^{CW3}-linked induction of IFNλ controls replication of pCW3-NS1^{D94E}. Nevertheless, pCW3 does not persist in *Ifnlr-/-* (57). This implies that VP1 and NS1/2 work in concert to avoid induction of IFNλ and replicate in the intestine, respectively, to establish persistence. Could persistent NS1/2 antagonize IFNλ? It remains unclear if NS1/2 function intersects IFNλ signaling. Nevertheless, the observation that persistently replicating pCR6 is cleared by IFNλ treatment indicates pCR6 is susceptible to IFNλ signaling, if IFNλ is produced sufficiently (57). However, pCR6-VP1^{CW3} persists and induces IFNλ (57). Therefore, evasion of IFNλ expression is not the sole correlate of MNoV persistence. In conclusion, unless it is true that NS1/2^{CR6} antagonizes IFNλ function, another viral gene within CR6 contributes to persistence by evading IFNλ. Should NS1/2^{CR6} antagonize IFNλ, why isn't pCW3-NS1^{D94E} sufficient to persist at high dose? Perhaps NS1^{D94E} does not have the full potency of activity as NS1^{CR6}. Experiments elucidating the specific cells inducing and responding to IFNλ, the

mechanism of VP1^{CW3} induction of IFNλ, IFNλ ISGs that are antiviral against MNoV, the function of the NS1 domain, and MNoV tropism will be needed to fully answer these questions.

Clues for how NS1/2 functions in persistence may be found from studies in cell lines. NS1/2 is associated with replication complexes (59, 60) and disrupts intracellular membrane trafficking (39). Furthermore, the NS1 domains from persistent variants of NS1/2, CR6 and D94E, differ structurally from non-persistent CW3 (36). Lastly, the NS2 domain contains a predicted permutated NlpC/p60 fold that among closely related sequences modifies lipids (38, 61-64). Therefore, it is possible that *in vivo* persistence is linked to the function of NS1/2 in infected cells to modify lipids or membranes. We did observe a delay of viral release from cells for pCR6-NS1^{CW3}, though it was unclear how this virus grew equivalently in a multi-step growth curve. How MNoV virions are released from cells is poorly understood, so the viral and host factors that contribute to viral egress are unknown. The observation that NS1/2 mutants impair accumulation of virus in media is the first example of a NoV protein involved in viral egress. It is possible earlier events are dysfunctional but are only revealed by impaired release. More evidence is needed to establish a role for NS1/2 in viral egress, if viral egress is related to persistence, and finally, a molecular mechanism for the role of NS1/2 in MNoV persistence.

2.4.4 VP1 and tropism

NoV tropism is incompletely understood (27). MNoV-1 non-structural proteins were detected in macrophages in *Stat1-/-* mice (41). Subsequently MNoV-1 has been cultured in primary macrophages and macrophage-like cell lines RAW264.7 and BV2 cells. Evidence for replication in intestinal epithelial cells is currently lacking, though other gastrointestinal viruses replicate predominately in these cells. More recently, both MNoV and HNoV are reported to

replicate in B cells (65, 66), but the definitive cells *in vivo* that support persistent viral replication are yet unknown.

Among many phenotypic differences in mice (30, 34, 45), CR6 and CW3 replicate in different tissues in mice, and this is partially governed by VP1 (51). This argues either these strains have different cellular tropism, different tissue entry portals, and/or are trafficked differently. The observation that CR6 and CW3 replicate differently in BMDMs argues cellular tropism may be a major factor for tissue tropism. Direct detection of virus *in situ* has been problematic in WT mice. Therefore, further studies looking at MNoV growth in different macrophage or dendritic cell subsets will be critical to connect a role for VP1 determining cellular tropism *in vivo*. This will be important to mechanistically associate *in vivo* phenotypic differences between CR6 and CW3 to replication in different cell types. Identifying VP1 residues that correlate with cell tropism, then correlating these residues with *in vivo* phenotypes will be a powerful method to approach this question.

Electroporated vRNA from pCR6 and pCW3 produced equivalent levels of virus at 12 hours post infection, arguing the block for CR6 replication is at entry. However, CR6 had diminished levels of virus later in infection. Either CR6 replicates less robustly over time, or existing virus degrades over time. This may occur from a process intrinsic to CR6 or a degradative process in BMDMs that CR6 is uniquely susceptible to. It will be important to elucidate if this process is dependent on VP1 because it would provide evidence that VP1 functions at a role downstream of entry to enhance viral growth in BMDMs.

2.5 Materials and Methods

2.5.1 Cells and Media

293T and RAW264.7 cells were maintained in DMEM with 10% FBS, 1% Pen/Strep, 2mM L-Glutamine, and 10mM HEPES. To generate bone marrow derived macrophages (BMDM), mouse bone marrows were isolated and cultured on non-tissue-culture treated plate for seven days in BMDM media (Dulbecco's Modified Eagle Medium, 10% fetal bovine serum, 5% horse serum, 10% CMG14-12 (67), 1x MEM nonessential amino acids, 1mM sodium pyruvate, 2 mM L-glutamine). At day 7, adherent BMDMs were dissociated from the plate and frozen in fetal bovine serum with 10% DMSO. Cells were thawed and incubated three days when they were detached and plated at $1x10^5$ cells/24-well plate, and infected the next day for MNoV analysis.

2.5.2 Cloning

Cloning mutant MNoV done by site-directed mutagenesis using Phusion high-fidelity polymerase (New England BioLabs). Virus-encoding region of plasmids were fully Sanger-sequenced prior to producing virus.

2.5.3 MNoV

Viral stocks. Stocks were generated as described (37). Briefly, infectious clones were transfected (Transit-LT1 (Mirus)) into 293T cells. 48 hours post transfection, plates were frozen and thawed to liberate virus (passage zero), centrifuged, and supernatants were inoculated onto RAW264.7 cells. 48 hours post infection (HPI), RAW264.7 cells were frozen, thawed, centrifuged, and supernatants were titered (passage one). Virus was further passaged on RAW264.7 cells at an MOI 0.01 PFU/cell, and clarified supernatant was ultracentrifuged at

30000 RPM for 3h. Pellets were resuspended in DMEM with 10% FBS and triply titered, constituting a passage two working stock of virus.

Viability of mutant infectious clones. MNoV infectious clones with novel mutations were transfected as above, and frozen at 48 HPT. Virus titer was assessed using plaque assay.

Virus infections. $5x10^4$ cells were seeded into each well of a 24 well plate the night before infection. MNoV was inoculated at indicated MOI onto cells in 200 µl final volume for 30m on ice, then subsequently washed three times with complete media. 500 µl pre-warmed complete media was added back, immediately frozen for time 0, or incubated for the indicated time.

Plaque assay. RAW264.7 cells were plated at $3x10^6$ cells/well in six well plates the night before the assay. Freeze-thawed samples were serially diluted on the day of the assay. 500µl of each dilution was inoculated onto RAW264.7 cell monolayers and rocked for one hour at room temperature. Inoculum was aspirated and cells were overlaid with methylcellulose media (MEM, 10%FBS, 1% Pen/Strep, 2mM L-Glutamine, and 10mM HEPES). When plaques resolved in 2-3 days, overlay was aspirated and replaced with 0.01% Crystal violet in 20% ethanol for greater than 1hr. Fixed monolayers were rinsed with water, dried, and plaques were counted.

2.5.4 Mice and infections.

C57BL/6J mice (stock number 000664) were purchased from Jackson Laboratories (Bar Harbor, ME) and housed at Washington University School of Medicine under specific-pathogen-free conditions (45) according to university guidelines. Cages of male or female mice were inoculated with virus at 6 to 8 weeks of age by the oral route in a volume of 25 to 35 µl. A dose of $3x10^4$ PFU was used for all experiments, with one exception ($1x10^6$ PFU; see Fig. 2.5E). Stool and tissues were harvested into 2-ml tubes (Sarstedt, Germany) with 1-mm diameter

zirconia/silica beads (Biospec, Bartlesville, OK). Tissues were flash frozen in a bath of ethanol and dry ice and either processed on the same day or stored at-80°C.

2.5.5 Quantitative reverse transcription-PCR.

RNA from stool was isolated using either an RNeasy Miniprep (Qiagen, Valencia, CA) or Quick-RNA Miniprep (Zymoresearch, Irvine, CA) kit. RNA from tissues was isolated using TRIzol (Life Technologies, Carlsbad, CA) according to the manufacturer's protocol. Five µl of RNA from stool or 1 µg of RNA from tissue was used as a template for cDNA synthesis with the ImPromII reverse transcriptase system (Promega, Madison, WI). When evident in the melting curve analysis, DNA contamination was removed using the DNAfree kit (Life Technologies). MNoV TaqMan was performed as described previously (68). MNoV genome quantities from tissue samples were normalized to the house- keeping gene of ribosomal protein S29 (RPS29). SYBR green quantitative PCR for RPS29 was performed with the forward primer 5'-AGCAGCTC TACTGGAGTCACC-3' and reverse primer 5'-AGGTCGCTTAGTCCAACTTAATG-3' at a concentration of 0.2 µM in 1x Power SYBR green master mix (Life Technologies). Cycling parameters were identical to those for MNoV TaqMan with the exception of an additional melting curve analysis.

2.5.6 Statistics and Software

All statistics were calculated using Graphpad Prism software. ns = $p>0.05$, *= $p\leq0.05$, **= $p\leq0.01$, ***= $p\leq0.001$, ****= $p\leq0.0001$, all error bars signify standard error mean. Sequence alignments and analysis were performed in Geneious 9.1 (69).

2.6 Acknowledgements

At the time this work was completed, the work was supported by National Institutes of Health (NIH) grants to H.W.V. (AI0544483 and AI084887). T.J.N. was supported by an NIH training grant (5T32A100716334) and postdoctoral fellowships from the Cancer Research Institute and American Cancer Society. Washington University and H.W.V. receive income based on licenses for MNV technology. We thank members of the Virgin laboratory for their comments on the manuscript, P. Vachharajani for technical support, and D. Kreamalmeyer for managing mouse colonies

2.7 References

1. **Patel MM, Hall AJ, Vinje J, Parashar UD.** 2009. Noroviruses: a comprehensive review. J Clin Virol **44:**1-8.

2. **Chan CM, Chan CW, Ma CK, Chan HB.** 2011. Norovirus as cause of benign convulsion associated with gastro-enteritis. J Paediatr Child Health **47:**373-377.

3. **Stuart RL, Tan K, Mahar JE, Kirkwood CD, Andrew Ramsden C, Andrianopoulos N, Jolley D, Bawden K, Doherty R, Kotsanas D, Bradford J, Buttery JP.** 2010. An outbreak of necrotizing enterocolitis associated with norovirus genotype GII.3. Pediatr Infect Dis J **29:**644-647.

4. **Obinata K, Okumura A, Nakazawa T, Kamata A, Niizuma T, Kinoshita K, Shimizu T.** 2010. Norovirus encephalopathy in a previously healthy child. Pediatr Infect Dis J **29:**1057-1059.

5. **Medici MC, Abelli LA, Dodi I, Dettori G, Chezzi C.** 2010. Norovirus RNA in the blood of a child with gastroenteritis and convulsions--A case report. J Clin Virol **48:**147-149.

6. **Chen SY, Tsai CN, Lai MW, Chen CY, Lin KL, Lin TY, Chiu CH.** 2009. Norovirus Infection as a Cause of Diarrhea-Associated Benign Infantile Seizures. Clinical Infectious Diseases **48:**849-855.

7. **Turcios-Ruiz RM, Axelrod P, St JK, Bullitt E, Donahue J, Robinson N, Friss HE.** 2008. Outbreak of necrotizing enterocolitis caused by norovirus in a neonatal intensive care unit. J Pediatr **153:**339-344.

8. **Marshall JK, Thabane M, Borgaonkar MR, James C.** 2007. Postinfectious irritable bowel syndrome after a food-borne outbreak of acute gastroenteritis attributed to a viral pathogen. Clin GastroenterolHepatol **5:**457-460.

9. **Lopman BA, Hall AJ, Curns AT, Parashar UD.** 2011. Increasing rates of gastroenteritis hospital discharges in US adults and the contribution of norovirus, 1996-2007. Clin Infect Dis **52:**466-474.

10. **Milbrath MO, Spicknall IH, Zelner JL, Moe CL, Eisenberg JN.** 2013. Heterogeneity in norovirus shedding duration affects community risk. Epidemiol Infect **141:**1572-1584.

11. **Atmar RL, Opekun AR, Gilger MA, Estes MK, Crawford SE, Neill FH, Graham DY.** 2008. Norwalk virus shedding after experimental human infection. Emerg Infect Dis **14:**1553-1557.

12. **Gallimore CI, Lewis D, Taylor C, Cant A, Gennery A, Gray JJ.** 2004. Chronic excretion of a norovirus in a child with cartilage hair hypoplasia (CHH). Journal of Clinical Virology **30:**196-204.

13. **Gallimore CI, Cubitt D, du Plessis N, Gray JJ.** 2004. Asymptomatic and symptomatic excretion of noroviruses during a hospital outbreak of gastroenteritis. Journal of Clinical Microbiology **42:**2271-2274.

14. **Rockx B, de Wit M, Vennema H, Vinje J, De Bruin E, van Duynhoven Y, Koopmans M.** 2002. Natural history of human calicivirus infection: a prospective cohort study. Clin InfectDis **35:**246-253.

15. **Murata T, Katsushima N, Mizuta K, Muraki Y, Hongo S, Matsuzaki Y.** 2007. Prolonged norovirus shedding in infants <or=6 months of age with gastroenteritis. PediatrInfectDisJ **26:**46-49.

16. **Graham DY, Jiang X, Tanaka T, Opekun AR, Madore HP, Estes MK.** 1994. Norwalk virus infection of volunteers: new insights based on improved assays. JInfectDis **170:**34-43.

17. **Sukhrie FH, Siebenga JJ, Beersma MF, Koopmans M.** 2010. Chronic shedders as reservoir for nosocomial transmission of norovirus. J Clin Microbiol **48:**4303-4305.

18. **Barrabeig I, Rovira A, Buesa J, Bartolome R, Pinto R, Prellezo H, Dominguez A.** 2010. Foodborne norovirus outbreak: the role of an asymptomatic food handler. BMC Infect Dis **10:**269.

19. **Ozawa K, Oka T, Takeda N, Hansman GS.** 2007. Norovirus infections in symptomatic and asymptomatic food handlers in Japan. J Clin Microbiol **45:**3996-4005.

20. **Schmid D, Kuo HW, Hell M, Kasper S, Lederer I, Mikula C, Springer B, Allerberger F.** 2011. Foodborne gastroenteritis outbreak in an Austrian healthcare facility caused by asymptomatic, norovirus-excreting kitchen staff. J Hosp Infect **77:**237-241.

21. **Zheng DP, Ando T, Fankhauser RL, Beard RS, Glass RI, Monroe SS.** 2006. Norovirus classification and proposed strain nomenclature. Virology **346:**312-323.

22. **Sosnovtsev SV, Belliot G, Chang KO, Prikhodko VG, Thackray LB, Wobus CE, Karst SM, Virgin HW, Green KY.** 2006. Cleavage map and proteolytic processing of the murine norovirus nonstructural polyprotein in infected cells. J Virol **80:**7816-7831.

23. **Thorne LG, Goodfellow IG.** 2014. Norovirus gene expression and replication. J Gen Virol **95:**278-291.

24. **McFadden N, Bailey D, Carrara G, Benson A, Chaudhry Y, Shortland A, Heeney J, Yarovinsky F, Simmonds P, Macdonald A, Goodfellow I.** 2011. Norovirus regulation of the innate immune response and apoptosis occurs via the product of the alternative open reading frame 4. PLoS Pathog **7:**e1002413.

25. **Taube S, Kolawole AO, Hohne M, Wilkinson JE, Handley SA, Perry JW, Thackray LB, Akkina R, Wobus CE.** 2013. A mouse model for human norovirus. MBio **4**.

26. **Jones MK, Watanabe M, Zhu S, Graves CL, Keyes LR, Grau KR, Gonzalez-Hernandez MB, Iovine NM, Wobus CE, Vinje J, Tibbetts SA, Wallet SM, Karst SM.** 2014. Enteric bacteria promote human and mouse norovirus infection of B cells. Science **346:**755-759.

27. **Karst SM, Wobus CE, Goodfellow IG, Green KY, Virgin HW.** 2014. Advances in Norovirus Biology. Cell Host Microbe **15:**668-680.

28. **Karst SM, Wobus CE, Lay M, Davidson J, Virgin HW.** 2003. STAT1-dependent innate immunity to a Norwalk-like virus. Science **299:**1575-1578.

29. **Thackray LB, Duan E, Lazear HM, Kambal A, Schreiber RD, Diamond MS, Virgin HW.** 2012. Critical role for interferon regulatory factor 3 (IRF-3) and IRF-7 in type I interferon-mediated control of murine norovirus replication. J Virol **86:**13515-13523.

30. **Thackray LB, Wobus CE, Chachu KA, Liu B, Alegre ER, Henderson KS, Kelley ST, Virgin HW.** 2007. Murine noroviruses comprising a single genogroup exhibit biological diversity despite limited sequence divergence. J Virol **81:**10460-10473.

31. **Hsu CC, Riley LK, Wills HM, Livingston RS.** 2006. Persistent infection with and serologic cross-reactivity of three novel murine noroviruses. Comp Med **56:**247-251.

32. **Ward VK, McCormick CJ, Clarke IN, Salim O, Wobus CE, Thackray LB, Virgin HW, Lambden PR.** 2007. Recovery of infectious murine norovirus using pol II-driven expression of full-length cDNA. Proc Natl Acad Sci U S A **104:**11050-11055.

33. **Bailey D, Thackray LB, Goodfellow IG.** 2008. A single amino acid substitution in the murine norovirus capsid protein is sufficient for attenuation in vivo. JVirol **82:**7725-7728.

34. **Strong DW, Thackray LB, Smith TJ, Virgin HW.** 2012. Protruding domain of capsid protein is necessary and sufficient to determine murine norovirus replication and pathogenesis in vivo. J Virol **86:**2950-2958.

35. **Baker ES, Luckner SR, Krause KL, Lambden PR, Clarke IN, Ward VK.** 2012. Inherent structural disorder and dimerisation of murine norovirus NS1-2 protein. PLoS ONE **7:**e30534.

36. **Borin BN, Tang W, Nice TJ, McCune BT, Virgin HW, Krezel AM.** 2013. Murine norovirus protein NS1/2 aspartate to glutamate mutation, sufficient for persistence, reorients side chain of surface exposed tryptophan within a novel structured domain. Proteins doi:10.1002/prot.24484.

37. **Nice TJ, Strong DW, McCune BT, Pohl CS, Virgin HW.** 2013. A single-amino-acid change in murine norovirus NS1/2 is sufficient for colonic tropism and persistence. J Virol **87:**327-334.

38. **Anantharaman V, Aravind L.** 2003. Evolutionary history, structural features and biochemical diversity of the NlpC/P60 superfamily of enzymes. GenomeBiol **4:**R11.

39. **Ettayebi K, Hardy ME.** 2003. Norwalk virus nonstructural protein p48 forms a complex with the SNARE regulator VAP-A and prevents cell surface expression of vesicular stomatitis virus G protein. J Virol **77:**11790-11797.

40. **Fernandez-Vega V, Sosnovtsev SV, Belliot G, King AD, Mitra T, Gorbalenya A, Green KY.** 2004. Norwalk virus N-terminal nonstructural protein is associated with disassembly of the Golgi complex in transfected cells. J Virol **78:**4827-4837.

41. **Wobus CE, Karst SM, Thackray LB, Chang KO, Sosnovtsev SV, Belliot G, Krug A, Mackenzie JM, Green KY, Virgin HW.** 2004. Replication of Norovirus in cell culture reveals a tropism for dendritic cells and macrophages. PLoS Biol **2:**e432.

42. **Cinek O, Witso E, Jeansson S, Rasmussen T, Drevinek P, Wetlesen T, Vavrinec J, Grinde B, Ronningen KS.** 2006. Longitudinal observation of enterovirus and adenovirus in stool samples from Norwegian infants with the highest genetic risk of type 1 diabetes. J Clin Virol **35:**33-40.

43. **Maldonado Y, Cantwell M, Old M, Hill D, Sanchez ML, Logan L, Millan-Velasco F, Valdespino JL, Sepulveda J, Matsui S.** 1998. Population-based prevalence of

symptomatic and asymptomatic astrovirus infection in rural Mayan infants. J Infect Dis **178:**334-339.

44. **Phillips G, Lopman B, Rodrigues LC, Tam CC.** 2010. Asymptomatic rotavirus infections in England: prevalence, characteristics, and risk factors. Am J Epidemiol **171:**1023-1030.

45. **Cadwell K, Patel KK, Maloney NS, Liu TC, Ng AC, Storer CE, Head RD, Xavier R, Stappenbeck TS, Virgin HW.** 2010. Virus-plus-susceptibility gene interaction determines Crohn's disease gene Atg16L1 phenotypes in intestine. Cell **141:**1135-1145.

46. **Kernbauer E, Ding Y, Cadwell K.** 2014. An enteric virus can replace the beneficial function of commensal bacteria. Nature **516:**94-98.

47. **Tomov VT, Osborne LC, Dolfi DV, Sonnenberg GF, Monticelli LA, Mansfield K, Virgin HW, Artis D, Wherry EJ.** 2013. Persistent enteric murine norovirus infection is associated with functionally suboptimal virus-specific CD8 T cell responses. J Virol **87:**7015-7031.

48. **Nice TJ, Osborne LC, Tomov VT, Artis D, Wherry EJ, Virgin HW.** 2016. Type I Interferon Receptor Deficiency in Dendritic Cells Facilitates Systemic Murine Norovirus Persistence Despite Enhanced Adaptive Immunity. PLoS Pathog **12:**e1005684.

49. **Osborne LC, Monticelli LA, Nice TJ, Sutherland TE, Siracusa MC, Hepworth MR, Tomov VT, Kobuley D, Tran SV, Bittinger K, A.G. B, Laughlin AL, Boucher JL, Wherry EJ, Bushman FD, Allen JE, Virgin HW, Artis D.** 2014. Coinfection. Virus-helminth coinfection reveals a microbiota-independent mechanism of immunomodulation. Science **345:**578-582.

50. **Arias A, Bailey D, Chaudhry Y, Goodfellow I.** 2012. Development of a reverse-genetics system for murine norovirus 3: long-term persistence occurs in the caecum and colon. J Gen Virol **93:**1432-1441.

51. **Taube S, Perry JW, McGreevy E, Yetming K, Perkins C, Henderson K, Wobus CE.** 2012. Murine noroviruses bind glycolipid and glycoprotein attachment receptors in a strain-dependent manner. J Virol **86:**5584-5593.

52. **Kane M, Golovkina T.** 2010. Common threads in persistent viral infections. J Virol **84:**4116-4123.

53. **Oldstone MB.** 2009. Anatomy of viral persistence. PLoS Pathog **5:**e1000523.

54. **Virgin HW, Wherry EJ, Ahmed R.** 2009. Redefining chronic viral infection. Cell **138:**30-50.

55. **Chachu KA, Strong DW, LoBue AD, Wobus CE, Baric RS, Virgin HW.** 2008. Antibody is critical for the clearance of murine norovirus infection. Journal of Virology **82:**6610-6617.

56. **Chachu KA, LoBue AD, Strong DW, Baric RS, Virgin HW.** 2008. Immune mechanisms responsible for vaccination against and clearance of mucosal and lymphatic norovirus infection. PLoS Pathog **4:**e1000236.

57. **Nice TJ, Baldridge MT, McCune BT, Norman JM, Lazear HM, Artyomov M, Diamond MS, virgin HW.** 2015. Interferon-lambda cures persistent murine norovirus infection in the absence of adaptive immunity. Science **347:**269-273.

58. **Baldridge MT, Nice TJ, McCune BT, Yokoyama CC, Kambal A, Wheadon M, Diamond MS, Ivanova Y, Artyomov M, Virgin HW.** 2015. Commensal microbes and interferon-λ determine persistence of enteric murine norovirus infection. Science **16:**266-269.

59. **Hyde JL, Sosnovtsev SV, Green KY, Wobus C, Virgin HW, Mackenzie JM.** 2009. Mouse norovirus replication is associated with virus-induced vesicle clusters originating from membranes derived from the secretory pathway. J Virol **83:**9709-9719.

60. **Hyde JL, Mackenzie JM.** 2010. Subcellular localization of the MNV-1 ORF1 proteins and their potential roles in the formation of the MNV-1 replication complex. Virology **406:**138-148.

61. **Golczak M, Kiser PD, Sears AE, Lodowski DT, Blaner WS, Palczewski K.** 2012. Structural basis for the acyltransferase activity of lecithin:retinol acyltransferase-like proteins. J Biol Chem **287:**23790-23807.

62. **Ren X, Lin J, Jin C, Xia B.** 2010. Solution structure of the N-terminal catalytic domain of human H-REV107--a novel circular permutated NlpC/P60 domain. FEBS Lett **584:**4222-4226.

63. **Senkevich TG, Wyatt LS, Weisberg AS, Koonin EV, Moss B.** 2008. A conserved poxvirus NlpC/P60 superfamily protein contributes to vaccinia virus virulence in mice but not to replication in cell culture. Virology **374:**506-514.

64. **Xu Q, Rawlings ND, Chiu HJ, Jaroszewski L, Klock HE, Knuth MW, Miller MD, Elsliger MA, Deacon AM, Godzik A, Lesley SA, Wilson IA.** 2011. Structural analysis

of papain-like NlpC/P60 superfamily enzymes with a circularly permuted topology reveals potential lipid binding sites. PLoS ONE **6:**e22013.

65. **Jones MK, Watanabe M, Zhu S, Graves CL, Keyes LR, Grau KR, Gonzalez-Hernandez MB, Iovine NM, Wobus CE, Vinjé J, Tibbetts SA, Wallet SM, Karst SM.** 2014. Enteric bacteria promote human and mouse norovirus infection of B cells. Science **346:**755-759.

66. **Zhu S, Jones MK, Hickman D, Han S, Reeves W, Karst SM.** 2016. Norovirus antagonism of B-cell antigen presentation results in impaired control of acute infection. Mucosal Immunol doi:10.1038/mi.2016.15.

67. **Takeshita S, Kaji K, Kudo A.** 2000. Identification and characterization of the new osteoclast progenitor with macrophage phenotypes being able to differentiate into mature osteoclasts. J Bone Miner Res **15:**1477-1488.

68. **Baert L, Wobus CE, Van Coillie E, Thackray LB, Debevere J, Uyttendaele M.** 2008. Detection of murine norovirus 1 by using plaque assay, transfection assay, and real-time reverse transcription-PCR before and after heat exposure. Appl Environ Microbiol **74:**543-546.

69. **Kearse M, Moir R, Wilson A, Stones-Havas S, Cheung M, Sturrock S, Buxton S, Cooper A, Markowitz S, Duran C, Thierer T, Ashton B, Meintjes P, Drummond A.** 2012. Geneious Basic: an integrated and extendable desktop software platform for the organization and analysis of sequence data. Bioinformatics **28:**1647-1649.

2.8 Figures

A

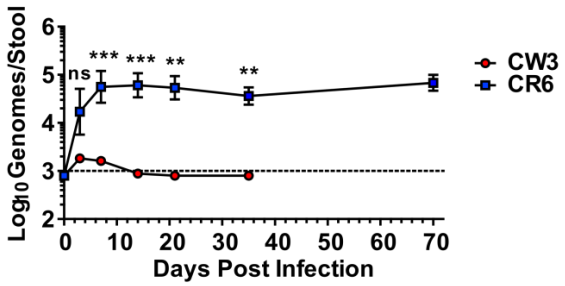
Log10 Genomes/Stool
Days Post Infection
ns
***
***
**
**
CW3
CR6

B

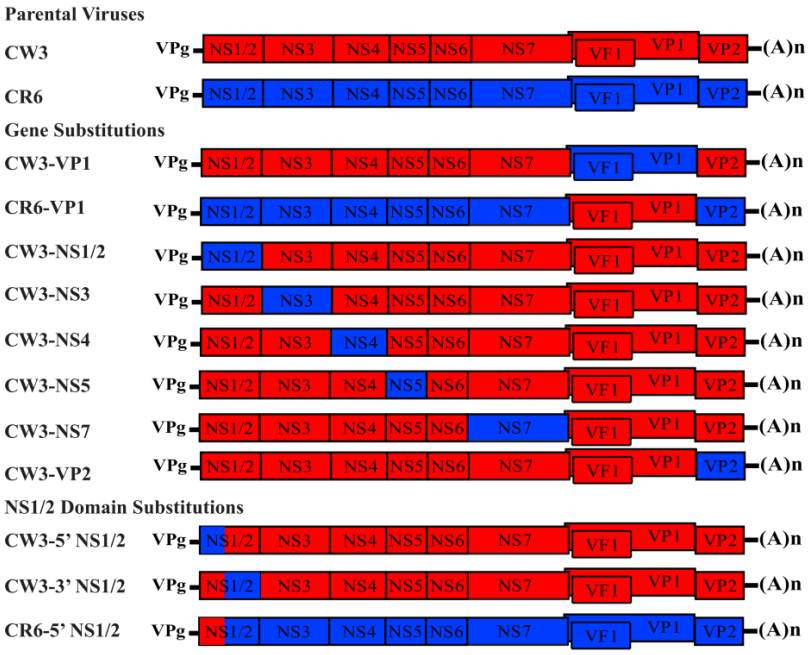
Parental Viruses
CW3
CR6
Gene Substitutions
CW3-VP1
CR6-VP1
CW3-NS1/2
CW3-NS3
CW3-NS4
CW3-NS5
CW3-NS7
CW3-VP2
NS1/2 Domain Substitutions
CW3-5' NS1/2
CW3-3' NS1/2
CR6-5' NS1/2
VPg
NS1/2
NS3
NS4
NS5
NS6
NS7
VF1
VP1
VP2
(A)n

C

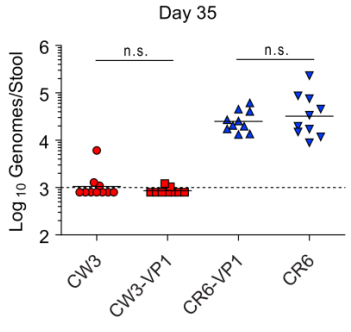
Day 35
Log 10 Genomes/Stool
n.s.
n.s.
CW3
CW3-VP1
CR6-VP1
CR6

D

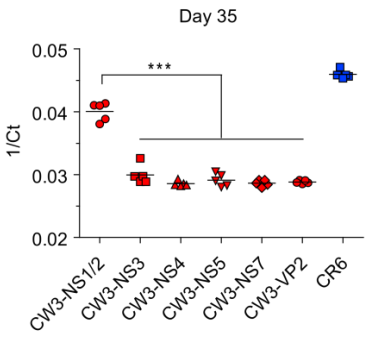
Day 35
1/Ct
***
CW3-NS1/2
CW3-NS3
CW3-NS4
CW3-NS5
CW3-NS7
CW3-VP2
CR6

E

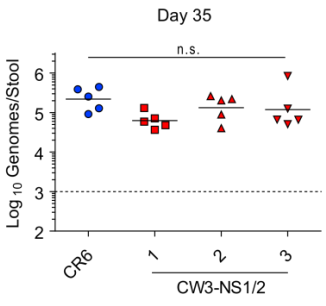
Day 35
Log 10 Genomes/Stool
n.s.
CR6
1
2
3
CW3-NS1/2

F

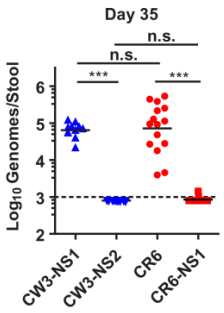
Day 35
Log10 Genomes/Stool
n.s.
n.s.
***
***
CW3-NS1
CW3-NS2
CR6
CR6-NS1

Figure 2.1. NS1^{CR6} domain is necessary and sufficient for MNoV persistence.

(A) Plasmid-derived pCR6 is persistently shed from stool but pCW3 is not persistently shed. Mice were infected $3x10^4$ PFU, stools collected at indicated time point, RNA was isolated from stool, and quantitative-RT-PCR for MNoV genomes was performed. Two-way ANOVA, Bonferroni's post-test. $n \geq 4$ for each time point.

(B) Schematic of MNoV gene chimera for pCW3 and pCR6 used in this study. Red and blue indicate CR6 and CW3 sequences, respectively.

(C) Mice were infected with indicated MNoV strains, stool collected 35 days post-infection, and MNoV genomes quantitated as in (A) . One-way ANOVA, Tukey's post-test.

(D) Single gene chimera were screened for their ability to establish persistent infection as in (B). 1/Ct indicates inverse of threshold cycle and indicates relative quantity of MNoV genomes/stool.

(E) Mice were infected with three independent preparations of pCW3-NS1/2^{CR6}, and MNoV genomes were quantitated in stool at 35 days post-infection.

(F) Comparison of MNoV genome shedding in stool for NS1/2 domain chimera during persistent infection. One-way ANOVA, Tukey's post-test.

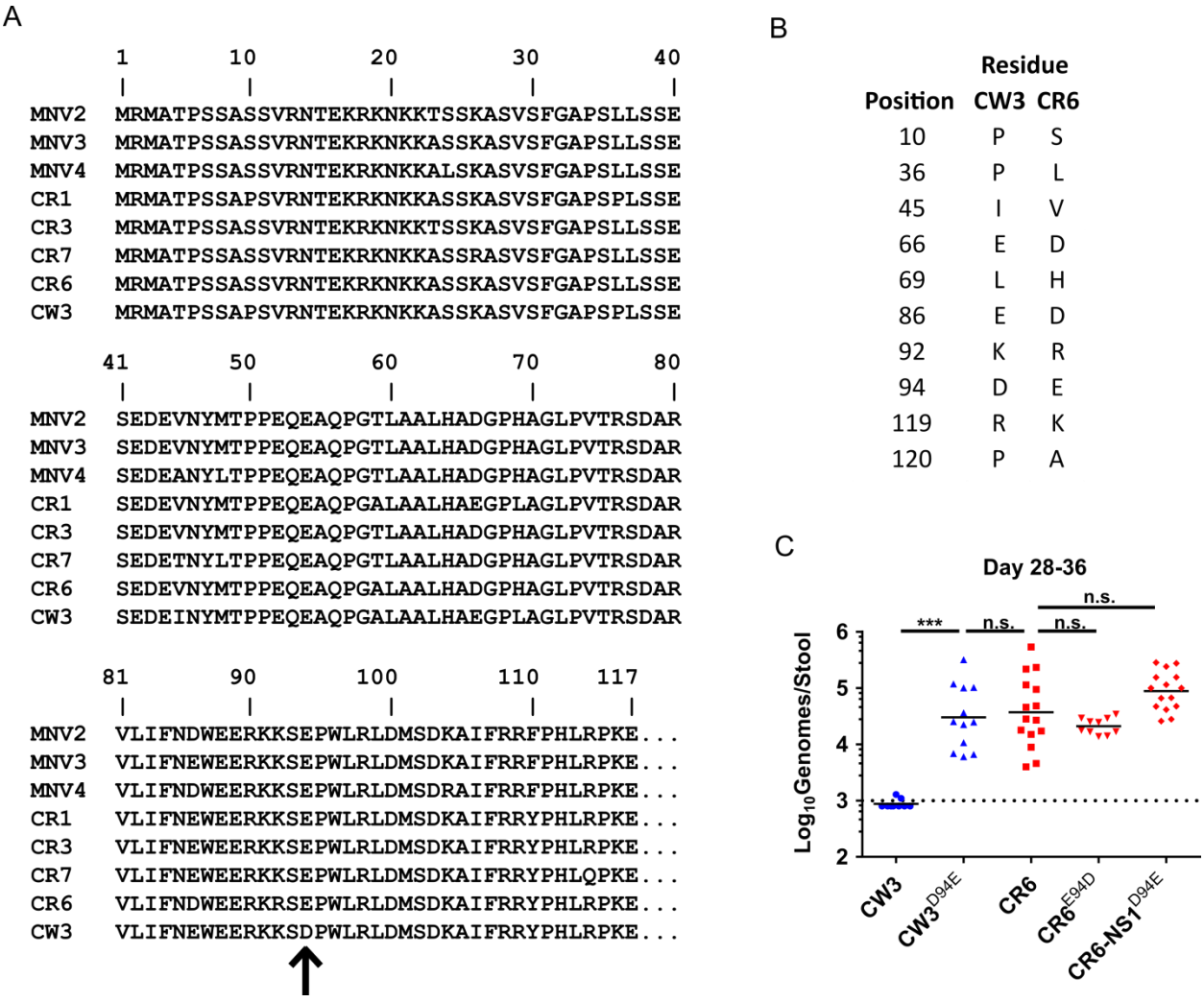

Figure 2.2. Mutation of aspartic acid residue 94 to glutamic acid in NS1^{CW3} is sufficient to confer persistence.

(A) Alignment of first 117 residues of NS1 for CR6, CW3, and six other persistent strains of MNoV (accession numbers DQ223041, DQ223042, DQ223043, EU004672, EU004673, and EU004677 (30, 31)).

(B) Ten residues in the NS1 domain differ between CR6 and CW3.

(C) Mice were inoculated with indicated MNoV strains and stool collected at the persistence time points 28-36 days post infection. MNoV genomes were quantified by q-RT-PCR, showing mice from two independent experiments, one-way ANOVA, Tukey's post-test.

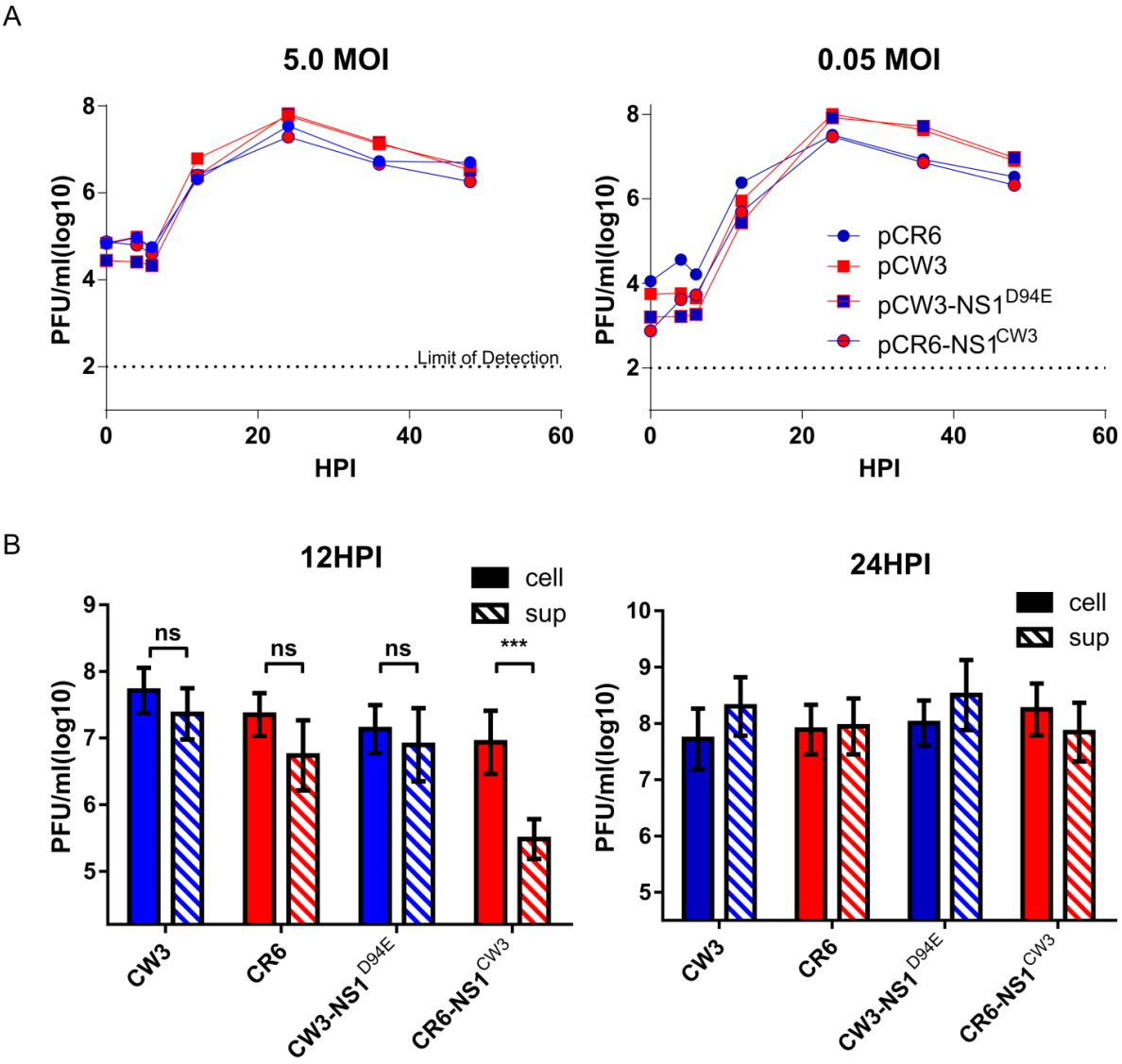

Figure 2.3. MNoV NS1/2 mutants grow equivalently in RAW264.7 cells, but pCR6-NS1^{CW3} release from cells is delayed.

(A) Viral growth of persistent and non-persistent NS1/2 mutants in RAW264.7 cells. MOI 5.0 left, MOI 0.05 right; virus was quantified by plaque assay and represented as plaque forming units/ml, n=3.

(B) MNoV NS1/2 mutants infected RAW264.7 cells. Supernatant was removed at indicated times, microcentrifuged to remove debris, and cells and supernatant were frozen. Virus was quantified as in (A). Two-way ANOVA, Bonferroni's post-test. MOI 5, n=3.

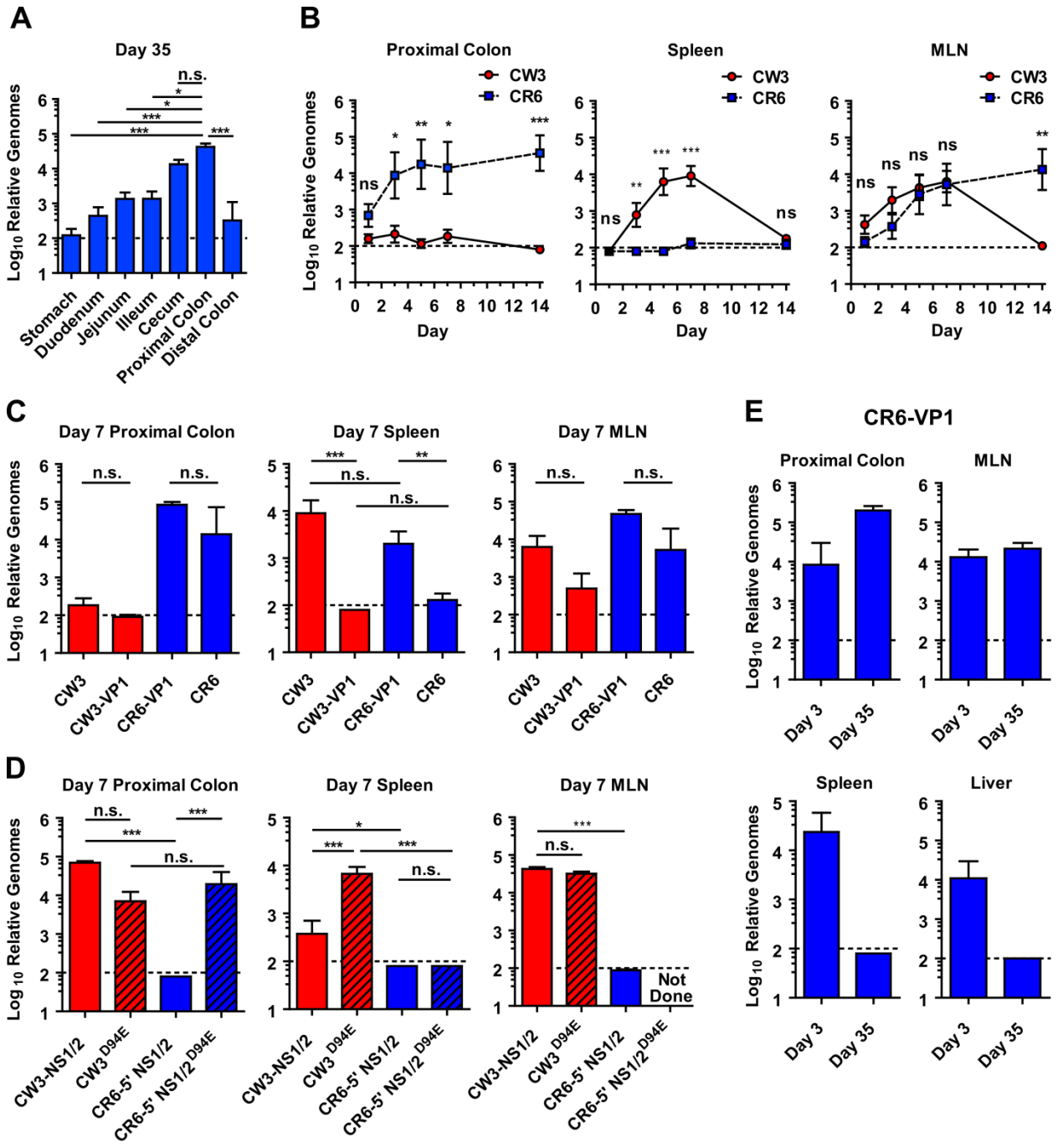

Figure 2.4. NS1/2 determines norovirus replication in colon, a major site of persistent infection, and VP1 determines viral replication in the spleen.

(A-E) Tissues were harvested at indicated times in MNoV infected mice. RNA was isolated and MNoV genomes were detected by quantitative-RT-PCR.

(A) Tissues from pCR6 infected mice were harvested at day 35 post infection, n=2 with 5 mice per data point. One-way ANOVA, Tukey's post-test.

(B) Time course of pCW3 or pCR6 infection in proximal colon, spleen, and MLN. Two-way ANOVA, Bonferroni's post-test, n=3 with 9 mice per data point.

(C-D) Tissues were harvested from proximal colon, spleen, and MLN at day 7 post infection with indicated MNoV strains. One-way ANOVA, Tukey's post-test, n=2 with 8 mice per data point.

(E) Proximal colon, MLN, spleen, and liver were harvested at days 3 and 35 from mice infected with pCR6-VP1^{CW3} at a dose of $1x10^6$, n=2 with 6 mice per data point.

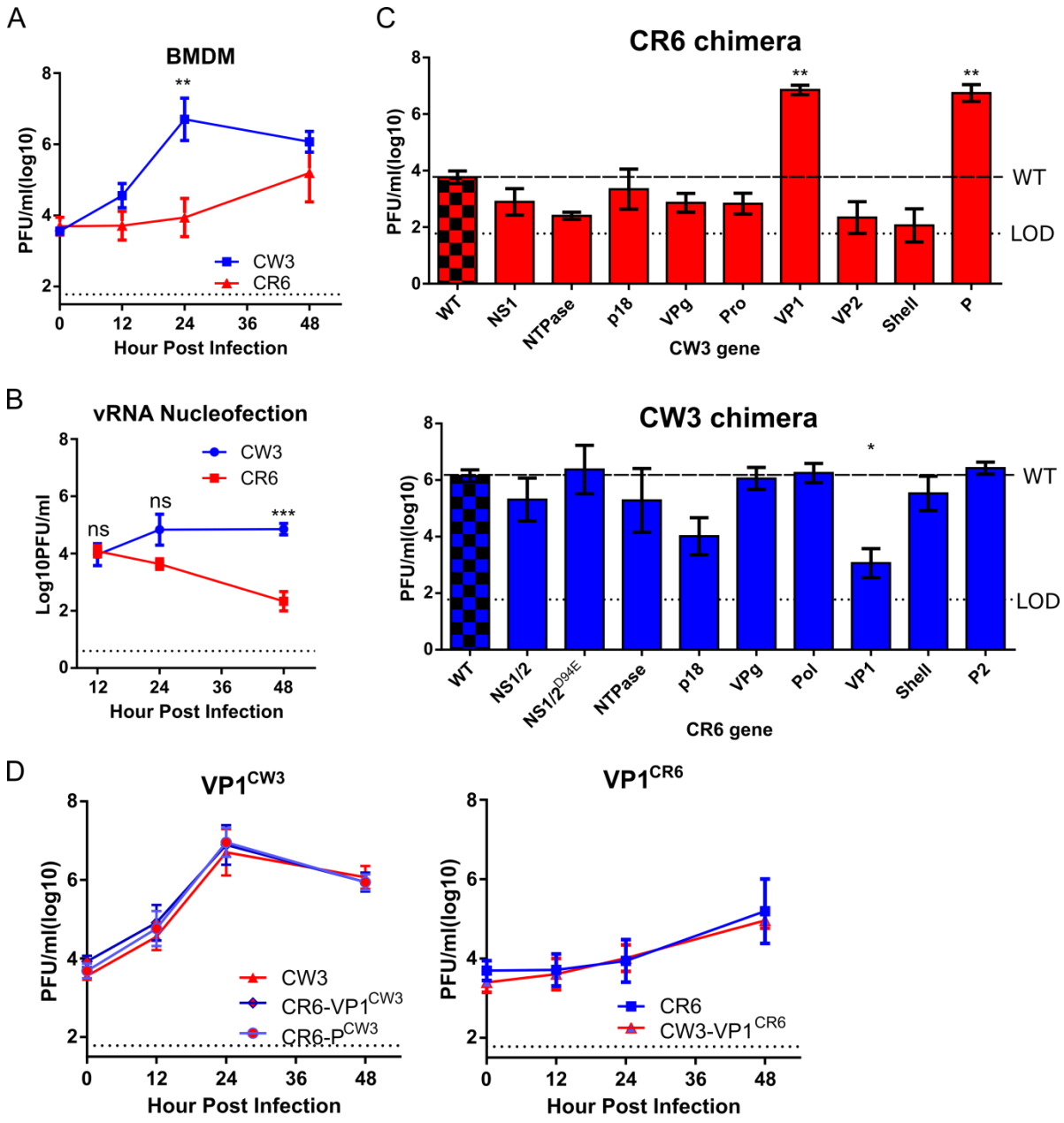

Figure 2.5. VP1 is the viral determinant for pCW3 growth in BMDMs

(A-D) Virus quantitated by plaque assay, dotted line limit of detection of plaque assay.

(A) Growth of pCR6 and pCW3 in BMDMs, MOI 0.5. Two-way ANOVA, Bonferroni's post-test, n=3.

(B) Replication of CR6 and CW3 following electroporation of vRNA into BMDMs. Two-way ANOVA, Bonferroni's post-test, n=3

(C) Screen of single gene or domain pCW3/pCR6 chimera for replication of virus 24 hours post infection, MOI 0.5. Upper dashed line represents average amount of virus for WT strain. One-way ANOVA, Tukey's post-test, n=2.

(D) Growth of indicated VP1 and VP1-domain chimera in BMDMs relative to WT pCR6 or pCW3. Non-significance was tested using two-way ANOVA, Bonferroni's post-test, n=3

Chapter 3:
Noroviruses coopt the function of host protein VAPA via an FFAT-motif mimic in nonstructural viral protein NS1/2

In addition to unpublished data, this chapter is adapted from:
McCune BT, Tang W, Lu J, Eagleshame J, Thorne L, Condiff E, Nice TJ, Goodfellow I, Krezel AM, Virgin HW. Noroviruses coopt the function of host protein VAPA for replication via a FFAT-motif mimic in nonstructural viral protein NS1/2. *Under Review*

3.1 Abstract

The *Norovirus* genus contains important human pathogens but the role of host pathways in norovirus replication is largely unknown. MNoV provide model systems to study norovirus replication in cell culture and in small animals. The human norovirus nonstructural protein NS1/2 interacts with the host protein Vamp-Associated Protein A (VAPA), but the significance of the NS1/2-VAPA interaction is unexplored. Herein we report decreased MNoV replication in VAPA-deficient cells. VAPA was required for the efficiency of step(s) in the viral replication cycle after entry of viral RNA into the cytoplasm but before the synthesis of viral minus-sense RNA. The interaction of VAPA with viral NS1/2 proteins is conserved between murine and human noroviruses. NS1/2 of MNoV directly binds the Major Sperm Protein (MSP) domain of VAPA through its poorly conserved NS1 domain. Mutations within the viral NS1 domain that disrupted interaction with VAPA inhibited viral replication. Investigation of the structural basis for interaction between the NS1 and MSP domains revealed that the viral NS1 domain contains a mimic of the phenylalanine-phenylalanine-acidic-tract (FFAT)-motif that enables host proteins to bind to the VAPA MSP domain. The NS1/2-FFAT-mimic region interacted with the VAPA-MSP domain in a manner similar to *bona fide* host FFAT motifs. Amino acids in the FFAT mimic region of the NS1 domain that are important for viral replication are highly conserved across MNoV strains. Thus, VAPA interaction with a norovirus protein that functionally mimics host FFAT motifs is important for MNoV replication.

3.2 Introduction

Noroviruses are non-enveloped positive-sense single-stranded RNA viruses that primarily infect the gastrointestinal tract. Human noroviruses are a leading cause of epidemic gastroenteritis (1-3), but study of human noroviruses has been difficult due to the lack of robust culture systems, though recent work has demonstrated human norovirus replication in mice and cell lines (4, 5). NoVs are divided into genogroups GI-GVII. Of these, GI, GII, and GIV viruses cause human disease, and GV encompasses more recently discovered rodent NoVs, including MNoV (6). As MNoV replicates robustly in mice and cells, it serves as a powerful model for molecular studies of norovirus replication, tropism, and pathogenesis (7, 8).

The norovirus genome encodes nine known proteins: seven non-structural (NS) proteins derived by proteolysis of the ORF 1 polyprotein (9), and two structural proteins, VP1 and VP2 derived from ORFs 2 and 3 respectively (7). MNoV encodes the virulence protein VF1 from ORF4, which overlaps ORF2 and has not been found in human noroviruses (10). The N-terminal protein in the norovirus polyprotein, NS1/2, is comprised of three domains: NS1, NS2, and a putative transmembrane domain (11). The MNoV NS1 domain in isolation has a structured region preceded by an unstructured domain (11, 12). A single aspartic acid to glutamic acid difference within NS1 confers an altered conformation within the NS1 structured domain (12) and is associated with enteric tropism and the capacity of MNoV to persistently infect and be shed from the mouse intestine (13). NS2 contains a domain with a predicted structural resemblance to domains found in a variety of enzymes (14). Ectopically expressed NS1/2 from GI human norovirus ($NS1/2^{GI}$) disrupts the Golgi apparatus and vesicular trafficking (15, 16) and is reported to interact with the host protein Vamp-Associated-Protein A (VAPA) (15). The role of VAPA interactions with NS1/2 during viral replication has not been defined.

VAPA is a type II endoplasmic reticulum (ER) resident protein that is conserved in eukaryotes (17). VAPA is comprised of a Major Sperm Protein (MSP) domain, a Coiled-Coil domain (CCD), and a transmembrane domain. Initially found to bind SNAREs (18-20), VAPA also binds a variety of client interacting proteins (17). Importantly, through the cytosolic MSP domain, VAPA interacts with client proteins primarily involved in lipid trafficking (17, 21-25). These proteins interact with VAPA-MSP via a phenylalanine-phenylalanine acidic tract (FFAT) linear motif (22, 26-29).

VAPA performs important functions during infection as both microbes and antimicrobial host molecules target VAPA and its client proteins. VAPA and its paralog VAPB enhance the replication of Hepatitis C virus (30, 31), rhinoviruses (32), tombusvirus (33, 34), and the intracellular bacteria *Chlamydia trachomatis* (35, 36). Some of these microbes encode molecules that interact with VAPA, VAPB, and/or its client proteins, including HCV proteins NS5a and NS5b (30, 31), tombusvirus p33 (33, 34), and *C. trachomatis* IncD (35, 36). Several observations support the idea that VAPA and VAPA client proteins assist in organization of membranous structures critical for virus replication (37, 38), possibly by manipulating the lipid composition of these membranes (32-34). Furthermore, VAPA binds to the interferon stimulated genes IFITM3 (39) and RSAD2 (40, 41), suggesting that VAPA may be involved in antiviral responses.

Herein we defined the function and molecular basis of NS1/2-VAPA interactions during MNoV infection. Disruption of VAPA in permissive cells delayed MNoV replication due to effects occurring after viral entry but prior to synthesis of viral minus-sense RNA. The interaction between NS1/2 and VAPA was conserved between human norovirus and MNoV NS1/2 proteins. The NS1 domain of MNoV NS1/2 interacted with the MSP domain of VAPA. This interaction occurred independent of other cellular or viral proteins, and mapped to a short

region in the NS1 domain sharing features of the FFAT motif found in host proteins that also interact with the VAPA MSP domain. NS1 engaged VAPA MSP domain residues crucial for interaction with FFAT motifs found in VAPA client proteins. Mutagenesis of conserved amino acids in NS1 to abrogate VAPA interaction impaired recovery of infectious MNoV after transfection of permissive cells with plasmids encoding the viral genome. These data indicate that NS1/2-VAPA binding is critical for efficient MNoV replication and that this occurs through viral mimicry of the host FFAT motif by amino acids in the NS1 domain of the nonstructural NS1/2 protein.

3.3 Results

3.3.1 MNoV replication is diminished in VAPA-deficient cells

To test the hypothesis that MNoV replication benefits from the function of VAPA, we genetically engineered RAW264.7 cells deficient in VAPA expression (hereafter *Vapa*$^{-/-}$) using CRISPR-Cas9. In two cloned *Vapa*$^{-/-}$ cell lines, 3A11 and 1E6, frameshifts in the first 37 nucleotides (Figure 3.1A) of coding sequence resulted in loss of VAPA protein expression (Figure 3.1B). *Vapa*$^{-/-}$ cells infected with MNoV strain CW3 had 2.2x (1E6) or 4.0x (3A11) fewer NS1/2 positive cells by flow cytometry 18 hours post infection than wild type cells (Figure 3.1E, F). We observed lower levels of replication of MNoV strains CW3 and CR6 in both *Vapa*$^{-/-}$ cell lines (Figure 3.1C). *Vapa*$^{-/-}$ cells also had increased viability during MNoV infection (Figure 3.1D). We also observed lower MNoV infectivity in BV2-Cas9 cells transduced with single guide RNAs targeting *Vapa* (Figure 3.1G). Reconstituting VAPA production in *Vapa*$^{-/-}$ cells via lentivirus transduction (Figure 3.2A) increased the percent of cells expressing NS1/2 at 18 hours post infection by 2.7 fold (3A11) or 4.1 fold (1E6) compared to transduction with GFP (Figure 3.2C, D). Expression of VAPA increased viral replication for the *Vapa*$^{-/-}$ 1E6 line (Figure 3.2B), but not the 3A11 cell line. These data together indicate that MNoV infectivity was enhanced by VAPA expression.

To test the role of VAPA in mice, we attempted to engineer *Vapa*$^{-/-}$ mice. We were able to generate two mutant lines by transient expression of Cas9 and *Vapa* targeted sgRNA (Figure 3.3A). However, *Vapa*$^{+/-}$ crosses produced no *Vapa*$^{-/-}$ pups (Figure 3.3B), though we did detect two *Vapa*$^{-/-}$ embryos at E14.5 (Figure 3.3C). We concluded mutation of *Vapa* led to embryonic lethality.

3.3.2 VAPA is important for an early post-entry step in norovirus replication

To investigate the role of VAPA in MNoV replication, we analyzed non-structural protein expression by measuring NS1/2 protein levels in infected cells by western blot. Infected *Vapa*$^{-/-}$ cells expressed lower levels of NS1/2 protein four and six hours after infection (Figure 3.4A) with the difference diminishing later in infection. This supports a role for VAPA in early events of MNoV replication. Because VAPA is associated with efficient entry of an enveloped virus (39) as well as the function of endosomes (21, 39, 42) through which MNoV likely passes to establish infection (43-45), we tested whether impaired viral entry in *Vapa*$^{-/-}$ cells accounted for decreased NS1/2 production and viral replication. We reasoned that transfection of viral RNA would bypass any effect of VAPA on viral entry and uncoating. After electroporating purified viral RNA into cells, we detected decreased NS1/2 levels in *Vapa*$^{-/-}$ cells (Figure 3.4B), despite observing no difference in transfectability as measured by plasmid-driven GFP expression (Figure 3.4B, middle). These data indicate that VAPA plays a role in viral protein expression downstream of viral entry. After the viral RNA accesses the cytoplasm, NS1/2 protein can be produced by either translating in-coming plus-sense virion RNA or from viral plus-sense RNA transcribed from newly synthesized minus-sense RNA. Using strand-specific quantitative RT-PCR (46), we observed delayed accumulation of both negative- and positive-sense MNoV RNA in *Vapa*$^{-/-}$ cells (Figure 3.4C) indicating that production of NS1/2 is impaired prior to synthesis of new viral minus-sense RNA. Collectively, these observations support a role for VAPA downstream of viral RNA delivery into the cytosol, but upstream of minus-sense viral RNA synthesis.

3.3.3 NS1/2 interaction with VAPA is conserved among norovirus strains

Prior work showed that VAPA binds to human NoV NS1/2^{GI} (15). To determine the

evolutionary conservation of the NS1/2^{GI}-VAPA interaction we tested NS1/2^{MNoV} interaction with VAPA. Consistent with published observation (15), Flag-tagged NS1/2^{GI} reciprocally co-immunoprecipitated with HA-tagged VAPA (Figure 3.5A). Flag-tagged NS1/2^{MNoV} (strain CR6) immunoprecipitated weakly with VAPA (Figure 3.5A) and with NS4 as previously shown (47).

To test for direct NS1/2-VAPA interaction using a system with which we could more easily map interactions, we assessed NS1/2 interaction with VAPA by mammalian 2-hybrid (M2H). In this assay, interaction between a "bait" and "prey" protein generates a luciferase signal. As previously reported (15, 23, 48), we detected VAPA interaction with itself, the host protein OSBP, and human norovirus NS1/2^{GI}, validating use of M2H as an approach to assess VAPA interactions (Figure 3.5B). NS1/2^{MNoV} from either MNoV strain CW3 or CR6 interacted with VAPA (Figure 3.5B). We also detected interaction of NS1/2^{MNoV} with VAPB, a paralogue of VAPA (17) with 62% amino acid identity.

3.3.4. VAPA interacts with NS1/2 during MNoV infection

To test if VAPA interacts with NS1/2 during infection, we engineered MNoV to express a FLAG tag in NS1/2 (nucleotide 383) and used a previously described virus with a FLAG tag in NS4 (nucleotide 2600) (Figure 3.6A) (47). We selected NS4 for this experiment as it is known to bind NS1/2 (47). Both MNoV-NS1/2^{FLAG} and MNoV-NS4^{FLAG} replicated similarly to wild type virus (Figure 3.6B). FLAG-tagged viral proteins of appropriate molecular weight were expressed during infection (Figure 3.6A, top left). As expected, virus-derived FLAG-NS1/2 and FLAG-NS4 localized with the viral replication complex (Figure 3.6C) (49). Having validated the use of FLAG-tagged viruses to study viral replication, we infected the BV2 microglial cell line with MNoV-NS1/2^{FLAG} and MNoV-NS4^{FLAG}. Both FLAG-NS1/2 and FLAG-NS4 co-precipitated

with VAPA, but not NS7 or GAPDH (Figure 3.6D). Thus NS1/2, either independently or together with NS4, interacts with VAPA (47).

3.3.5 NS1/2 interacts with FFAT-binding residues in VAPA MSP domain

Many VAPA protein-protein interactions occur between the VAPA MSP domain and host cell proteins containing FFAT motifs. Structure-function analyses of FFAT-VAPA interactions support a model in which FFAT motifs from VAPA client proteins rest within a groove present on the surface of the VAPA-MSP domain (26, 28, 29). Within this groove, VAPA residues K50, K52, K94, M96, and K125 are critical for interaction with FFAT motifs. To test if these residues also engage NS1/2, we introduced the following mutations into VAPA: K50E/K52E, K94A/M96A, and K125E/R127E (Figure 3.7A). Each of these mutation pairs decreased VAPA interaction with NS1/2 (Figure 3.7A) as measured by M2H. To test if NS1/2 interacts with sets of positively charged residues elsewhere in VAPA, we mutated additional sites in VAPA selected to have the sequence (H/R/K)X(H/R/K). Mutations K161E/H163E, H195E/R197E, and R202E/R204E had no effect on NS1/2-VAPA interaction (Figure 3.7A). We conclude that NS1/2 interaction specifically required positively charged residues within the VAPA MSP domain.

To test if NS1/2 must interact with VAPA to rescue MNoV infectivity in *Vapa*$^{-/-}$ cells, we reconstituted *Vapa*$^{-/-}$ with VAPA that did (K161E/H163E, H195E/R197E, and R202E/R204E) or did not (K50E/K52E, K94A/M96A, and K125E/R127E) interact with NS1/2. VAPA variants that did not interact with NS1/2 failed to rescue MNoV infectivity in *Vapa*$^{-/-}$ cells, while mutants that interacted with NS1/2 rescued MNoV infectivity (Figure 3.7B). This result is consistent with the model that VAPA must interact with NS1/2 to enhance MNoV infectivity.

In work presented below, we found that the NS1 domain of NS1/2 is required for NS1/2-VAPA interactions (Figure 3.8B). To map the physical interactions between NS1 and the VAPA-MSP domain, we used NMR to analyze the chemical shift perturbations of the ^{15}N-labeled VAPA-MSP domain (M8-M132 of VAPA) titrated with increasing amounts of unlabeled NS1 (S28-R114 of NS1/2). This analysis revealed interactions between NS1/2 and four groups of residues on VAPA, K52-T54, C60-N64, K92-V97, and D123-L126 (Figure 3.7C). These groups of residues all mapped to the FFAT binding groove on a positively charged surface of the MSP domain. Furthermore, the VAPA residues that bind NS1/2 coincide with the FFAT-motif interaction surface on the MSP domain (26, 28). Using the same experimental approach, we did not observe any interactions of NS1 with the isolated coiled-coil domain (P133-S226 of VAPA, data not shown).

We independently verified the role of the VAPA residues identified above in NS1/2-VAPA interactions using M2H. To this end, we replaced selected amino acids in the VAPA MSP domain with either glutamate or alanine and tested for the interaction of these mutant molecules with NS1/2. No interaction was detected with glutamate or alanine substitutions at positions V51, K52, T54, K94, and K125 (Figure 3.7D). No interaction occurred after mutation of R62 to glutamate, but interaction was present with alanine at this site (Figure 3.7D). However, at positions K50, T53, V61, N64, M96, and R127 we observed interaction after replacing these residues with either glutamate or alanine (Figure 3.7D). These results indicate NS1/2 interaction with VAPA requires many of same residues FFAT motifs bind within a groove on the VAPA-MSP domain (Figure 3.7E).

3.3.6 Residues 47-54 of MNoV NS1 are necessary for interaction with VAPA

While the NS2 domain is well conserved within the NoV genus, NS1 is not (Figure 3.8A). Accordingly, we predicted that the conserved NS2 domain contributed to the NS1/2 interaction with VAPA. To test this hypothesis, we cloned a panel of N- and C-terminal NS1/2 truncations. Surprisingly, the MNoV NS1 domain containing residues 1-131 was sufficient to interact with VAPA while the NS2 domain did not interact (Figure 3.8B). Furthermore, a region between residues 31-57 was necessary to interact with VAPA (Figure 3.8B).

To define the specific NS1 residues interacting with VAPA-MSP, we analyzed the chemical shift perturbations of the NMR spectra of ^{15}N-labeled NS1 (S28-R11 of NS1/2) with increasing amounts of unlabeled VAPA (M8-S226 of VAPA). The largest perturbations in NS1 from both the CR6 and CW3 strains of MNoV were observed for a core of interacting residues centered on Y47-Q53 (YMTPPEQ) (Figure 3.9A, B). A longer sequence encompassing residues I45 to A61, showed consistent but smaller perturbations (Figure 3.9A, B). The VAPA interacting residues are predominantly within the segment K26-P57 that shows a highly dynamic conformation in isolated NS1 (50). The last few interacting residues of the core residues of NS1 that interact with VAPA are in the structured domain of NS1 (G58-R114) (50). There are no observable amides in prolines; hence, no data were available for P50, P51, and P57.

To test the importance of this core of interacting residues, we carried out experiments with three mutant forms of NS1, NS1-CR6^{M48G}, CW3^{T49G}, and CW3^{E52K}. The Heteronuclear Single Quantum Coherence (HSQC) spectra obtained for mutants were similar indicating that these mutations did not destabilize tertiary structures (data not shown). NS1-CW3^{T49G} and CW3^{E52K} mutations decreased binding to VAPA to undetectable levels, while NS1-CR6^{M48G} interacted with VAPA (Figure 3.9B).

3.3.7 MNoV NS1 contains a mimic of host FFAT domains

Since this core domain of NS1 interacted with the MSP domain of VAPA, and the FFAT motif is responsible for interactions of host proteins with this same domain, we considered the possible relationship of this NS1 region and FFAT motifs. Generally, FFAT motifs contain a core sequence containing a bulky aromatic residue flanked N- and C-terminally by acidic residues (22, 27). Similar to FFAT motifs, NS1/2 encodes acidic residues (residues 40-44, 52, 54) surrounding tyrosine 47 (Figure 3.9C). This sequence is conserved across MNoV strains (Figure 3.9C, Figure 3.10), though positions 45, 46, and 48 are variable. The strong conservation of certain amino acids in this region suggested that the motif is functionally important.

To test which residues within this domain contribute to interaction with VAPA, we introduced single residue mutations and assessed their effect by M2H analysis. For positions in the N-terminal acidic segment, mutations E40A, E40K, E42A, E42K, D43A, D43K, E44A, and E44K blocked NS1/2-VAPA interaction, while S41G maintained detectable interaction (Figure 3.9D). Within the FFAT-like core segment, Y47A, Y47G, T49A, and T49G ablated NS1/2 interactions with VAPA. Residues at positions 45, 46, and 48 are variable across MNoV strains (Figure 3.9C, Figure 3.10). To test the function of amino acids in these positions, we introduced variants observed in other MNoV strain, including V45A, V45I, N46C, N46D, M48A, and M48L, as well as variants not observed in MNoV isolates, including V45G, N46G, M48D, M48I, and M48G. Mutations at these positions did not disrupt interaction, suggesting that the interaction is preserved for sequences that vary in these positions across strains (Figure 3.9D). For C-terminal acidic residues, E52K mutation disrupted the interaction, but E54K maintained interaction. Additionally, mutations outside of this region including H69L, D121G, and D131G did not prevent interaction (Figure 3.9D).

Therefore, residues in the S40-E54 region of NS1/2 were necessary for interaction with

VAPA. The 1) chemical nature of the amino acids present (acidic, bulky aromatic), 2) their positions, 3) their importance for binding VAPA, 4) the interaction of this region with the region of VAPA that binds to FFAT motifs in host proteins, 5) the conservation of the critical amino acids across strains and 6) the arrangement of the acidic amino acids surrounding and FFAT-like core argue that this region of NS1 is mimicking host FFAT motifs as a basis for interacting with the MSP domain of VAPA.

3.3.8 NS1/2-VAPA interactions are required for recovery of MNoV from infectious clones

To determine the importance of the NS1/2-VAPA interaction and specific amino acids in the NS1/2 FFAT-like domain for MNoV growth we assessed the effect of mutations in NS1/2 using an infectious molecular clone of the virus. Mutations were introduced in a plasmid encoding the CR6 viral genome and recovery of infectious virus was assessed after transfection of the plasmid into permissive cells. We noticed three patterns of recovery of infectious virus in these experiments (Figure 3.11A): (i) some NS1/2 mutations had no discernable effect on virus recovery (V45G, V45A, V45I, N46D, M48A, M48L, H69L, D121G, and D131G); (ii) some NS1/2 mutations resulted in variable recovery (S41G, N46G, M48I, M48D, and E54K); (iii) some NS1/2 mutations completely eliminated virus recovery (E40A, E40K, E42A, E42K, D43A, D43K, E44A, E44K, Y47G, Y47A, M48G, T49G, T49A, and E52K). We saw similar patterns of virus recovery after insertion of mutations into NS1/2 in the CW3 genome with the following exceptions. NS1/2 mutations S41G, N46C, M48I, M48D, and E54K resulted in consistent recovery of virus; E40A, D43A mutations resulted in variable virus recovery; I45G mutation completely prevented virus recovery (Figure 3.11B).

Importantly, this mutational analysis of the NS1 domains of two strains of MNoV

revealed a strong correlation between mutations that perturbed VAPA interaction (Figure 3.11C top panel) and those which diminished recovery of virus (Figure 3.11C bottom two panels). Side-chains for residues that were critical for recovery of virus primarily mapped to a sequence showing highly dynamic behavior in free NS1 and a few N-terminal residues of the NS1 structured domain (50) (Figure 3.11D). The specificity of the relationship between side-chain and function within this region is strikingly revealed by comparing the role of the tyrosine at position 47, which was important for virus recovery, and the immediately adjacent methionine at position 48 at which multiple amino acids substitutions were tolerated.

3.4 Discussion

3.4.1 Summary

In this study, we define the importance of the host protein VAPA and its interaction with the viral nonstructural protein NS1/2 in replication of MNoV. We confirmed the previously identified interaction between a human norovirus NS1/2 protein and VAPA (15) and found that this interaction is shared with the NS1/2 proteins of two MNoV strains. Using a variety of approaches including analysis of the interaction of the proteins *in vitro* and in cells, we delineate the structural basis for the interaction between VAPA and NS1/2 and used these data to test for the importance of specific amino acids in NS1/2 for viral replication and for the interaction between VAPA NS1/2. These studies support the concept that VAPA is a pro-viral host protein for MNoV infection, and that interaction between NS1/2 and VAPA is important for viral replication. Remarkably, the MNoV NS1 domains appear to mimic host VAPA-binding proteins through the conservation of a region that mimics host FFAT domains present in VAPA MSP domain-interacting proteins.

3.4.2 Norovirus mimicry of host FFAT motifs

Mimicry of host molecules and motifs is a pervasive evolutionary theme enabling microbes to hijack host processes (51). While efforts have been made to predict mimicry on large-scale (50, 51), detecting structural and/or functional domain mimics requires validation through detailed studies of individual microbial molecules. For other microbial proteins involved in targeting VAPA mimicry via an FFAT motif has not been reported. It will be interesting to determine whether FFAT domain mimicry is a common strategy for microbial proteins that target VAPA. If so, small molecules that target this interaction surface may have antiviral or

antimicrobial properties for multiple microbes that similarly bind VAPA. In this regard, it is important that FFAT motifs tolerate variation at many positions (22, 27), are relatively short, and are unstructured in solution (26), potentially enabling viruses or other organisms to evolve strategies to target VAPA. It is interesting that much of the region of MNoV NS1/2 that contains the FFAT mimic is unstructured in the purified NS1 domain (50). It seems possible that the interaction of these domains with the MSP domain of VAPA is somehow enhanced by the unstructured nature of this region.

This mimicry likely arose from convergent evolution, exploiting the partially unstructured, highly diverging, and evolving sequence of the NS1 domain. The observation that the NS1 domain, including the MNoV NS1-FFAT mimic, is poorly conserved across NoV genogroups bolsters this idea. Future work revealing how NS1 from HNoV interacts with VAPA and how broadly conserved this interaction is across a comprehensive set of NoV strains will test this hypothesis. Furthermore, no naturally occurring variants of MNoV disturbed NS1/2-VAPA interaction. This introduces the possibility that the NS1/2-VAPA interaction has undergone purifying selection in MNoV.

The greatest similarity of the MNoV NS1/2 sequences to host FFAT motifs was identified in the N-terminal and C-terminal portions of the motif. The core sequence was less similar, notably lacking a phenylalanine followed by D/E, instead encoding a tyrosine without a flanking acidic residue. The third position of host FFAT motifs (the second of the two Phe residues defining the motif in host proteins) tolerates wide range of residue substitutions without loss of functionality. Similarly, both NMR and M2H experiments with the NS1 M48G mutant are consistently tolerant of variability at this site. Nonetheless, at the structural level, the binding mode of NS1/2 to VAPA showed remarkable similarity to the binding of host FFAT motifs to

VAPA, for example by interacting with specific VAPA amino acids in the MSP domain. It is therefore interesting that the core portions of host and norovirus FFAT motifs differs in some regards, suggesting that there may be specific properties of the interaction that are unique to the viral FFAT motif. Future work revealing the molecular basis of the interaction between human norovirus NS1/2 and VAPA and examining the conservation of relevant amino acids across norovirus genogroups and strains will be of interest.

3.4.3 Role of VAPA in norovirus replication

Our work does not reveal the mechanism by which VAPA participates in the viral life cycle. However, it is clear that the stages of viral replication after entry and before minus-sense viral RNA synthesis are affected by VAPA. We have considered two non-mutually exclusive possibilities for the function of the NS1/2-VAPA interaction at this early stage of viral replication. First, the NS1/2-VAPA interaction could localize NS1/2 to the ER in order to initiate formation of the membranous viral replication compartment. Notably, the advantage afforded by direct interactions of viral proteins with VAPA and VAPB proteins has been reported for Hepatitis C Virus (30, 31) which also required rearrangements of intracellular membranes to create a replication complex. MNoV NS1/2 is associated with the ER when expressed independent of other viral proteins (49, 52), and VAPA is an ER-resident protein, suggesting the possibility of a role for VAPA in NS1/2 localization. It is notable that the NS1 domain that contains the FFAT motif mimic would be the first portion of the polyprotein synthesized from viral plus-sense RNA, and could therefore contribute to coordination of initial steps of viral replication at the ER prior to synthesis and processing of the rest of the viral polyprotein.

Second, it is also conceivable that the interaction of NS1/2 with VAPA alters lipid

metabolism through competition for the interactions between VAPA and VAPA-client proteins that also have FFAT domains. In this regard, it is not known whether any of the specific processes carried out by VAPA client proteins are important for enhancing or inhibiting norovirus replication. Answering this question is likely to be complex since VAPA interacts with multiple client proteins such as OSBP and CERT and to be involved in a range of processes in the cell including non-vesicular lipid transfer (23, 25, 53), lipid metabolism (53, 54) and is present at membrane contact sites (55-59). Nevertheless, the conservation of a structural motif related to the FFAT motifs found in proteins that interact with the MSP domain of VAPA indicates the value of dissecting the possible role of VAPA-dependent functions in the viral life cycle and of the impact of NS1/2 function on VAPA-dependent proteins.

3.5 Materials and Methods

3.5.1 Cells and Media

293T, BV2, and RAW264.7 cells were maintained in DMEM with 10% FBS, 1% Pen/Strep, 2mM L-Glutamine, and 10mM HEPES. The Genome Engineering and iPSC Center (St. Louis, MO) engineered VAPA-knockout RAW 264.7 cell lines 1E6 and 3A11. Briefly, guide RNAs (5'-GGCGAAGCACGAGCAGATCCTGG-3' and 5'-GATCTGCTCGTGCTTCGCCATGG-3') targeting VAPA were transfected into RAW 264.7 cells transiently expressing Cas9. Cells were clonally selected and verified for disruption of endogenous locus via the Cel-1 nuclease assay, then deep sequenced to identify frameshift mutations.

3.5.2 Cloning

NS1/2 from MNoV strains CR6 and CW3 infectious clones (13), and GI (NC_001959), as well as VAPA (NM_013933), were cloned into Gateway vector pDONR221 (Life Technologies), and subcloned using Gateway recombination and expression vectors. Cloning mutant MNoV done by site-directed mutagenesis using Q5/KLD mix or Phusion (New England BioLabs) and as described previously (60). The generation of the MNoV-NS4^{FLAG} infectious clone was described previously (47), and MNoV-NS1/2^{FLAG} was generated similarly with FLAG tag nucleotide sequence inserted after nucleotide 383 of the MNoV-1 genome by overlapping PCR.

3.5.3 MNoV

Viral stocks. Stocks were generated as described (13). Briefly, infectious clones were transfected (Transit-LT1 (Mirus)) into 293T cells. 48 hours post transfection, plates were frozen and thawed to liberate virus (passage zero), centrifuged, and supernatants were inoculated onto

RAW264.7 cells. 48 hours post infection (HPI), RAW264.7 cells were frozen, thawed, centrifuged, and supernatants were titered (passage one). Virus was further passaged on RAW264.7 cells at an MOI 0.01 PFU/cell, and clarified supernatant was ultracentrifuged at 30000 RPM for 3h. Pellets were resuspended in DMEM with 10% FBS and triply titered, constituting working stock of virus (passage two). The recovery of infectious FLAG-tagged MNoV was described previously (61). Briefly, infectious clones were transfected in BSRT7 cells infected with fowlpox virus expressing T7 RNA polymerase at MOI 0.5 to 1. 24 hours post transfection, MNoV were released by freeze-thawing plates. Then BV2 cells were inoculated with the recovered viruses at MOI 0.01 $TCID_{50}$ per cell, and viral stocks (passage one) were generated by freeze thawing the infected cells upon appearance of cytopathic effect and spinning down of cell debris at 4000 RPM for 5 minutes. The stability of FLAG tag insertions at passage three was verified by RT-PCR and sequencing of the viruses at relevant genomic locations, and Western Blot against FLAG tag using infected lysate (data not shown).

Viability of mutant infectious clones. MNoV infectious clones with novel mutations were transfected as above, and frozen at 48 HPT. Virus titer was assessed using plaque assay.

Virus infections. MNoV was inoculated at indicated MOI into cells in suspension for 30m on ice, and subsequently washed three times with complete media. For growth curves and FACS analysis, cells were plated and harvested at indicated times post infection.

Plaque assay and $TCID_{50}$. RAW264.7 cells were plated at $3x10^6$ cells/well in six well plates the night before the assay. Freeze-thawed samples were serially diluted on the day of the assay. 500µl of each dilution was inoculated onto RAW264.7 cell monolayers and rocked for one hour at room temperature. Inoculum was aspirated and cells were overlaid with methylcellulose

media (MEM, 10%FBS, 1% Pen/Strep, 2mM L-Glutamine, and 10mM HEPES). When plaques resolved in 2-3 days, overlay was aspirated and replaced with 0.01% Crystal violet in 20% ethanol for greater than 1hr. Fixed monolayers were rinsed with water, dried, and plaques were counted. $TCID_{50}$ was determined on BV2 cells as described previously (62).

3.5.4 Flow cytometry

Cells were infected as above. At indicated time, supernatant was collected for viral titering. Cells were washed once in PBS, scraped and transferred to a U-bottom 96well plate. All subsequent steps occurred at RT. Samples were incubated with fixable live/dead stain for 10 minutes, pelleted, and resuspended in 4% formaldehyde. After 10 minutes of fixation, cells were permeabilized in 0.2% Triton-X100 in PBS (PBS-T) for 20 minutes at RT or overnight at 4°C. Cells were then blocked (PBS-T, 3%FBS, 1% normal mouse serum, 1% normal goat serum) for 10 minutes, and incubated with 1:5000 dilution of polyclonal anti-NS1/2 Rabbit sera (Vernon Ward) for one hour. After three washes in PBS-T, cells were stained for 30-60 minutes with 1:500 dilution of anti-Rabbit secondary antibody conjugated to either Dylight 649 (BioLegend, 406406) or PE (Caltag, L43004), or anti-FLAG PE (BioLegend, 637310). After three PBS-T washes, cells were resuspended in PBS-T with 3% FBS passed through a cell strainer, and analyzed on an LSR II or FACS Calibur flow cytometer. All analysis was performed on FlowJo (Treestar, OR).

Cell Viability. Scraped cells were resuspended in 1:500 Fixable Aqua Live/Dead stain (Thermo Fisher), incubated at RT for 10m, microcentrifuged, then resuspended in fixative.

3.5.5 Confocal microscopy

2 x 10^5 BV2 cells were seeded on glass coverslips and were infected at MOI 1 $TCID_{50}$/cell. At 12 hours post infection, cells were fixed with 4% paraformaldehyde (PFA) in

PBS, quenched with 0.1M Glycine in PBS and permeabilized with 0.2% Triton X-100 in PBS. After blocking with 0.1% TWEEN 20 in PBS (PBST) containing 1% BSA and 1% Normal Goat Serum (Sigma Aldrich), mouse monoclonal anti-FLAG M2 (Sigma Aldrich) and rabbit polyclonal anti-NS7 antibodies were diluted 1:1000 in blocking solution and added to cells at room temperature for 1 hour. After washing three times with PBST, Goat anti-mouse IgG Alexa Fluor® 488 conjugate and Goat anti-rabbit IgG Alexa Fluor® 546 were added at dilution of 1:1000 in PBST. After incubation at room temperature for 1 hour protected from light, the coverslips were washed three times with PBST before mounting with Mowiol medium containing DAPI (4′,6-diamidino-2-phenylindole) stain. The confocal images were taken using a Zeiss 510 Meta laser confocal microscope.

3.5.6 Lentivirus

Lentiviral constructs, packaging plasmid, and VSV-G were transfected (TransIT-LT1, Mirus) into ~70% confluent 293T cells. 60 hours post-transfection, supernatant was filtered (0.45 micron) and inoculated onto ~5% confluent RAW 264.7 cells. The next day, media was replaced with complete media. 72 HPI, media was replaced with media with puromycin (5ug/ml). Cells were subsequently maintained in puromycin.

3.5.7 Immunoprecipitation

For ectopic expression, ~85% confluent 293Ts were transfected (TransIT-LT1, Mirus). 48 hours later, cells were washed once with PBS. Cells were washed once with PBS and lysed (50mM Tris-HCl (pH 7.5), 125mM NaCl, 1.5mM MgCl2, 5% Glycerol, 0.2% NP-40, fresh Protease Inhibitor Cocktail III (Roche)), and kept on ice. Lysates were passed through 29G needle five times, rested 5 minutes, repeated, then spun 16000 xg at 4°C. An aliquot of supernatant was removed for analysis of lysate. The remainder of supernatant was incubated with

Protein A/G beads (Santa Cruz) resuspended in lysis buffer for 30 minutes, then spun 1000 xg for one minute. Supernatant was incubated with 1µg/mL antibody for one hour, after which 50 µl Protein A/G beads were added and rotated overnight at 4°C. Beads were washed four times with one mL lysis buffer, then boiled with two times in laemmeli buffer for two to three minutes, and supernatant was frozen prior to analysis.

For anti-FLAG immunoprecipitation, BV2 cells were infected at MOI 10 $TCID_{50}$/cell and were harvested at 8 hours post infection. Cells were washed three times with cold PBS before lysis with 50mM Tris-HCl pH7.4, 150mM NaCl, 1mM EDTA, 2 mM $MgCl_2$, 1% Triton X-100, 1% v/v Protease Inhibitors Cocktail (Promega), 0.1% benzonase (Sigma Aldrich). The lysates were incubated on ice for 30 minutes to allow benzonase digestion of DNA and RNA, before spinning down for 10 minutes at 15000 RPM at 4°C. The supernatants were collected and the protein concentrations were determined by BCA assay (Thermo Fisher). The ANTI-FLAG M2 affinity agarose gel (Sigma Aldrich) was pre-washed twice with TBS buffer (50mM Tris-HCl pH7.5, 150mM NaCl. 2 mg total protein in 1ml lysis buffer was loaded to 40 µl ANTI-FLAG agarose and incubated at 4°C overnight with rotation. After removing the unbound protein by centrifugation at 5000 x g for 30 seconds at 4°C and three more washes with TBS buffer, the bound proteins were eluted by adding 50 µl 2X SDS-PAGE sample buffer and heating at 95°C for 3 minutes.

3.5.8 Western Blot

Laemmeli buffer was added to samples, then boiled 10-15 minutes. Protein was resolved on either 10% or 4-20% (Bio-Rad) SDS-PAGE Tris-Glycine gels. Protein was transferred semi-dry to PVDF membranes, blocked with 5% milk in TBS-tween, then incubated with antibody overnight at 4°C. Membranes were triply washed with TBS-tween, then incubated for an hour

with HRP-conjugated secondary antibody. After three TBS-tween washes, membranes were incubated with ECL or ECL2 reagent (Pierce), and signal was detected on film (MidSci). For densitometry, NS1/2 band density was calculated using ImageJ, normalized to Gapdh band density, then reported as a ratio to WT from each respective time point.

3.5.9 Antibodies

Polyclonal rabbit NS1/2 antisera was a kind gift from Vernon Ward. Anti-VAPA clone K-15 (sc-48698) was obtained from Santa Cruz Biotechnology. Anti-FLAG (M2) (Sigma Aldrich) anti-HA (H9658, Sigma Aldrich) were conjugated to HRP using Lightning-Link HRP Antibody Labeling Kit (701-0000, Innova Bioscience), and anti-Strep-tag II-HRP was acquired (71591-3, Novagen). Gapdh-HRP (G9295-25UL, Sigma Aldrich), and anti-actin (A5316, Sigma Aldrich) were used for normalization. Anti-VP16 (sc-7546) and anti-Gal4 BD (sc-510) (Santa Cruz Biotechnology) were used for M2H expression validation. Secondary antibodies obtained from Jackson Immunoresearch: Anti-Rabbit HRP (111-035-003), Anti-Goat-HRP (705-035-003), and Anti-mouse HRP (115-035-146).

3.5.10 Strand-specific qPCR

Cells were infected as above. At each time point post infection, cells were lysed and total cellular RNA was extracted using GenElute™ mammalian total RNA Miniprep Kit (Sigma Aldrich). Quantities of genomic positive/negative RNAs were determined using strand-specific RT-qPCR according to (46) with the following changes: 100ng total RNA was used in each RT reaction and 5µl of cDNA was used for genomic negative qPCR. The mean of log10 gEq/ng total RNA of mock-infected cells was used as the limit of detection (LOD). The results were obtained using ViiA™7 Real-Time PCR System.

3.5.11 Mammalian 2-Hybrid

Checkmate Vectors (Promega) pACT (prey) and pBIND (bait) were converted to Gateway destination vectors and genes were subcloned used Gateway LR reactions (Life Technology). Subsequent M2H analysis was performed as described previously (63). In brief, 7.5 fmol Bait and Prey plasmids with 100ng pG5 reporter plasmid were incubated with 40 µl Optimem (Life Technology) and 2 µl Transit-LT1. DNA-reagent complexes were added to 293T cells 50-75% confluent. 48-51h post transfection, cells were lysed using Passive Lysis Buffer, and luminescence was measured using Dual-Luciferase Reporter Assay (Promega) on an Opticomp II (MGM Instruments) luminometer. Firefly luciferase luminescence was reported as percentage of Renilla luciferase for each sample. All data shown are $n \geq 3$, determined normally distributed, comparing the greater of bait- or prey-only with bait+prey. Fold-change calculated from average of bait+prey/average highest background (bait or prey).

3.5.12 Vapa Mutant Mouse

Day 0.5 B6/J inbred embryos underwent pronuclear microinjection with gRNA and Cas9-mRNA, then embryos were implanted in surrogate mothers as described (64). Mutations in live born pups were identified by isolating tail DNA, PCR amplifying the Vapa targeted locus, and Sanger sequencing. Genotypes were verified by TOPO-TA (Life Sciences) cloning the amplicons and Sanger sequencing.

Genotyping. Mutant line 1: Primers were designed to amplify Vapa locus (F-CTGCTGAGCGGACAGGCTG, R- CGCAAGATGGCGGCGGAG), wt: 500 bp, deletion: 440 bp. Mutant line 2: Genotyping to detect single base pair insertion was designed as in (65). In brief, primers designed to detect specifically WT (F- GGCCCCGTCCTAGAGCTCCG, R-ATATGATAGTAACTATCCAGGATCTGCTCGTGCTACGC) amplified a 180 bp product. Primers designed to detect mutant (F- GGCCCCGTCCTAGAGCTCCG, R-

AAAAACCAGGATCTGCTCGTGCTTAGG) amplified a 159 bp product. Genotyping was verified by PCR amplifying locus and Sanger sequencing.

3.5.13 NMR

Protein Sample Preparation for NMR experiments. We purified natural abundance and ^{15}N-labeled N-terminally His_6-tagged 28-114 domain of MNoV NS1/2 protein as described (12). Single amino acid mutations were introduced with QuickChange approach. We also constructed *E. coli* expression plasmids and purified three fragments of natural abundance and ^{15}N-labeled N-terminally His_6-tagged murine VAPA protein. The isolated VAPA MSP domain, residues 8-132, gave excellent NMR spectra. Similarly, MSP domain with the following linker and coiled-coil domain, residues 8-226, gave excellent NMR spectra. As expected, VAPA residues 8-226 formed stable dimers in solution, confirmed by a size exclusion chromatography and diffusion NMR experiments. The third VAPA fragment consisting of residues 133-226, also showed dimeric size in solution, and NMR spectra indicative of contributions from α-helical and disordered segments. Protein samples were concentrated and dialyzed extensively against 10 mM KH_2PO_4, 20 mM KCl, pH 7.0. Final concentrations of NS1/2 28-114 (ε280=13,940 $M^{-1}cm^{-1}$) and VAPA (ε280=8,250 $M^{-1}cm^{-1}$) were 0.4 mM and 1.6 mM, respectively, as determined spectrophotometrically. All samples contained reducing reagent 1 mM dTECP, 5% D_2O for lock signal and 0.5 mM DSS as a chemical shift reference.

Chemical Shift Perturbation Experiments. After 24 h dialysis against the same buffer solution, protein samples were mixed by step-wise addition of VAPA solution. Each addition was followed by NMR experiments, carried out at 25 ˚C on a Bruker 600 MHz instrument equipped with a cryoprobe. First, for each ^{15}N-labeled NS1/2 protein construct, ^{15}N-^{1}H HSQC spectrum was recorded for a NS1/2 protein only. Following 5-6 spectra were recorded after each

addition of natural abundance VAPA, typically from 0.5 to 10.0-fold excess over the NS1/2 concentration present. NMR data were processed (Topspin 3.2, Bruker), and the chemical shift perturbations were analyzed using NMRFAM-SPARKY (66). The chemical shift assignments for NS1/2 (Accession nos. 19439, 19444) and closely related human VAPA (Accession no. 7025) are available in BMRB database. The specific values of chemical shifts for the buffer conditions and protein constructs used here were verified by acquisition of standard suite of triple resonance experiments on $^{13}C/^{15}N$–labeled samples. Chemical shift perturbations on ^{15}N-labeled VAPA were analyzed in analogous fashion, except that initial concentrations of VAPA and NS1/2 were 0.1 mM and 2.2 mM, respectively and the step-wise addition of NS1/2 was performed. Figures show combined difference of ^{1}H and ^{15}N chemical shifts observed between zero and the highest concentration of unlabeled protein used. The combined differences in ppm units were calculated as $\Delta\delta = \sqrt{\left\{\frac{1}{2}\left[(\Delta\delta_H)^2 + (\frac{\Delta\delta_N}{5})^2\right]\right\}}$, and hereafter they are referred to as chemical shift perturbations. The threshold for perturbations interpreted as specific protein-protein interactions was set at a value of four standard deviation above the mean perturbation excluding the highest perturbations for each data set.

3.5.14 Statistics and Software

All statistics were calculated using Graphpad Prism software. ns = $p>0.05$, *= $p\leq0.05$, **= $p\leq0.01$, ***= $p\leq0.001$, ****= $p\leq0.0001$, all error bars signify standard error mean. Sequence alignments and analysis were performed in Geneious 9.1 (http://www.geneious.com) (67). Molecular graphics were produced using UCSF Chimera (68).

3.6 Acknowledgments:

We thank the Alvin J. Siteman Cancer Center at WUSM and Barnes-Jewish Hospital in St. Louis, MO, for the use of the Genome Engineering and iPSC Center. Mice were generated using the WUSM Department of Pathology Microinjection Core. We thank Megan Baldridge, Robert Orchard, Craig Wilen, and Donna MacDuff, for intellectual contributions and reviewing the manuscript, Vernon Ward for the generous gift of anti-NS1/2 rabbit sera, and Darren Kreamalmeyer for handling and breeding mice.

The Siteman Cancer Center was supported in part by NCI Cancer Center Support Grant P30CA091842. The Washington University School of Medicine (WUSM) Department of Pathology Microinjection Core was supported by P30AR048335. HWV was supported by U19 AI 109725. BTM was supported by NCI-NIH award F31CA177194-01. TJN was supported by NIH training grant 5T32A100716334 and postdoctoral fellowships from the Cancer Research Institute and American Cancer Society. IG was supported by funding from the Wellcome Trust (ref: 097997/Z/11/Z) and the Biotechnology and Biological Sciences Research Council (ref: BB/N001176/1). JE was supported by a Churchill Scholarship. The funders did not influence study design, data collection or interpretation, or preparation of the manuscript. Neither the authors nor this study represent the official views of the funding agencies.

3.7 References

1. **Atmar RL, Estes MK.** 2006. The epidemiologic and clinical importance of norovirus infection. GastroenterolClinNorth Am **35:**275-290, viii.

2. **Hall AJ, Lopman BA, Payne DC, Patel MM, Gastanaduy PA, Vinje J, Parashar UD.** 2013. Norovirus disease in the United States. Emerg Infect Dis **19:**1198-1205.

3. **Patel MM, Hall AJ, Vinje J, Parashar UD.** 2009. Noroviruses: a comprehensive review. J Clin Virol **44:**1-8.

4. **Taube S, Kolawole AO, Hohne M, Wilkinson JE, Handley SA, Perry JW, Thackray LB, Akkina R, Wobus CE.** 2013. A mouse model for human norovirus. MBio **4**.

5. **Jones MK, Watanabe M, Zhu S, Graves CL, Keyes LR, Grau KR, Gonzalez-Hernandez MB, Iovine NM, Wobus CE, Vinje J, Tibbetts SA, Wallet SM, Karst SM.** 2014. Enteric bacteria promote human and mouse norovirus infection of B cells. Science **346:**755-759.

6. **Zheng DP, Ando T, Fankhauser RL, Beard RS, Glass RI, Monroe SS.** 2006. Norovirus classification and proposed strain nomenclature. Virology **346:**312-323.

7. **Thorne LG, Goodfellow IG.** 2014. Norovirus gene expression and replication. J Gen Virol **95:**278-291.

8. **Karst SM, Wobus CE, Goodfellow IG, Green KY, Virgin HW.** 2014. Advances in Norovirus Biology. Cell Host Microbe **15:**668-680.

9. **Sosnovtsev SV, Belliot G, Chang KO, Prikhodko VG, Thackray LB, Wobus CE, Karst SM, Virgin HW, Green KY.** 2006. Cleavage map and proteolytic processing of the murine norovirus nonstructural polyprotein in infected cells. J Virol **80:**7816-7831.

10. **McFadden N, Bailey D, Carrara G, Benson A, Chaudhry Y, Shortland A, Heeney J, Yarovinsky F, Simmonds P, Macdonald A, Goodfellow I.** 2011. Norovirus regulation of the innate immune response and apoptosis occurs via the product of the alternative open reading frame 4. PLoS Pathog **7:**e1002413.

11. **Baker ES, Luckner SR, Krause KL, Lambden PR, Clarke IN, Ward VK.** 2012. Inherent structural disorder and dimerisation of murine norovirus NS1-2 protein. PLoS ONE **7:**e30534.

12. **Borin BN, Tang W, Nice TJ, McCune BT, Virgin HW, Krezel AM.** 2013. Murine norovirus protein NS1/2 aspartate to glutamate mutation, sufficient for persistence, reorients side chain of surface exposed tryptophan within a novel structured domain. Proteins doi:10.1002/prot.24484.

13. **Nice TJ, Strong DW, McCune BT, Pohl CS, Virgin HW.** 2013. A single-amino-acid change in murine norovirus NS1/2 is sufficient for colonic tropism and persistence. J Virol **87:**327-334.

14. **Anantharaman V, Aravind L.** 2003. Evolutionary history, structural features and biochemical diversity of the NlpC/P60 superfamily of enzymes. GenomeBiol **4:**R11.

15. **Ettayebi K, Hardy ME.** 2003. Norwalk virus nonstructural protein p48 forms a complex with the SNARE regulator VAP-A and prevents cell surface expression of vesicular stomatitis virus G protein. J Virol **77:**11790-11797.

16. **Fernandez-Vega V, Sosnovtsev SV, Belliot G, King AD, Mitra T, Gorbalenya A, Green KY.** 2004. Norwalk virus N-terminal nonstructural protein is associated with disassembly of the Golgi complex in transfected cells. J Virol **78:**4827-4837.

17. **Lev S, Ben Halevy D, Peretti D, Dahan N.** 2008. The VAP protein family: from cellular functions to motor neuron disease. Trends Cell Biol **18:**282-290.

18. **Skehel PA, Martin KC, Kandel ER, Bartsch D.** 1995. A VAMP-binding protein from Aplysia required for neurotransmitter release. Science **269:**1580-1583.

19. **Weir ML, Klip A, Trimble WS.** 1998. Identification of a human homologue of the vesicle-associated membrane protein (VAMP)-associated protein of 33 kDa (VAP-33): a broadly expressed protein that binds to VAMP. Biochem J **333 (Pt 2):**247-251.

20. **Weir ML, Xie H, Klip A, Trimble WS.** 2001. VAP-A binds promiscuously to both v- and tSNAREs. Biochem Biophys Res Commun **286:**616-621.

21. **Alpy F, Rousseau A, Schwab Y, Legueux F, Stoll I, Wendling C, Spiegelhalter C, Kessler P, Mathelin C, Rio MC, Levine TP, Tomasetto C.** 2013. STARD3 or STARD3NL and VAP form a novel molecular tether between late endosomes and the ER. J Cell Sci **126:**5500-5512.

22. **Loewen CJ, Roy A, Levine TP.** 2003. A conserved ER targeting motif in three families of lipid binding proteins and in Opi1p binds VAP. EMBO J **22:**2025-2035.

23. **Wyles JP, McMaster CR, Ridgway ND.** 2002. Vesicle-associated membrane protein-associated protein-A (VAP-A) interacts with the oxysterol-binding protein to modify export from the endoplasmic reticulum. J Biol Chem **277:**29908-29918.

24. **Kumagai K, Kawano M, Shinkai-Ouchi F, Nishijima M, Hanada K.** 2007. Interorganelle trafficking of ceramide is regulated by phosphorylation-dependent cooperativity between the PH and START domains of CERT. J Biol Chem **282:**17758-17766.

25. **Kawano M, Kumagai K, Nishijima M, Hanada K.** 2006. Efficient trafficking of ceramide from the endoplasmic reticulum to the Golgi apparatus requires a VAMP-associated protein-interacting FFAT motif of CERT. J Biol Chem **281:**30279-30288.

26. **Furuita K, Jee J, Fukada H, Mishima M, Kojima C.** 2010. Electrostatic interaction between oxysterol-binding protein and VAMP-associated protein A revealed by NMR and mutagenesis studies. J Biol Chem **285:**12961-12970.

27. **Mikitova V, Levine TP.** 2012. Analysis of the key elements of FFAT-like motifs identifies new proteins that potentially bind VAP on the ER, including two AKAPs and FAPP2. PLoS One **7:**e30455.

28. **Kaiser SE, Brickner JH, Reilein AR, Fenn TD, Walter P, Brunger AT.** 2005. Structural basis of FFAT motif-mediated ER targeting. Structure **13:**1035-1045.

29. **Loewen CJ, Levine TP.** 2005. A highly conserved binding site in vesicle-associated membrane protein-associated protein (VAP) for the FFAT motif of lipid-binding proteins. J Biol Chem **280:**14097-14104.

30. **Tu H, Gao L, Shi ST, Taylor DR, Yang T, Mircheff AK, Wen Y, Gorbalenya AE, Hwang SB, Lai MM.** 1999. Hepatitis C virus RNA polymerase and NS5A complex with a SNARE-like protein. Virology **263:**30-41.

31. **Evans MJ, Rice CM, Goff SP.** 2004. Phosphorylation of hepatitis C virus nonstructural protein 5A modulates its protein interactions and viral RNA replication. Proc Natl Acad Sci U S A **101:**13038-13043.

32. **Roulin PS, Lotzerich M, Torta F, Tanner LB, van Kuppeveld FJ, Wenk MR, Greber UF.** 2014. Rhinovirus uses a phosphatidylinositol 4-phosphate/cholesterol counter-current for the formation of replication compartments at the ER-Golgi interface. Cell Host Microbe **16:**677-690.

33. **Barajas D, Xu K, de Castro Martin IF, Sasvari Z, Brandizzi F, Risco C, Nagy PD.** 2014. Co-opted oxysterol-binding ORP and VAP proteins channel sterols to RNA virus replication sites via membrane contact sites. PLoS Pathog **10:**e1004388.

34. **Barajas D, Xu K, Sharma M, Wu CY, Nagy PD.** 2014. Tombusviruses upregulate phospholipid biosynthesis via interaction between p33 replication protein and yeast lipid sensor proteins during virus replication in yeast. Virology **471-473:**72-80.

35. **Elwell CA, Jiang S, Kim JH, Lee A, Wittmann T, Hanada K, Melancon P, Engel JN.** 2011. Chlamydia trachomatis co-opts GBF1 and CERT to acquire host sphingomyelin for distinct roles during intracellular development. PLoS Pathog **7:**e1002198.

36. **Derre I, Swiss R, Agaisse H.** 2011. The lipid transfer protein CERT interacts with the Chlamydia inclusion protein IncD and participates to ER-Chlamydia inclusion membrane contact sites. PLoS Pathog **7:**e1002092.

37. **Gao L, Aizaki H, He JW, Lai MM.** 2004. Interactions between viral nonstructural proteins and host protein hVAP-33 mediate the formation of hepatitis C virus RNA replication complex on lipid raft. J Virol **78:**3480-3488.

38. **Berger KL, Randall G.** 2009. Potential roles for cellular cofactors in hepatitis C virus replication complex formation. Commun Integr Biol **2:**471-473.

39. **Amini-Bavil-Olyaee S, Choi YJ, Lee JH, Shi M, Huang IC, Farzan M, Jung JU.** 2013. The antiviral effector IFITM3 disrupts intracellular cholesterol homeostasis to block viral entry. Cell Host Microbe **13:**452-464.

40. **Wang S, Wu X, Pan T, Song W, Wang Y, Zhang F, Yuan Z.** 2012. Viperin inhibits hepatitis C virus replication by interfering with binding of NS5A to host protein hVAP-33. J Gen Virol **93:**83-92.

41. **Helbig KJ, Eyre NS, Yip E, Narayana S, Li K, Fiches G, McCartney EM, Jangra RK, Lemon SM, Beard MR.** 2011. The antiviral protein viperin inhibits hepatitis C virus replication via interaction with nonstructural protein 5A. Hepatology **54:**1506-1517.

42. **Rocha N, Kuijl C, van der Kant R, Janssen L, Houben D, Janssen H, Zwart W, Neefjes J.** 2009. Cholesterol sensor ORP1L contacts the ER protein VAP to control Rab7-RILP-p150 Glued and late endosome positioning. J Cell Biol **185:**1209-1225.

43. **Perry JW, Wobus CE.** 2010. Endocytosis of murine norovirus 1 into murine macrophages is dependent on dynamin II and cholesterol. J Virol **84:**6163-6176.

44. **Gerondopoulos A, Jackson T, Monaghan P, Doyle N, Roberts LO.** 2010. Murine norovirus-1 cell entry is mediated through a non-clathrin-, non-caveolae-, dynamin- and cholesterol-dependent pathway. J Gen Virol **91:**1428-1438.

45. **Shivanna V, Kim Y, Chang KO.** 2015. Ceramide formation mediated by acid sphingomyelinase facilitates endosomal escape of caliciviruses. Virology **483:**218-228.

46. **Vashist S, Urena L, Goodfellow I.** 2012. Development of a strand specific real-time RT-qPCR assay for the detection and quantitation of murine norovirus RNA. J Virol Methods **184:**69-76.

47. **Thorne L, Bailey D, Goodfellow I.** 2012. High-resolution functional profiling of the norovirus genome. J Virol **86:**11441-11456.

48. **Nishimura Y, Hayashi M, Inada H, Tanaka T.** 1999. Molecular cloning and characterization of mammalian homologues of vesicle-associated membrane protein-associated (VAMP-associated) proteins. Biochem Biophys Res Commun **254:**21-26.

49. **Hyde JL, Sosnovtsev SV, Green KY, Wobus C, Virgin HW, Mackenzie JM.** 2009. Mouse norovirus replication is associated with virus-induced vesicle clusters originating from membranes derived from the secretory pathway. J Virol **83:**9709-9719.

50. **Borin BN, Tang W, Nice TJ, McCune BT, Virgin HW, Krezel AM.** 2014. Murine norovirus protein NS1/2 aspartate to glutamate mutation, sufficient for persistence, reorients side chain of surface exposed tryptophan within a novel structured domain. Proteins **82:**1200-1209.

51. **Hagai T, Azia A, Babu MM, Andino R.** 2014. Use of host-like peptide motifs in viral proteins is a prevalent strategy in host-virus interactions. Cell Rep **7:**1729-1739.

52. **Hyde JL, Mackenzie JM.** 2010. Subcellular localization of the MNV-1 ORF1 proteins and their potential roles in the formation of the MNV-1 replication complex. Virology **406:**138-148.

53. **Nikawa J, Murakami A, Esumi E, Hosaka K.** 1995. Cloning and sequence of the SCS2 gene, which can suppress the defect of INO1 expression in an inositol auxotrophic mutant of Saccharomyces cerevisiae. J Biochem **118:**39-45.

54. **Kagiwada S, Zen R.** 2003. Role of the yeast VAP homolog, Scs2p, in INO1 expression and phospholipid metabolism. J Biochem **133:**515-522.

55. **Loewen CJ, Young BP, Tavassoli S, Levine TP.** 2007. Inheritance of cortical ER in yeast is required for normal septin organization. J Cell Biol **179:**467-483.

56. **Weber-Boyvat M, Kentala H, Peranen J, Olkkonen VM.** 2015. Ligand-dependent localization and function of ORP-VAP complexes at membrane contact sites. Cell Mol Life Sci **72:**1967-1987.

57. **Mesmin B, Bigay J, Moser von Filseck J, Lacas-Gervais S, Drin G, Antonny B.** 2013. A four-step cycle driven by PI(4)P hydrolysis directs sterol/PI(4)P exchange by the ER-Golgi tether OSBP. Cell **155:**830-843.

58. **Wakana Y, Kotake R, Oyama N, Murate M, Kobayashi T, Arasaki K, Inoue H, Tagaya M.** 2015. CARTS biogenesis requires VAP-lipid transfer protein complexes functioning at the endoplasmic reticulum-Golgi interface. Mol Biol Cell **26:**4686-4699.

59. **Kumagai K, Kawano-Kawada M, Hanada K.** 2014. Phosphoregulation of the ceramide transport protein CERT at serine 315 in the interaction with VAMP-associated protein (VAP) for inter-organelle trafficking of ceramide in mammalian cells. J Biol Chem **289:**10748-10760.

60. **Liu H, Naismith JH.** 2008. An efficient one-step site-directed deletion, insertion, single and multiple-site plasmid mutagenesis protocol. BMC Biotechnol **8:**91.

61. **Chaudhry Y, Skinner MA, Goodfellow IG.** 2007. Recovery of genetically defined murine norovirus in tissue culture by using a fowlpox virus expressing T7 RNA polymerase. JGenVirol **88:**2091-2100.

62. **Hwang S, Alhatlani B, Arias A, Caddy SL, Christodoulou C, Cunha JB, Emmott E, Gonzalez-Hernandez M, Kolawole A, Lu J, Rippinger C, Sorgeloos F, Thorne L, Vashist S, Goodfellow I, Wobus CE.** 2014. Murine norovirus: propagation, quantification, and genetic manipulation. Curr Protoc Microbiol **33:**15K 12 11-61.

63. **Greninger AL, Knudsen GM, Betegon M, Burlingame AL, DeRisi JL.** 2013. ACBD3 interaction with TBC1 domain 22 protein is differentially affected by enteroviral and kobuviral 3A protein binding. MBio **4:**e00098-00013.

64. **Parikh BA, Beckman DL, Patel SJ, White JM, Yokoyama WM.** 2015. Detailed phenotypic and molecular analyses of genetically modified mice generated by CRISPR-Cas9-mediated editing. PLoS One **10:**e0116484.

65. **Gaudet M, Fara AG, Beritognolo I, Sabatti M.** 2009. Allele-specific PCR in SNP genotyping. Methods Mol Biol **578:**415-424.

66. **Lee W, Tonelli M, Markley JL.** 2015. NMRFAM-SPARKY: enhanced software for biomolecular NMR spectroscopy. Bioinformatics **31:**1325-1327.

67. **Kearse M, Moir R, Wilson A, Stones-Havas S, Cheung M, Sturrock S, Buxton S, Cooper A, Markowitz S, Duran C, Thierer T, Ashton B, Meintjes P, Drummond A.** 2012. Geneious Basic: an integrated and extendable desktop software platform for the organization and analysis of sequence data. Bioinformatics **28:**1647-1649.

68. **Pettersen EF, Goddard TD, Huang CC, Couch GS, Greenblatt DM, Meng EC, Ferrin TE.** 2004. UCSF Chimera--a visualization system for exploratory research and analysis. J Comput Chem **25:**1605-1612.

3.8 Figures

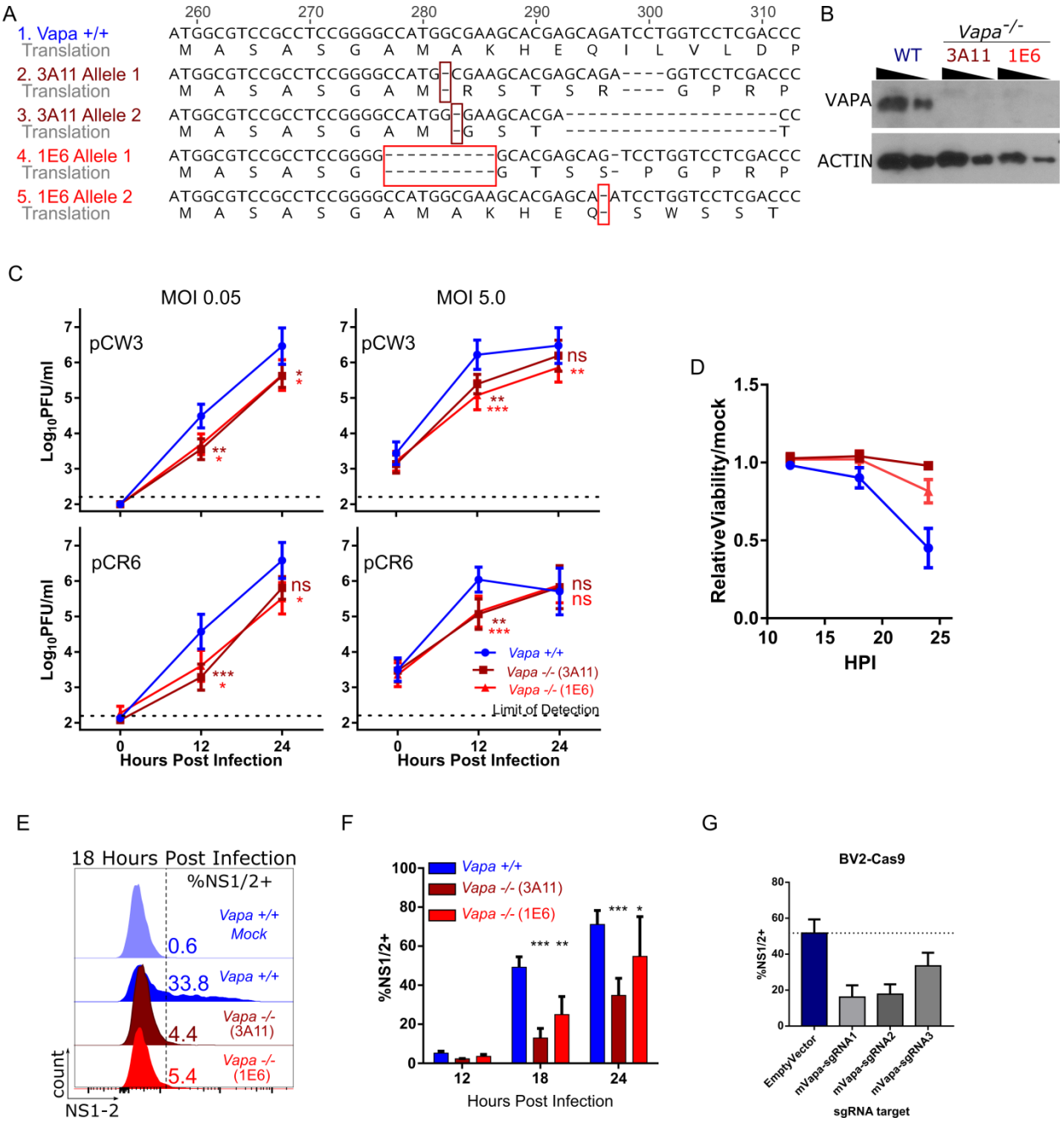

Figure 3.1. MNoV replication in *Vapa*$^{-/-}$ cells is diminished.

(A) Alignment of genomic sequence and translation for two *Vapa* edited RAW264.7 cell lines with WT *Vapa*$^{+/+}$ (NM_013933) (top), showing both mutant alleles for each cell line. Numbering relative to transcript start.

(B) Western blot against VAPA and ACTIN (loading control) in WT and *Vapa*$^{-/-}$ cell lines.

(C) Murine norovirus strains-CW3 (top) or CR6 (bottom) growth in *Vapa*$^{-/-}$ and *Vapa*$^{+/+}$ cell lines, MOI 0.05 (left) or 5.0 (right) PFU/ml. Repeated measure one-way ANOVA, Dunnett post-test.

(D) Cell viability of MNoV infected *Vapa*$^{-/-}$ and *Vapa*$^{+/+}$ cell lines determined by live/dead fixable stain followed by FACS, relative to WT mock infected.

(E) Representative infection frequency of MNoV-CW3 in *Vapa*$^{-/-}$ cells, measured by intracellular FACS of NS1/2, 18 hours post infection.

(F) Same as (E), combined experiments, repeated measure two-way ANOVA, Dunnett post-test, n=3.

(G) Infection frequency of BV2-Cas9 cells transduced with one of three lentiviruses expressing unique sgRNA against *Vapa.* MOI 0.1, n=3.

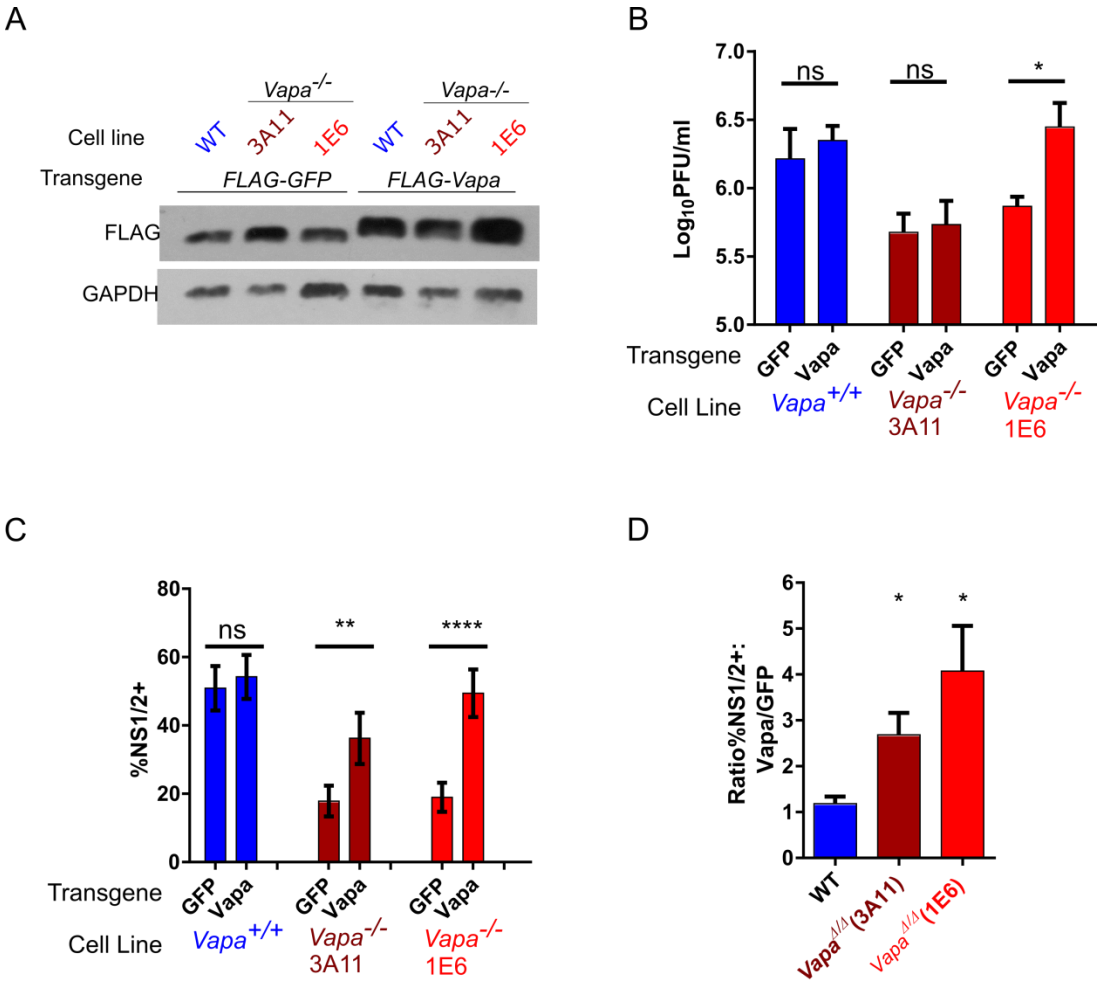

Figure 3.2. Reconstitution of VAPA expression in *Vapa*$^{-/-}$ cells rescues MNoV infectivity.

(A) Western blot of *Vapa*$^{+/+}$ or *Vapa*$^{-/-}$ cell lines lentivirally transduced with *FLAG-GFP* or *FLAG-Vapa*, GAPDH loading control.

(B) MNoV-CW3 growth 18hpi in *Vapa* or *GFP* in transduced cells as in (A). Two-way ANOVA, Sidak post-test.

(C) MNoV infection frequency in *FLAG-Vapa* or *FLAG-GFP* transduced cells as in (A), two-way ANOVA Sidak post-test, n=9.

(D) Relative MNoV infectivity in *FLAG-Vapa* transduced cells, relative to *FLAG-GFP* transduced cells for each cell line. Two-tailed t-test relative to H_0=1.

A

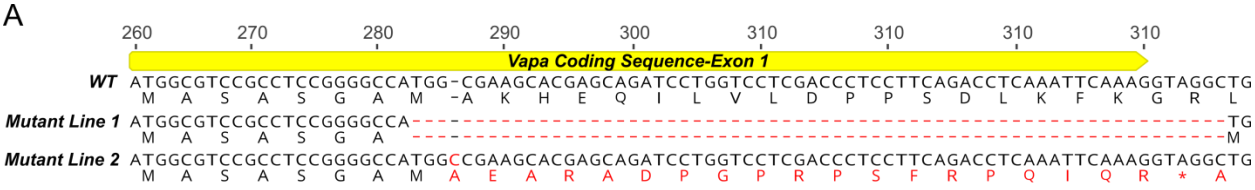

B

Genotype of Live Pups from Heterozygote Crosses.

	Line 1	Line 2	Total
Total	62	59	121
Vapa+/+	26	21	47
Vapa+/-	36	38	74
Vapa-/-	0	0	0
Ratio	1.4:1:0	1.8:1:0	1.6:1:0

C

Genotype of Day 14 Embryos.

	Line 1	Line 2	Total
Vapa+/+	5	6	11
Vapa+/-	3	12	15
Vapa-/-	1	1	2
Undetermined	0	2	2

Figure 3.3. *Vapa*$^{-/-}$ mice are embryonic lethal.

(A) Alignment of two *Vapa* mutant mouse lines generated by electroporating embryonic stem cells with Cas9 and gRNA targeting *Vapa*. Note mutant line 1 has splice junction deleted, and mutant line 2 has single base pair insertion. Numbering relative to transcript start.

(B) Number of live pups of indicated genotypes from heterozygote crosses.

(C) Number of day 14 embryos of indicated genotype. Embryonic day 14 embryos were isolated from heterozygote crosses and genotyped, four litters total. Undetermined refers to samples for which PCR failed to amplify.

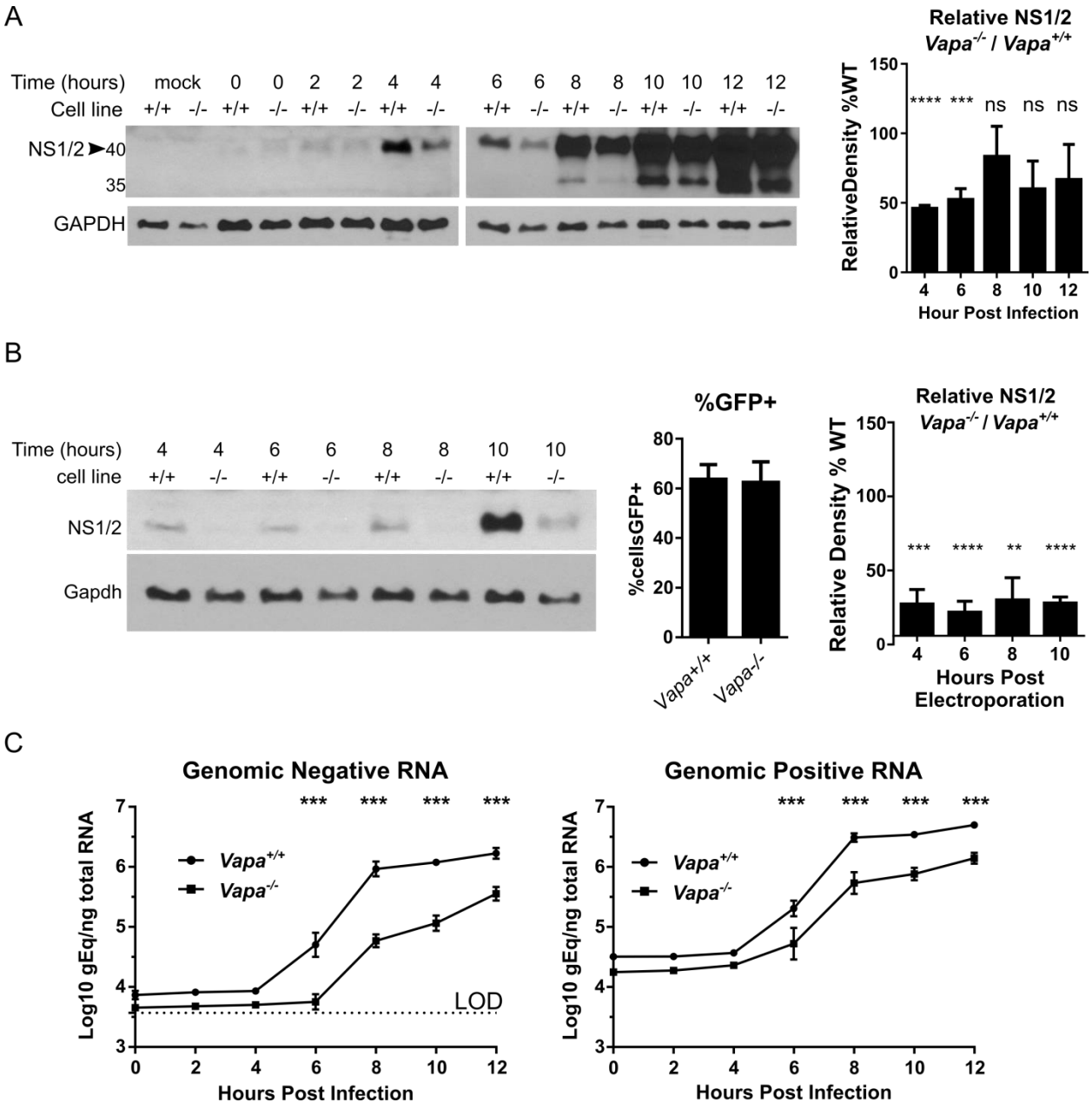

Figure 3.4. MNoV replication in RAW264.7-*Vapa*$^{-/-}$ cells is impaired early in viral life cycle.

(A) Western blot of NS1/2 in *Vapa*$^{+/+}$ and *Vapa*$^{-/-}$ (3A11) cell lines, MOI 5. Right, combined densitometry from multiple experiments performed on film exposures for each time point within linear range of assay (n=2-4), (unpaired t-test, means compared to H_O=1).

(B) NS1/2 western blot after electroporating vRNA into *Vapa*$^{+/+}$ and *Vapa*$^{-/-}$ cells (representative, n=3-5). Middle, *Vapa*$^{+/+}$ and *Vapa*$^{-/-}$ cells are transfected equivalently with

pMAX-GFP. Right, combined densitometry as in (A) (n=3-5).

(C) Viral strand-specific quantitative PCR for negative strand (left) and positive strand (right) over time in infected *Vapa*$^{+/+}$ and *Vapa*$^{-/-}$ cells, MOI 5 (n=3, two-way ANOVA).

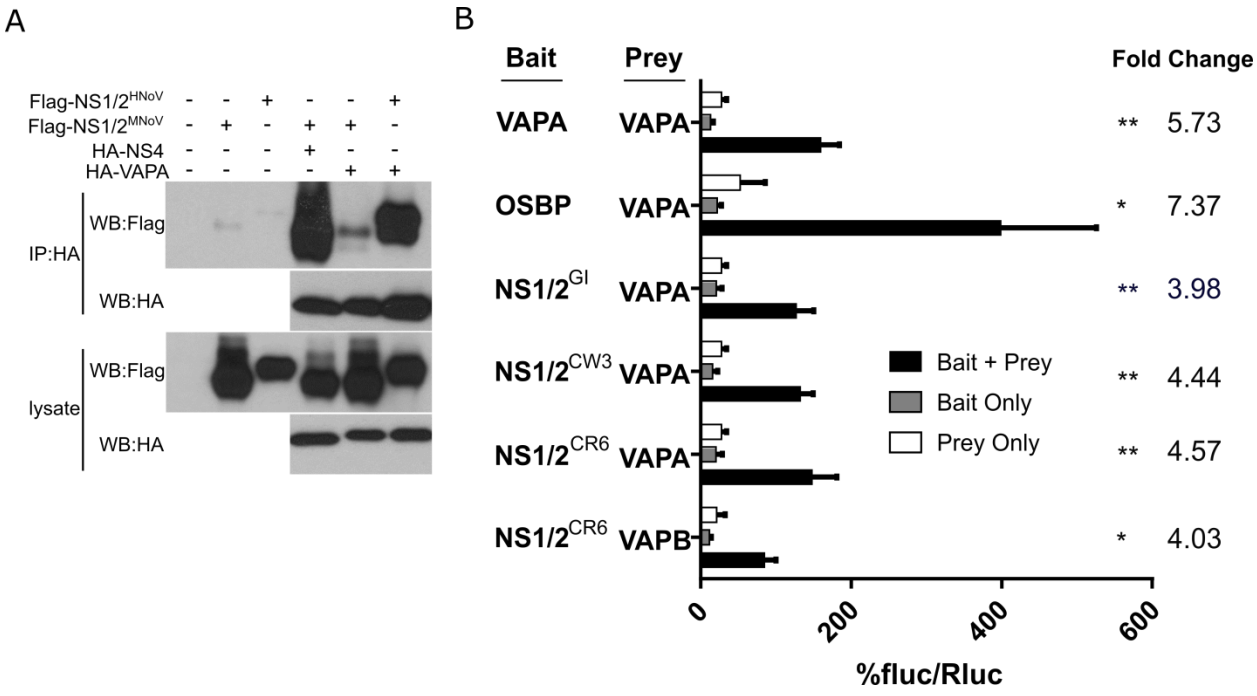

Figure 3.5. NS1/2 interaction with VAPA is conserved among norovirus strains.

(A) Representative immunoprecipitation of Flag-NS1/2-HNoV (GI), -MNoV (CR6) with HA-VAPA or HA-NS4 (n=3).

(B) M2H interaction of NS1/2^{GI}, NS1/2^{MNoV} (CR6 and CW3), OSBP, and VAPA with VAPA, as well as NS1/2^{CR6} with VAPB (one-way ANOVA, Dunnett; fold change on right).

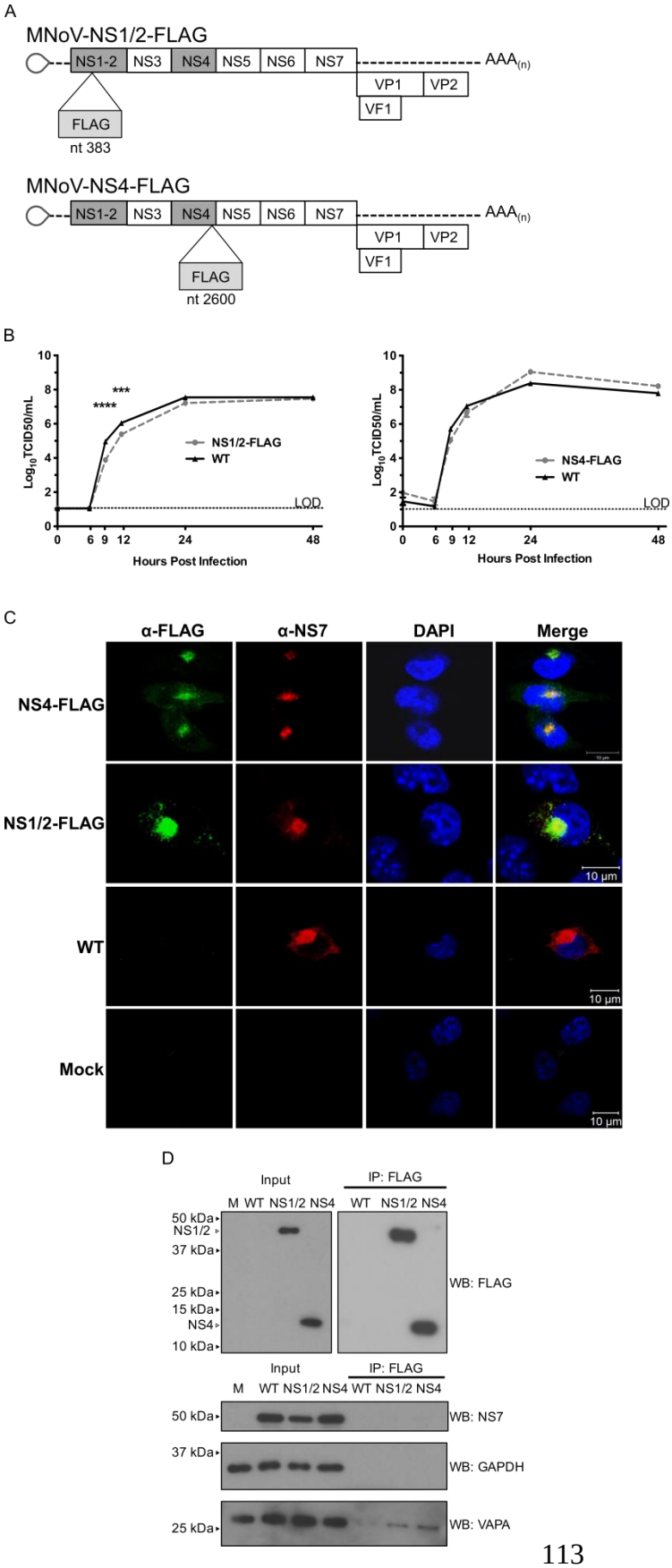
A
MNoV-NS1/2-FLAG
NS1-2
NS3
NS4
NS5
NS6
NS7
AAA(n)
VP1
VP2
VF1
FLAG
nt 383
MNoV-NS4-FLAG
NS1-2
NS3
NS4
NS5
NS6
NS7
AAA(n)
VP1
VP2
VF1
FLAG
nt 2600
B
Log10TCID50/mL
***
****
NS1/2-FLAG
WT
LOD
Hours Post Infection
Log10TCID50/mL
NS4-FLAG
WT
LOD
Hours Post Infection
C
α-FLAG
α-NS7
DAPI
Merge
NS4-FLAG
NS1/2-FLAG
WT
Mock
10 μm
D
Input
IP: FLAG
M WT NS1/2 NS4
WT NS1/2 NS4
50 kDa
NS1/2
37 kDa
25 kDa
15 kDa
NS4
10 kDa
WB: FLAG
Input
IP: FLAG
M WT NS1/2 NS4 WT NS1/2 NS4
50 kDa
WB: NS7
37 kDa
WB: GAPDH
25 kDa
WB: VAPA

Figure 3.6. NS1/2 interacts with VAPA during infection.

(A) Engineering infectious FLAG-tagged MNoV. The FLAG epitope tag was inserted into sites in NS1/2 (top) or in NS4 (bottom) (47).

(B) Growth characterization of the NS1/2-FLAG (left) and NS4-FLAG (right) viruses. A multistep growth curve was performed by infecting BV2 cells with either virus at an MOI of 0.01 $TCID_{50}$/cell. Virus was harvested at the specified time points and viral titer determined by $TCID_{50}$. Two-way ANOVA, Bonferroni post-test compared WT and FLAG-insertion virus at each time point, n=3. LOD: limit of detection, 11.2 $TCID_{50}$/ml.

(C) Immunofluorescence in BV2 cells infected with NS1/2-FLAG, NS4-FLAG or WT virus, labeled on left of panels, MOI 5 $TCID_{50}$/cell, 12hpi. Samples were stained for FLAG, NS7, and DAPI, labeled on top of panels.

(D) BV2 cells were infected with NS1/2-FLAG or NS4-FLAG MNV for 8 hours, MOI 10 $TCID_{50}$/cell. FLAG pulldowns were performed on lysates, and immunoblotted with the specified antibodies.

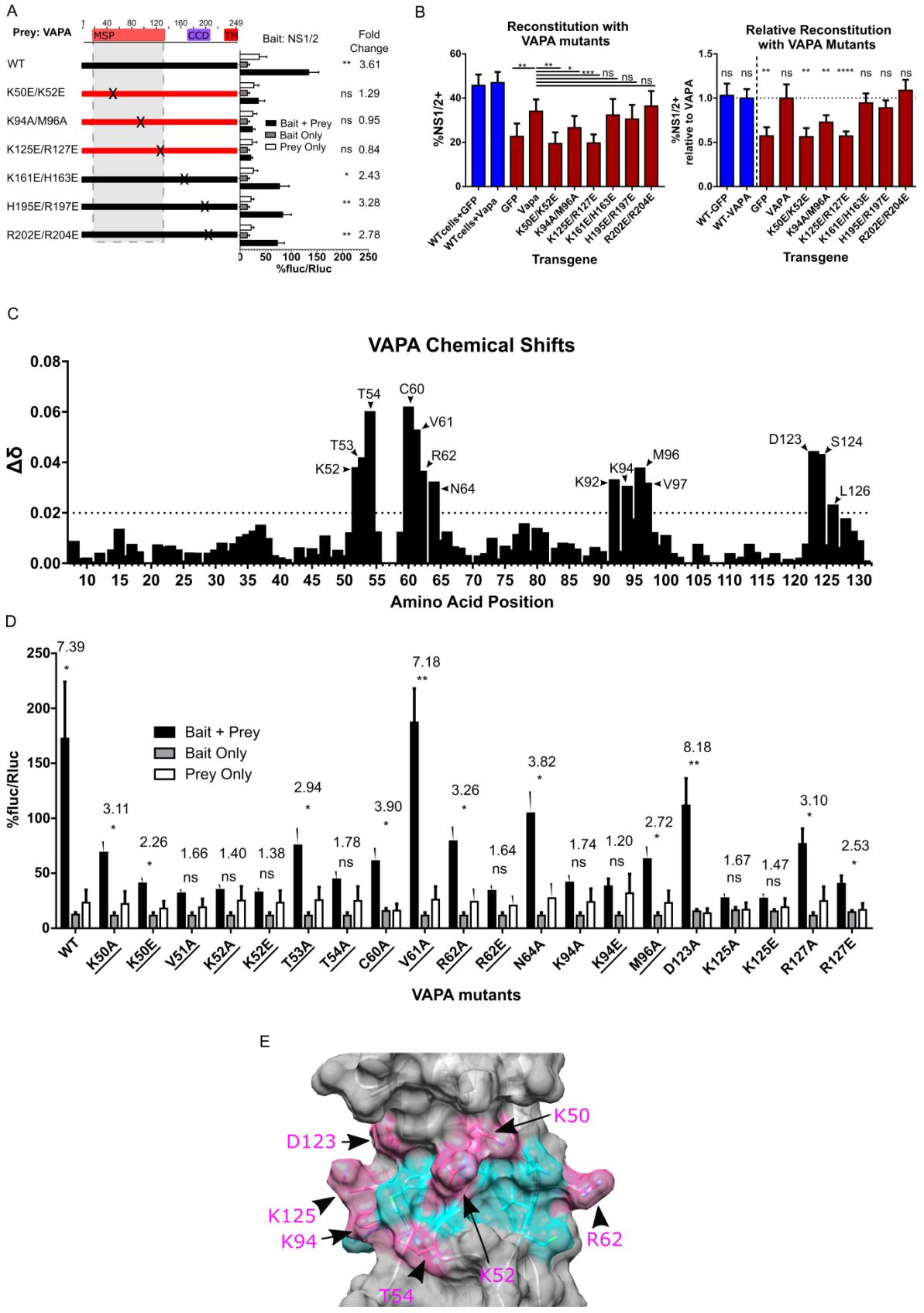
A
Prey: VAPA
MSP
CCD
TM
Bait: NS1/2
Fold Change
WT
K50E/K52E
K94A/M96A
K125E/R127E
K161E/H163E
H195E/R197E
R202E/R204E
Bait + Prey
Bait Only
Prey Only
%fluc/Rluc
B
Reconstitution with VAPA mutants
%NS1/2+
Transgene
Relative Reconstitution with VAPA Mutants
%NS1/2+ relative to VAPA
C
VAPA Chemical Shifts
Δδ
Amino Acid Position
D
%fluc/Rluc
Bait + Prey
Bait Only
Prey Only
VAPA mutants
E
K50
D123
K125
K94
R62
K52
T54

Figure 3.7. NS1/2 binds FFAT-interacting residues in MSP domain of VAPA.

(A) M2H interaction of NS1/2^{MNoV} with VAPA mutants.

(B) MNoV infectivity in *Vapa*$^{-/-}$ cells transduced with lentivirus expressing GFP, VAPA, and VAPA mutants. Showing fold change %NS1/2+ cells in VAPA (or VAPA mutant) transduced cells over GFP transduced cells.

(C) Chemical shift perturbations of amide resonances upon unlabeled-NS1^{CW3} titration into ^{15}N-labeled VAPA MSP. Horizontal broken line represents threshold.

(D) M2H analysis of additional single residue mutant VAPA. Underline=residues interacting with FFAT as shown by NMR and crystal structure (26, 28).

(E) Murine VAPA MSP domain (PDB: 2CRI). Pink residues disrupted NS1/2-VAPA interaction in M2H when mutated; mutations in cyan-colored residues did not disrupt interaction.

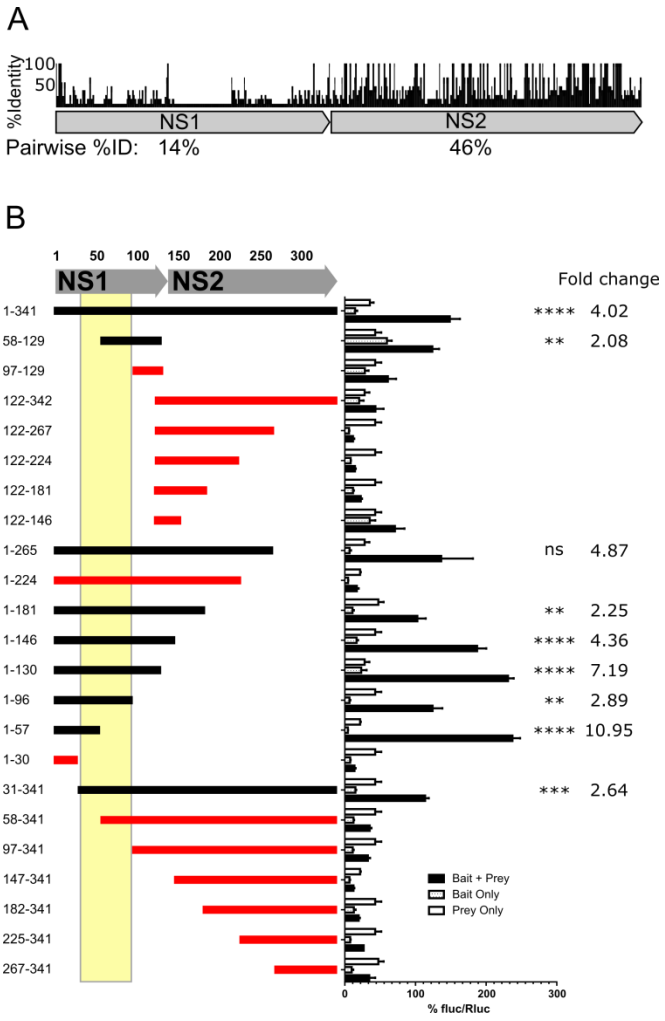

Figure 3.8. Poorly conserved NS1 domain within NS1/2^{MNoV} interacts with VAPA.

(A) Alignment of NS1/2 from representative strains from each norovirus genogroup.

(B) M2H of full length or truncations of NS1/2^{MNoV} (CR6) with VAPA.

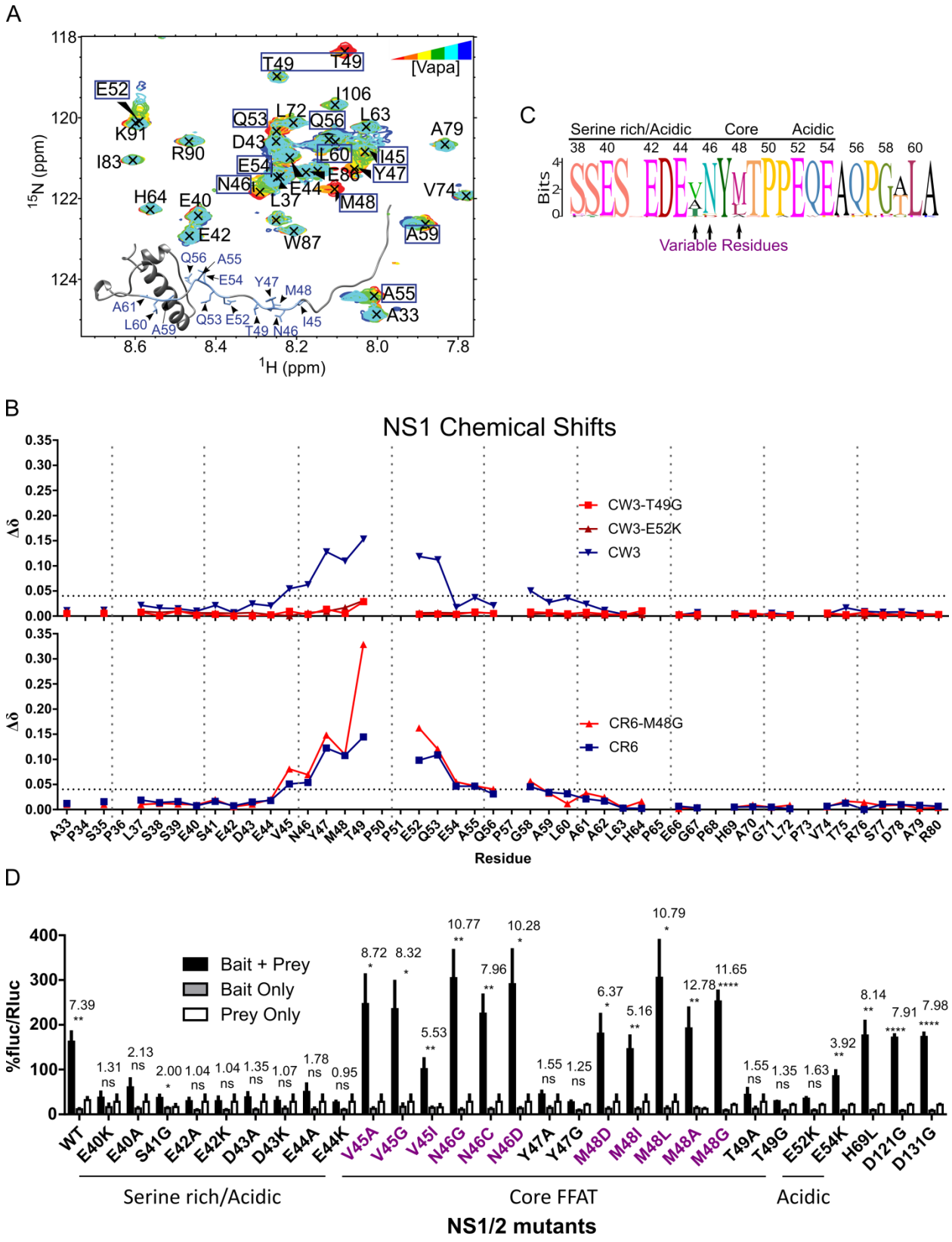
A
[Vapa]
^{15}N (ppm)
^{1}H (ppm)
C
Serine rich/Acidic
Core
Acidic
Bits
Variable Residues
B
NS1 Chemical Shifts
CW3-T49G
CW3-E52K
CW3
CR6-M48G
CR6
Δδ
Residue
D
%fluc/Rluc
Bait + Prey
Bait Only
Prey Only
Serine rich/Acidic
Core FFAT
Acidic
NS1/2 mutants

Figure 3.9. N-terminal segment of NS1-MNoV interacts with VAPA.

(A) A portion of superimposed ^{1}H-^{15}N HSQC spectra of $NS1^{CW3}$ with increasing levels of VAPA. Molar ratio NS1:VAPA: 1:0.0, red; 1:0.3, orange; 1:0.6, yellow; 1:1.2, green; 1:2.6, cyan; 1:4.9, blue. Assignments and peak positions are shown for free NS1 sample. Insert shows structure of NS1 28-114 (PDB: 2MCH), with core VAPA interacting residues labeled in blue.

(B) Chemical shift perturbations of amide resonances upon unlabeled-VAPA titration into ^{15}N-labeled NS1-CR6, CW3, $CR6^{M48G}$, $CW3^{T49G}$, and $CW3^{E52K}$. Horizontal broken line is threshold.

(C) Sequence logo of FFAT-like amino acid sequence of NS1/2 derived from BLAST alignment (Supplemental Figure 6). Font size for each amino acid proportional to percent conservation at each position.

(D) M2H interaction with NS1/2 substitutions (NS1/2: bait, VAPA: prey). Residues 69, 121, and 131 are not predicted to interact with VAPA. Purple residues same as (C).

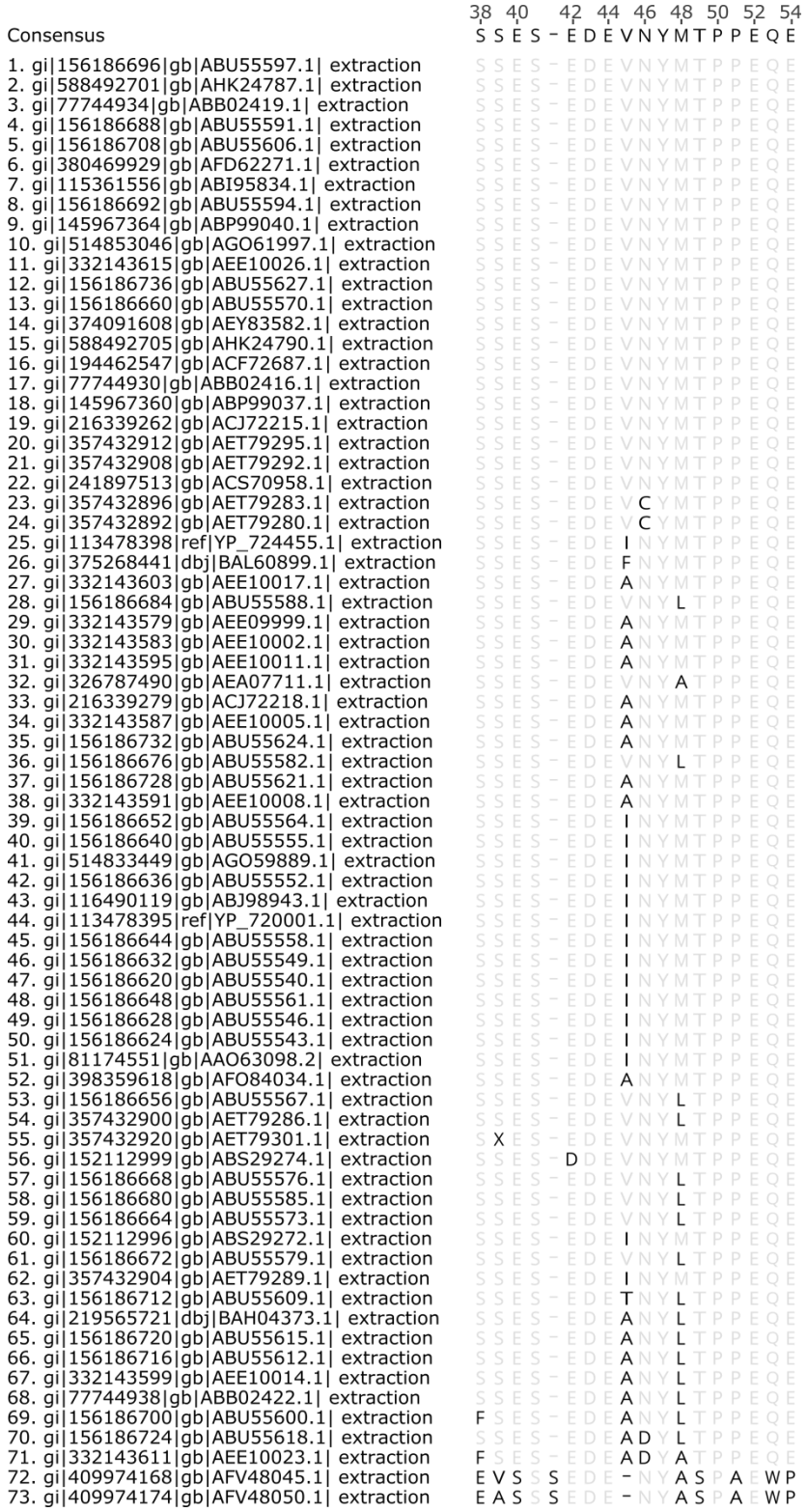

Figure 3.10.BLAST alignment of NS1/2 sequence resembling FFAT.

Bottom two sequences are from Rat Norovirus, the most divergent NS1/2 sequence within GV.

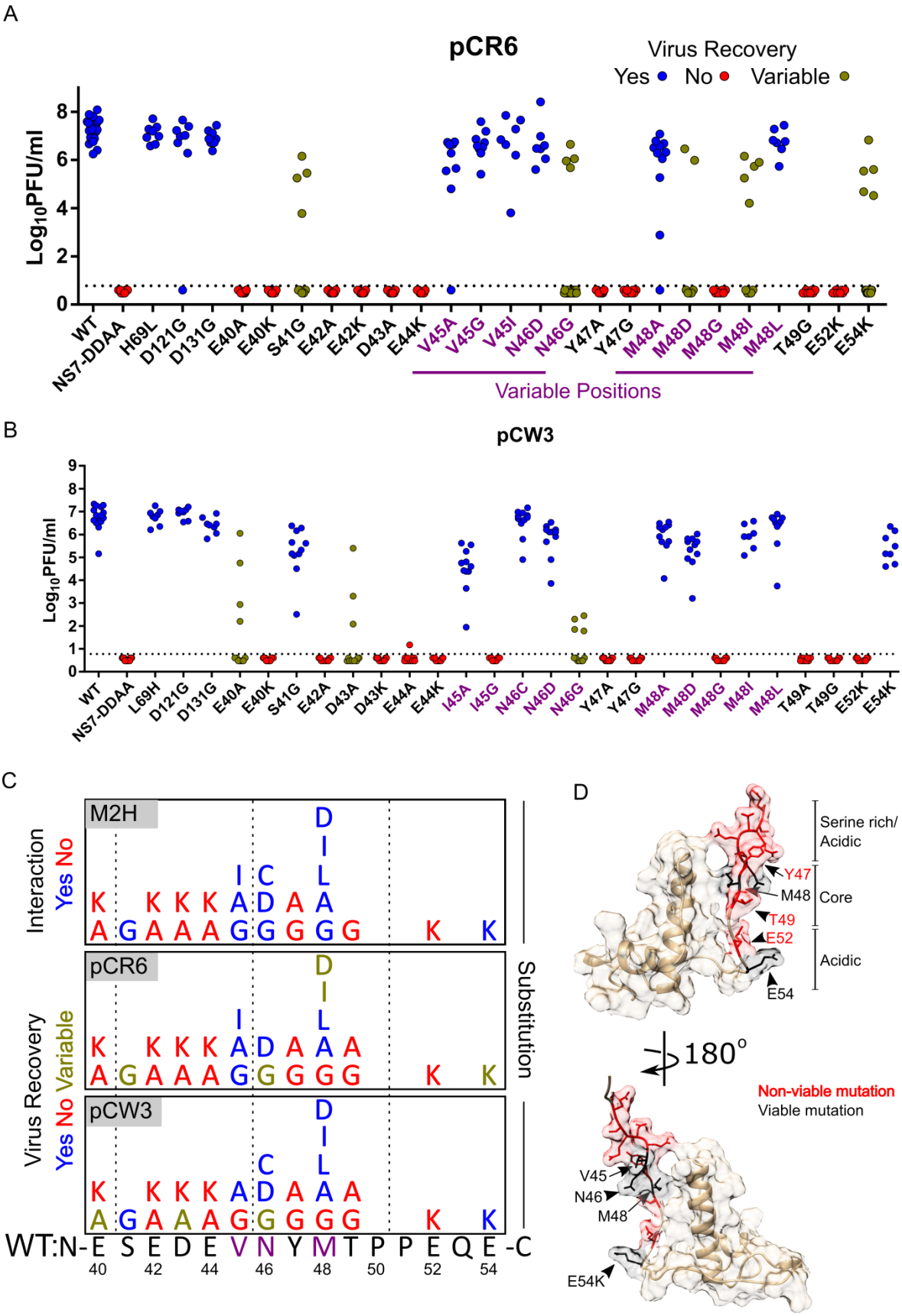
A
pCR6
Virus Recovery
Yes
No
Variable
Log10PFU/ml
WT
NS7-DDAA
H69L
D121G
D131G
E40A
E40K
S41G
E42A
E42K
D43A
E44K
V45A
V45G
V45I
N46D
N46G
Y47A
Y47G
M48A
M48D
M48G
M48I
M48L
T49G
E52K
E54K
Variable Positions
B
pCW3
Log10PFU/ml
WT
NS7-DDAA
L69H
D121G
D131G
E40A
E40K
S41G
E42A
D43A
D43K
E44A
E44K
I45A
I45G
N46C
N46D
N46G
Y47A
Y47G
M48A
M48D
M48G
M48I
M48L
T49A
T49G
E52K
E54K
C
M2H
Interaction
Yes No
pCR6
Virus Recovery
Yes No Variable
pCW3
Substitution
WT:N-E S E D E V N Y M T P P E Q E -C
40 42 44 46 48 50 52 54
D
Serine rich/
Acidic
Y47
M48
Core
T49
E52
Acidic
E54
180°
Non-viable mutation
Viable mutation
V45
N46
M48
E54K

Figure 3.11. NS1/2 interaction with VAPA enhances recovery of MNoV from infectious clones.

(A) Recovery titers of mutants of MNoV strain pCR6. Showing passage one titers (n=7-20). Virus was quantified by plaque assay. Purple text indicates less conserved residue as in Fig 3.9C.

(B) Same as (A) but using MNoV-pCW3.

(C) Summary of interaction of NS1/2 mutants with Vapa in M2H, and recovery of virus from infectious clones for CW3 and CR6 NS1/2 mutants. Purple text same as (A).

(D) Solution structure of NS1-MNoV with viable (black) and non-viable (red) mutants.

Chapter 4:
Summary and Future Directions

4.1 Summary

The unifying theme in this dissertation is the molecular mechanisms of NoV replication in mice and cells. We directed the work to the following questions: 1) what are the viral mechanisms to establish persistent infection in mice, and 2) what is the function of NoV protein NS1/2? The work presented herein described the importance of the viral molecule NS1/2 during persistent infection in mice and viral replication in cell culture. VP1 was an important determinant of tropism *in vivo* and *ex vivo* for different MNoV strains. Lastly, this work uncovered a role for the host molecule VAPA during MNoV infection.

In Chapter 2, we found NS1/2 and VP1 are major determinants of persistence and tropism. The NS1 domain of the NS1/2 protein from MNoV strain CR6 conferred persistence and colonic tropism on CW3. This mapped to a single amino acid change within NS1, D94E, which conferred persistence on CW3. While E94D did not prevent CR6 persistence, other mutants within NS1 domain did not persist, including mutations that disrupt proteolytic cleavage of NS1 and NS2 domains. Viruses with NS1/2 mutants replicated equivalently to WT virus in cell culture, but many NS1/2 mutant viruses had delayed release of virus from cells. This work establishes important functions for NS1/2 in establishing persistent infection in mice and viral replication in cell culture. NS1/2 has hitherto been poorly characterized, and these observations expand what is known about NS1/2.

$VP1^{CW3}$ conferred splenic tropism on CR6, and $VP1^{CR6}$ prevented splenic tropism on CW3. Furthermore, viruses with $VP1^{CW3}$ grew robustly in BMDMs in cell culture while viruses with $VP1^{CR6}$ grew poorly. These studies 1) strengthen a role for VP1 as a determinant of tropism and 2) highlight a role for cellular tropism as a mechanism for phenotypic differences among MNoV strains.

In Chapter 3, we found MNoV replication is enhanced by the host protein VAPA. Loss of VAPA expression led to a delay in production of NS1/2 very early in infection. VAPA enhanced viral infection in part by directly interacting with NS1/2. The sequence in NS1/2 that interacted with VAPA closely resembled the FFAT host motif that mediates host protein interaction with VAPA. Furthermore, the mechanism for interaction with VAPA by NS1/2 was similar to FFAT interaction with VAPA. This represents the first detailed cellular mechanism described for NS1/2. This is also the first reported example of microbial mimicry of FFAT motifs.

4.2 Future Directions

4.2.1 Persistence

NS1/2^{CR6} conferred colonic tropism and persistent shedding of MNoV in mice but the functions of NS1/2 during infection is unknown. NS1/2 variants associated with persistence are structurally different in the NS1 domain, and how this alters NS1/2 functionally is an important question. Because both NS1/2^{CR6} and NS1/2^{CW3} equivalently bind VAPA, and are similarly affected by loss of VAPA expression, it is unlikely that VAPA alone is related to persistence. Therefore, more fundamental information about the function of NS1/2 is required to assess how this conformational change affects persistence. One approach will be to determine what other proteins NS1/2 interact with during infection using NS1/2-FLAG tagged virus for different MNoV strains, and performing immunoprecipitations. This approach was validated herein, and promises to be a powerful strategy to discover additional NS1/2 interacting proteins during infection.

While this work did not focus on innate immune responses, emerging studies have identified connections among persistence, tropism, and innate immunity for MNoV. Therefore, innate

immunity against MNoV is a key future direction to understand persistence and tropism. MNoV is controlled by type I and type III interferons (IFN) in systemic and intestinal tissues, respectively (1, 2). $VP1^{CW3}$ is linked to induction of type III IFN, IFNλ, which correlates with clearance of MNoV from mice (1). It is nevertheless unclear if VP1 is the sole determinant of IFNλ sensitivity or if NS1/2 also modulates MNoV sensitivity to the functions of IFNλ. Further studies are needed to uncover how VP1 regulates IFNλ induction and any potential role for NS1/2 in IFN induction, signaling, or ISG function. For example, what cell subsets induce IFNλ during infection? Does VP1 confer tropism in those subsets? Will pCR6-$NS1^{CW3}$ (and other non-persistent pCR6-NS1/2 mutants) persist in *Ifnlr*$^{-/-}$ mice? Studies to address these questions are ongoing.

Key to these studies is identifying a cell type in which CW3 and CR6 differentially induce and are differentially sensitive to IFNλ. An interesting nuance to these studies is that IFNλ did not affect viral growth in myeloid cells *ex vivo* (Tim Nice personal communication, data not shown) and does not act on myeloid cells *in vivo*, but rather on intestinal epithelial cells (3). This is significant because current evidence argues that NoV replicates in myeloid cells but not epithelial cells. How is MNoV regulated by IFNλ when IFNλ does not directly act on infected cells? Several non-mutually exclusive possibilities may reconcile this conundrum: 1) MNoV does replicate in epithelial cell; 2) there is cross-talk between infected myeloid cells producing IFNλ and IFNλ responsive epithelial cells that restricts infection; 3) epithelial cells can restrict virus without being infected, such as by regulating barrier integrity. Germane to the first possibility is the need to identify the cell type MNoV infects in wild-type mice, as discussed below. Myeloid-epithelial cell cross talk is important during infection (4); to determine if this occurs during MNoV infection, we can infect macrophages in the presence of intestinal epithelial

cells using trans-wells, then measure viral growth. Alternatively, it would be interesting to treat epithelial cells with IFNλ, harvest the conditioned media, and treat infected myeloid cells with this conditioned media. Biochemical fractionation of the conditioned media could help determine which factor(s) contribute to MNoV control. The development of mice with *Ifnlr* deleted in specific cell types will corroborate with these studies. Lastly, IFNλ is known to affect barrier in different tissues (5), and this could be assessed in the intestine during infection, in *Ifnlr*$^{-/-}$ mice, and upon IFNλ treatment using a tissue diffusible dye that variably diffuses across the intestine dependent upon barrier integrity.

As sequence outside NS1 for either CW3 or CR6 were not necessary for persistence, and E94 was not necessary for CR6 to persist, we reasoned other residues within NS1 were necessary for persistence. In preliminary work, mutations that disrupted caspase cleavage sites separating NS1 and NS2 domains (6) did not persist in mice (data not shown). Furthermore, products correlating with NS1 and NS2 sizes accumulate during infection MNoV infection of cell lines. These observations argue NS1 and NS2 are cleaved during infection and that cleavage is necessary to establish persistent infection. Further studies are needed to determine the mechanism of cleavage, if it is spatiotemporally regulated, and the importance of cleavage in cell culture as well as mice. It is particularly interesting if NS1/2 is cleaved by caspases, as this may provide a way for MNoV to sense cellular responses to infection and subsequently alter replication or antagonize innate immune responses. Caspase activation and cleavage of viral proteins is important in other viral systems (reviewed in (7)), but this observation could provide novel significance for caspase regulation of viral proteins. To determine the mechanism of cleavage, MNoV infected cells can be treated with pan-caspase inhibitors then monitor NS1/2 cleavage. To test a role for caspases on replication, virus titers can also be monitored during treatment.

Furthermore, NS1/2 cleavage during infection with MNoV caspase-cleavage-site mutants will demonstrate which sites are targeted during infection. Detailed growth curves are needed to assess the effect of these mutants on viral growth. Preliminary studies using *Caspase3*$^{-/-}$ mice did not show any effect on MNoV replication or persistence (data not shown), but this may be related to extensive redundancy of caspases. Therefore, to demonstrate a role for caspase activation in persistent MNoV infection, mice can be treated with pan-caspase inhibitors and viral shedding monitored. If it is validated that NS1 are cleaved, the function of the divided proteins will be interesting to pursue. It is possible that NS1 function(s) during persistent viral infection are independent of NS2.

4.2.2 Tropism in vivo

The work herein provides new evidence for viral factors that contribute to tissue tropism, NS1/2 and VP1. Furthermore, the assays used herein (qRT-PCR) did not differentiate from the presence of virus and replicating virus. Detecting replicating virus may require development of techniques that detect viral antigens or products only present during viral replication, such as detection of minus strand RNA, or viral non-structural proteins. Nevertheless, a clear challenge to detecting persistent virus infection is there are low levels of viral antigens across the intestine. This may be the consequence of infrequent infection with high level of antigen/virion production, or frequent infection with low level of antigen/virion production. In the first case, higher throughput assays are needed to analyze cells in bulk, such as FACS or whole organ immunohistochemistry. In the second case, methods that are more sensitive are needed to detect viral antigen. Single molecule FISH assays coupled with FACS, *in situ* PCR, and novel genetic viral reporters, may help with this hurdle. Genetically overexpressing or deleting host factors regulating NoV infection in specific cell types will provide evidence for the cell types involved

in infection (pathogenesis, immune responses, persistence, etc.). These factors may include STAT1, IFNLR, IFNAR, HSP90, and VAPA. For example, *CD11c-Ifnar*$^{-/-}$ and *LyzM-Ifnar*$^{-/-}$, but not *Villin-Ifnar*$^{-/-}$ mice, did not clear acute CW3 infection (8, 9). This indicates that Type I IFN signaling in CD11c+ or LyzM+ cells is necessary to clear CW3 infection. This was likely due to unrestrained replication of CW3 in dendritic cells and macrophages and occurred in the face of an adaptive immune response typical for WT animals, thus strengthening the evidence that MNoV replicates in dendritic cells and macrophages *in vivo*. More studies like this will be important. Nevertheless, direct detection of virus will be required to definitively conclude the cell type NoV infects.

As current assays are insufficiently sensitive to directly detect virus, it will be difficult to directly assess the question how NS1/2 and VP1 contribute to tropism. Relying on growth of virus in *ex vivo* cells may help overcome this hurdle. In this work, we presented that CW3 and CR6 replicate differently in BMDMs *ex vivo*. This difference may reflect a different tropism for different macrophage subsets *in vivo*. Performing MNoV growth curves in macrophages and dendritic cell subsets from intestines, spleens, etc., can help further refine cellular tropism. Additionally, it will be interesting to differentiate cells into different macrophage and dendritic cell subsets to determine if differentiation or activation state determines cellular tropism for viral strains. Subsequently performing gene expression analysis to identify differentially expressed genes may help correlate host pathways associated with CR6 or CW3 infection. Further mapping of viral determinants to replicate in these cell subsets may correlate *in vivo* phenotypes such as persistence with these host pathways. Therefore, it may be possible to use different cell types to help identify host factors involved in regulating persistent infection.

Growth in BMDMs mapped to $VP1^{CW3}$. While VP1 can enhance viral RNA synthesis (10, 11), this is mediated by the shell domain that had no influence on viral replication in BMDMs. VP1, and particularly the protruding domain, is the major determinant for cellular tropism (12). These observations together suggest CR6 and CW3 may utilize different cellular factors to mediate entry into the cell. Recent observations that CD300lf is a protein receptor for MNoV (in press), but CR6 and CW3 similarly require CD300lf. Two possibilities to explain differences in BMDM growth are 1) there are other co-factors uniquely used by CR6 or CW3 in BMDMs, or 2) pathways downstream of binding are different. First, testing if CR6 and CW3 are recovered equivalently when added to BMDMs at 4°C will assess if these strains bind BMDMs differently. Second, MNoV-1 entry in BMDMs is dependent on dynamin and cholesterol (13, 14), but these studies did not analyze other strains of MNoV. Repeating these studies with CR6 and CW3 using 1) pharmacological inhibitors of endocytosis pathways and cholesterol trafficking, 2) knockouts of GTPases controlling endosomal trafficking, and 3) detailed time-course imaging of MNoV genomes with single-molecule FISH and subcellular markers, will assess if known MNoV entry pathways are similar between CR6 and CW3.

4.2.3 VAPA

This work establishes VAPA as a pro-MNoV factor. In this work, we did not use any functional systems for HNoV, which recently is becoming a more tractable system (15, 16) and may be assessed in the near future. What function VAPA plays during NoV function, and how broadly VAPA is used in other microbial infections are important questions.

Determining how VAPA enhances MNoV infection is a key aim to better understand the molecular and cellular requirements for efficient MNoV replication. Furthermore, it will be central to understanding the function of NS1/2 during infection. VAPA could serve at least two

non-mutually exclusive functions for MNoV: 1) VAPA enhances NS1/2 function and 2) VAPA is needed for NS1/2 to manipulate VAPA-client protein(s) function(s).

First, VAPA may regulate NS1/2 function. VAPA may influence NS1/2 subcellular localization. NS1/2 is the first protein translated from the MNoV genome, and binds other viral factors (17). Therefore, where NS1/2 localizes may influence the function of other viral proteins and subsequently virus replication. NS1/2 localizes to the ER (18), the major site of VAPA localization, but it is unknown if VAPA influences where NS1/2 localizes, either directly or indirectly. While ectopically expressed NS1/2 colocalized with overexpressed VAPA in 293T cells (data not shown), this study must be repeated during infection in *Vapa*$^{+/+}$ cells. Assessing if NS1/2 is mislocalized using subcellular markers against ER in 1) *Vapa*$^{-/-}$ cells, 2) reconstituted *Vapa*$^{-/-}$ cells with VAPA mutants that do not interact with NS1/2, and 3) MNoV-NS1/2 mutant viruses that disrupt VAPA interaction will determine if NS1/2-VAPA interaction is necessary for NS1/2 subcellular localization. Additionally, time courses analyzing VAPA localization with ER and other subcellular markers during the course of infection will test the hypothesis that NS1/2 redistributes VAPA during infection. These initial studies should be done using confocal microscopy. Because some VAPA-associated cellular structures are only detectable via high-resolution techniques, follow up studies should be done with EM and STORM.

VAPA may also affect the function of NS1/2 by regulating its function. Determining additional function(s) of NS1/2 is a key goal to learn if VAPA or other host factors regulate NS1/2. A simple yet challenging goal will be to discover the function of the NS2 domain. By sequence comparison NS2 has a fold found in diverse enzymes. Early structural determinations and mutagenesis indicate that NS2 adopts this fold (Krezel, unpublished communication) and the

key residues involved in catalysis are necessary for viral infection (unpublished). However, definitive proof will require defining the substrates of NS2, a challenging goal.

Second, NS1/2 may manipulate or coopt VAPA client proteins. In this scenario, NS1/2 turns on, off, redirects, or alters the normal function of VAPA client proteins. VAPA client proteins have roles in diverse cellular processes, including proteostasis (19-26), non-vesicular lipid transfer (27-32), membrane morphology (26, 33, 34), and membrane contacts (26, 30, 32, 35-37), but it is unknown if any of these processes influence NoV replication. A primary goal is to define which client proteins are pro- or antiviral to NoV replication. However, many VAPA interacting proteins perform redundant functions, or are otherwise spatiotemporally regulated. Therefore, direct studies on these cellular pathways in NoV infection are crucial.

One mechanism by which NS1/2 could regulate VAPA client protein function is to interact competitively with VAPA, thus disrupting physiological localization of client proteins. In this model, NS1/2 saturates VAPA interactions globally, locally, or redirects VAPA to subcellular locations where it no longer performs its physiological functions. To this end, preliminary estimations of NS1/2-VAPA dissociation constant are similar to those published for client proteins (Krezel private communication and (38)). One possibility for NS1/2 to outcompete other VAPA interactions at physiological levels would be for NS1/2 to have higher local concentrations. Regulation of VAPA-client proteins by competition has been observed in two settings. First, VAPA interacts competitively with FFAT motifs and either FAF1 or ATF6 that may mediate switching between regulating lipid trafficking and ER quality control (22). It is an attractive possibility that NS1/2 rewires host proteostatic/lipid dynamics by competitively binding VAPA. Second, IFITM3 competitively binds VAPA away from lipid transfer proteins (LTPs); this correlates with cholesterol accumulation in endosomes (39). It is unknown if IFITM

family members are antagonistic to NoV replication. Given the similar K_d of NS1/2-VAPA as LTP-VAPA, NS1/2-VAPA may likewise be susceptible to competition by IFITM3. Alternatively, NS1/2 may sequester VAPA into RCs, preventing competition by IFITM3. A separate IFN stimulated VAPA-client protein, RSAD2, antagonizes HCV infection by disrupting VAPA-NS5a interaction (40, 41). However, preliminary studies in mice did not find an antiviral role for RSAD2 against MNoV (Larissa Thackray, private communication). To test these hypotheses, biochemical competition assays to test NS1/2-VAPA-client protein interaction can be attempted. Furthermore, assessing client protein localization, including OSBP and IFITM3, during infection by microscopy will be important.

In addition to those discussed above, non-vesicular, protein-mediated lipid transfer is the primary function of VAPA and the most studied function in relation to microbial infection. Particularly, the role of PI4P and cholesterol are important during viral infection. To determine if PI4P and cholesterol localize to replication complexes, antibodies and genetic probes can be used to stain PI4P, and filipin can be used to stain cholesterol. Small molecules to inhibit PI4K family of enzymes can be used to disrupt the formation of PI4P, and itraconazole as well as osw-1 inhibit the activity of OSBP. Furthermore, knocking out OSBP, PI4K, and VAP-client proteins will be critical and simple with the advent of CRISPR-Cas9 genome editing technology.

VAP proteins make membrane contact sites (MCS) which are associated with the viral replication of tombusviruses, a genus of plant viruses. It may be that non-vesicular lipid transfer predominately occurs at MCSs. Therefore, establishing a role for lipid transfer proteins and lipids during NoV may infer that MCSs are involved in NoV replication. Furthermore, MCSs have been technically challenging to study as they are only detectable by careful analysis of electron micrographs. Therefore, electron microscopy of cells infected with NoV coupled with

high-resolution fluorescent microscopy techniques may facilitate studying MCSs during NoV infection. Lastly, ultrastructural reconstructions using EM tomography of infected cells has revealed remarkable detail of membrane interactions for a number of viruses (42-44). The study of membranes in NoV infection will benefit from EM tomography, albeit they are technically difficult to execute.

Lastly, the intracellular bacteria *Chlamydia trachomatis* also requires VAP proteins, but also encodes a virulence factor IncD that interacts with the VAP-client protein CERT (45, 46). VAP and CERT localize with IncD at ER-bacterial inclusion MCSs. At these sites, CERT transfers ceramide to the bacterial inclusion that is processed to sphingomyelin and used by the bacteria. There are no precedents for viruses requiring CERT. While there is some evidence for a role for ceramide in NoV entry into cells (47), it is unknown if CERT, ceramide, or sphingomyelin are required for viral replication. Studies looking at the localization of CERT and ceramide, as well as knocking out CERT will be informative.

How broadly among intracellular pathogens is VAPA utilized? Reported VAPA-dependent pathogens include positive-sense RNA viruses and intracellular bacteria, and we add NoV to this list. Furthermore, the flavivirus West Nile Virus (WNV) had diminished infectivity in *Vapa*$^{-/-}$ RAW264.7 cells, but viral replication was only diminished relative to *Vapa*$^{+/+}$ upon IFNb treatment (Matthew Gorman, Michael Diamond Lab, personal communication). A dependency on VAPA for WNV is unsurprising as WNV is related to HCV and utilizes the ER during infection. In contrast, preliminary studies showed diminished replication for lymphocytic Choriomeningitis virus (LCMV) in *Vapa*$^{-/-}$ cells LCMV only upon LPS treatment (Brian Sullivan, Oldstone Lab, personal communication). The replication life cycle of LCMV, which has an ambisense genome, is much different from currently described VAPA-dependent

microbes. Furthermore, the observation that replication was synergistically affected upon IFNβ or LPS treatment in *Vapa*$^{-/-}$ cells may provide additional insight into VAPA function under different stimuli. More studies with negative-sense viruses, DNA viruses, and parasites such as *Toxoplasma* will be informative. Of DNA viruses, poxviruses are particularly promising as they require extensive membrane rearrangements during replication. Nevertheless, screening a diverse set of pathogens with unique replication life-styles under different treatment conditions may reveal unique roles of VAPA during infection.

4.2.4 FFAT mimicry

Mimicry of host molecules and patterns is a pervasive evolutionary outcome for pathogens selected to hijack host processes (48). While efforts have been made to predict mimicry on large-scale (48), detecting structural and/or functional mimics requires validation of individual microbial molecules. For VAPA-microbe interactions, microbial mimicry of FFAT motifs is previously unreported.

NS1/2 is the first example of microbial mimicry of FFAT motifs. FFAT motifs tolerate variation at many positions (28, 49), are relatively short, and are unstructured in solution, making it unsurprising that a rapidly evolving virus could select these sequences. The advantage afforded by direct interactions with VAPA and VAPB proteins has been reported for Hepatitis C Virus (50, 51), which, in a similar way to many positive RNA viruses, rely on significant levels of membrane rearrangement for efficient viral replication. NS1/2 FFAT mimic was most similar N and C-terminally to host FFAT sequences. Further analyses of NoV NS1 sequences across diverse HNoV strains may further widen the definition of what constitutes a FFAT sequence (52).

It will be interesting to study how frequently FFAT mimicry occurs among microbes. HCV NS5a and NS5b both bind MSP domain in sites partially overlapping FFAT motif binding, yet neither protein contains sequences resembling FFAT motifs. This argues HCV evolved a unique way to interact with VAP proteins. A rigorous bioinformatic search for microbial FFAT motifs will be informative, but nonetheless would likely underrepresent the "VAPome" of microbial-VAPA interactors.

Finally, VAPB also interacts with NS1/2, probably through a common mechanism as VAPA. VAPA and VAPB demonstrably have overlapping functions, and it is currently unclear what, if any, functions are unique to each protein. The observation that *Vapb*$^{-/-}$ mice are viable but *Vapa*$^{-/-}$ mice are embryonic lethal, and that VAPB is linked to Amyotrophic Lateral Sclerosis, but VAPA is not, argues there are unique functions or spatiotemporal expression patterns between VAPA and VAPB. Nevertheless, VAPA and VAPB possibly have redundant functions during MNoV replication. It will be important to test a role for VAPB using VAPB knockout cells and VAPA/VAPB double knockout cells, which are currently under development.

4.3 References

1. **Nice TJ, Baldridge MT, McCune BT, Norman JM, Lazear HM, Artyomov M, Diamond MS, virgin HW.** 2015. Interferon-lambda cures persistent murine norovirus infection in the absence of adaptive immunity. Science **347:**269-273.

2. **Baldridge MT, Nice TJ, McCune BT, Yokoyama CC, Kambal A, Wheadon M, Diamond MS, Ivanova Y, Artyomov M, Virgin HW.** 2015. Commensal microbes and interferon-λ determine persistence of enteric murine norovirus infection. Science **16:**266-269.

3. **Pott J, Mahlakoiv T, Mordstein M, Duerr CU, Michiels T, Stockinger S, Staeheli P, Hornef MW.** 2011. IFN-lambda determines the intestinal epithelial antiviral host defense. Proc Natl Acad Sci U S A **108:**7944-7949.

4. **Sun L, Miyoshi H, Origanti S, Nice TJ, Barger AC, Manieri NA, Fogel LA, French AR, Piwnica-Worms D, Piwnica-Worms H, Virgin HW, Lenschow DJ, Stappenbeck TS.** 2015. Type I interferons link viral infection to enhanced epithelial turnover and repair. Cell Host Microbe **17:**85-97.

5. **Lazear HM, Daniels BP, Pinto AK, Huang AC, Vick SC, Doyle SE, Gale M, Jr., Klein RS, Diamond MS.** 2015. Interferon-lambda restricts West Nile virus neuroinvasion by tightening the blood-brain barrier. Sci Transl Med **7:**284ra259.

6. **Sosnovtsev SV, Belliot G, Chang KO, Prikhodko VG, Thackray LB, Wobus CE, Karst SM, Virgin HW, Green KY.** 2006. Cleavage map and proteolytic processing of the murine norovirus nonstructural polyprotein in infected cells. J Virol **80:**7816-7831.

7. **Richard A, Tulasne D.** 2012. Caspase cleavage of viral proteins, another way for viruses to make the best of apoptosis. Cell Death Dis **3:**e277.

8. **Nice TJ, Osborne LC, Tomov VT, Artis D, Wherry EJ, Virgin HW.** 2016. Type I Interferon Receptor Deficiency in Dendritic Cells Facilitates Systemic Murine Norovirus Persistence Despite Enhanced Adaptive Immunity. PLoS Pathog **12:**e1005684.

9. **Thackray LB, Duan E, Lazear HM, Kambal A, Schreiber RD, Diamond MS, Virgin HW.** 2012. Critical role for interferon regulatory factor 3 (IRF-3) and IRF-7 in type I interferon-mediated control of murine norovirus replication. J Virol **86:**13515-13523.

10. **Subba-Reddy CV, Goodfellow I, Kao CC.** 2011. VPg-primed RNA synthesis of norovirus RNA-dependent RNA polymerases by using a novel cell-based assay. J Virol **85:**13027-13037.

11. **Subba-Reddy CV, Yunus MA, Goodfellow IG, Kao CC.** 2012. Norovirus RNA synthesis is modulated by an interaction between the viral RNA-dependent RNA polymerase and the major capsid protein, VP1. J Virol **86:**10138-10149.

12. **Zhu S, Watanabe M, Kirkpatrick E, Murray AB, Sok R, Karst SM.** 2016. Regulation of Norovirus Virulence by the VP1 Protruding Domain Correlates with B Cell Infection Efficiency. J Virol **90:**2858-2867.

13. **Gerondopoulos A, Jackson T, Monaghan P, Doyle N, Roberts LO.** 2010. Murine norovirus-1 cell entry is mediated through a non-clathrin-, non-caveolae-, dynamin- and cholesterol-dependent pathway. J Gen Virol **91:**1428-1438.

14. **Perry JW, Wobus CE.** 2010. Endocytosis of murine norovirus 1 into murine macrophages is dependent on dynamin II and cholesterol. J Virol **84:**6163-6176.

15. **Katayama K, Murakami K, Sharp TM, Guix S, Oka T, Takai-Todaka R, Nakanishi A, Crawford SE, Atmar RL, Estes MK.** 2014. Plasmid-based human norovirus reverse genetics system produces reporter-tagged progeny virus containing infectious genomic RNA. Proc Natl Acad Sci U S A **111:**E4043-4052.

16. **Jones MK, Watanabe M, Zhu S, Graves CL, Keyes LR, Grau KR, Gonzalez-Hernandez MB, Iovine NM, Wobus CE, Vinje J, Tibbetts SA, Wallet SM, Karst SM.** 2014. Enteric bacteria promote human and mouse norovirus infection of B cells. Science **346:**755-759.

17. **Thorne L, Bailey D, Goodfellow I.** 2012. High-resolution functional profiling of the norovirus genome. J Virol **86:**11441-11456.

18. **Hyde JL, Mackenzie JM.** 2010. Subcellular localization of the MNV-1 ORF1 proteins and their potential roles in the formation of the MNV-1 replication complex. Virology **406:**138-148.

19. **Brickner JH, Walter P.** 2004. Gene recruitment of the activated INO1 locus to the nuclear membrane. PLoS Biol **2:**e342.

20. **Suzuki H, Kanekura K, Levine TP, Kohno K, Olkkonen VM, Aiso S, Matsuoka M.** 2009. ALS-linked P56S-VAPB, an aggregated loss-of-function mutant of VAPB, predisposes motor neurons to ER stress-related death by inducing aggregation of co-expressed wild-type VAPB. J Neurochem **108:**973-985.

21. **Gkogkas C, Middleton S, Kremer AM, Wardrope C, Hannah M, Gillingwater TH, Skehel P.** 2008. VAPB interacts with and modulates the activity of ATF6. Hum Mol Genet **17:**1517-1526.

22. **Ernst WL, Shome K, Wu CC, Gong X, Frizzell RA, Aridor M.** 2016. VAMP-associated Proteins (VAP) as Receptors That Couple Cystic Fibrosis Transmembrane

Conductance Regulator (CFTR) Proteostasis with Lipid Homeostasis. J Biol Chem **291:**5206-5220.

23. **Larroquette F, Seto L, Gaub PL, Kamal B, Wallis D, Lariviere R, Vallee J, Robitaille R, Tsuda H.** 2015. Vapb/Amyotrophic lateral sclerosis 8 knock-in mice display slowly progressive motor behavior defects accompanying ER stress and autophagic response. Hum Mol Genet **24:**6515-6529.

24. **Baron Y, Pedrioli PG, Tyagi K, Johnson C, Wood NT, Fountaine D, Wightman M, Alexandru G.** 2014. VAPB/ALS8 interacts with FFAT-like proteins including the p97 cofactor FAF1 and the ASNA1 ATPase. BMC Biol **12:**39.

25. **Moustaqim-Barrette A, Lin YQ, Pradhan S, Neely GG, Bellen HJ, Tsuda H.** 2014. The amyotrophic lateral sclerosis 8 protein, VAP, is required for ER protein quality control. Hum Mol Genet **23:**1975-1989.

26. **Manford AG, Stefan CJ, Yuan HL, Macgurn JA, Emr SD.** 2012. ER-to-plasma membrane tethering proteins regulate cell signaling and ER morphology. Dev Cell **23:**1129-1140.

27. **Wyles JP, McMaster CR, Ridgway ND.** 2002. Vesicle-associated membrane protein-associated protein-A (VAP-A) interacts with the oxysterol-binding protein to modify export from the endoplasmic reticulum. J Biol Chem **277:**29908-29918.

28. **Loewen CJ, Roy A, Levine TP.** 2003. A conserved ER targeting motif in three families of lipid binding proteins and in Opi1p binds VAP. EMBO J **22:**2025-2035.

29. **Kawano M, Kumagai K, Nishijima M, Hanada K.** 2006. Efficient trafficking of ceramide from the endoplasmic reticulum to the Golgi apparatus requires a VAMP-associated protein-interacting FFAT motif of CERT. J Biol Chem **281:**30279-30288.

30. **Peretti D, Dahan N, Shimoni E, Hirschberg K, Lev S.** 2008. Coordinated lipid transfer between the endoplasmic reticulum and the Golgi complex requires the VAP proteins and is essential for Golgi-mediated transport. Mol Biol Cell **19:**3871-3884.

31. **Tuuf J, Wistbacka L, Mattjus P.** 2009. The glycolipid transfer protein interacts with the vesicle-associated membrane protein-associated protein VAP-A. Biochem Biophys Res Commun **388:**395-399.

32. **Alpy F, Rousseau A, Schwab Y, Legueux F, Stoll I, Wendling C, Spiegelhalter C, Kessler P, Mathelin C, Rio MC, Levine TP, Tomasetto C.** 2013. STARD3 or STARD3NL and VAP form a novel molecular tether between late endosomes and the ER. J Cell Sci **126:**5500-5512.

33. **Amarilio R, Ramachandran S, Sabanay H, Lev S.** 2005. Differential regulation of endoplasmic reticulum structure through VAP-Nir protein interaction. J Biol Chem **280:**5934-5944.

34. **Kentala H, Pfisterer SG, Olkkonen VM, Weber-Boyvat M.** 2015. Sterol liganding of OSBP-related proteins (ORPs) regulates the subcellular distribution of ORP-VAPA complexes and their impacts on organelle structure. Steroids **99:**248-258.

35. **Wang P, Hawkins TJ, Richardson C, Cummins I, Deeks MJ, Sparkes I, Hawes C, Hussey PJ.** 2014. The plant cytoskeleton, NET3C, and VAP27 mediate the link between the plasma membrane and endoplasmic reticulum. Curr Biol **24:**1397-1405.

36. **Stoica R, De Vos KJ, Paillusson S, Mueller S, Sancho RM, Lau KF, Vizcay-Barrena G, Lin WL, Xu YF, Lewis J, Dickson DW, Petrucelli L, Mitchell JC, Shaw CE, Miller CC.** 2014. ER-mitochondria associations are regulated by the VAPB-PTPIP51 interaction and are disrupted by ALS/FTD-associated TDP-43. Nat Commun **5:**3996.

37. **Stefan CJ, Manford AG, Baird D, Yamada-Hanff J, Mao Y, Emr SD.** 2011. Osh proteins regulate phosphoinositide metabolism at ER-plasma membrane contact sites. Cell **144:**389-401.

38. **Furuita K, Jee J, Fukada H, Mishima M, Kojima C.** 2010. Electrostatic interaction between oxysterol-binding protein and VAMP-associated protein A revealed by NMR and mutagenesis studies. J Biol Chem **285:**12961-12970.

39. **Amini-Bavil-Olyaee S, Choi YJ, Lee JH, Shi M, Huang IC, Farzan M, Jung JU.** 2013. The antiviral effector IFITM3 disrupts intracellular cholesterol homeostasis to block viral entry. Cell Host Microbe **13:**452-464.

40. **Helbig KJ, Eyre NS, Yip E, Narayana S, Li K, Fiches G, McCartney EM, Jangra RK, Lemon SM, Beard MR.** 2011. The antiviral protein viperin inhibits hepatitis C virus replication via interaction with nonstructural protein 5A. Hepatology **54:**1506-1517.

41. **Wang S, Wu X, Pan T, Song W, Wang Y, Zhang F, Yuan Z.** 2012. Viperin inhibits hepatitis C virus replication by interfering with binding of NS5A to host protein hVAP-33. J Gen Virol **93:**83-92.

42. **Kopek BG, Perkins G, Miller DJ, Ellisman MH, Ahlquist P.** 2007. Three-dimensional analysis of a viral RNA replication complex reveals a virus-induced mini-organelle. PLoS Biol **5:**e220.

43. **den Boon JA, Diaz A, Ahlquist P.** 2010. Cytoplasmic viral replication complexes. Cell Host Microbe **8:**77-85.

44. **den Boon JA, Ahlquist P.** 2010. Organelle-like membrane compartmentalization of positive-strand RNA virus replication factories. Annu Rev Microbiol **64:**241-256.

45. **Elwell CA, Jiang S, Kim JH, Lee A, Wittmann T, Hanada K, Melancon P, Engel JN.** 2011. Chlamydia trachomatis co-opts GBF1 and CERT to acquire host sphingomyelin for distinct roles during intracellular development. PLoS Pathog **7:**e1002198.

46. **Derre I, Swiss R, Agaisse H.** 2011. The lipid transfer protein CERT interacts with the Chlamydia inclusion protein IncD and participates to ER-Chlamydia inclusion membrane contact sites. PLoS Pathog **7:**e1002092.

47. **Shivanna V, Kim Y, Chang KO.** 2015. Ceramide formation mediated by acid sphingomyelinase facilitates endosomal escape of caliciviruses. Virology **483:**218-228.

48. **Hagai T, Azia A, Babu MM, Andino R.** 2014. Use of host-like peptide motifs in viral proteins is a prevalent strategy in host-virus interactions. Cell Rep **7:**1729-1739.

49. **Mikitova V, Levine TP.** 2012. Analysis of the key elements of FFAT-like motifs identifies new proteins that potentially bind VAP on the ER, including two AKAPs and FAPP2. PLoS One **7:**e30455.

50. **Tu H, Gao L, Shi ST, Taylor DR, Yang T, Mircheff AK, Wen Y, Gorbalenya AE, Hwang SB, Lai MM.** 1999. Hepatitis C virus RNA polymerase and NS5A complex with a SNARE-like protein. Virology **263:**30-41.

51. **Evans MJ, Rice CM, Goff SP.** 2004. Phosphorylation of hepatitis C virus nonstructural protein 5A modulates its protein interactions and viral RNA replication. Proc Natl Acad Sci U S A **101:**13038-13043.

52. **Murphy SE, Levine TP.** 2016. VAP, a Versatile Access Point for the Endoplasmic Reticulum: Review and analysis of FFAT-like motifs in the VAPome. Biochim Biophys Acta doi:10.1016/j.bbalip.2016.02.009.